The Thesis Defense Committee for Machiraju P. Kashyap

Certifies that this is the approved version of the following Thesis or Report

Analyze the effect of urbanization and development over the flow regime and river channel hydraulics of the main Bear Creek channel

APPROVED BY

SUPERVISING COMMITTEE:

Dr. Nick Z Fang, Supervisor, Chair

Dr. Yu Zhang

Dr. Michelle Hummel

Analyze the effect of urbanization and development over the flow regime and river channel hydraulics of the Big Bear creek channel

By

Machiraju P. Kashyap

Presented to the Faculty of the Graduate School of The University of Texas at Arlington

in Partial Fulfillment of the Requirements

for the Degree of

Master of Science in Water Resources Engineering

THE UNIVERSITY OF TEXAS AT ARLINGTON

May 2023

Dedication

To my mother Machiraju Sarada, father V.K.R Machiraju and sister Machiraju Meher Jahnavi for giving me constant motivation and inspiration.

ACKNOWLEDGEMENTS

I would like to thank my supervising professor Dr. Nick Z. Fang for constantly motivating and encouraging me, and for his invaluable advice during my masters. I wish to thank Dr. Daniel Li and the whole Fang Research Group for providing their invaluable help to make my master thesis a success. Dr. Michelle Hummel and Dr. Yu Zhang for their interest in my research and for taking time to serve on my dissertation committee.

Finally, I would like to express my deep gratitude to my parents, sister and relatives who have encouraged and inspired me and sponsored my graduate studies. I am extremely fortunate to be so blessed. I am also extremely grateful to my father, mother and sister for their sacrifice, encouragement, and patience. I also thank my local guardian Mrs. Hema Malini Chavali and family for helping me throughout my stay at Arlington.

June 1st, 2023

ABSTRACT

Analyze the effect of urbanization and development over the flow regime and river channel hydraulics of the main Bear Creek channel

Machiraju P. Kashyap, M.S. in Water Resources Engineering

The University of Texas at Arlington, 2023

Supervising Professor:

This thesis focuses on investigating the influence of urbanization and development on flow regime and river channel hydraulics in the Bear Creek watershed, Texas using a comprehensive set of hydrologic and 1D/2D coupled hydraulic model. The Bear Creek watershed, located in North Texas, has experienced rapid urbanization and land development in recent years, raising concerns about the potential impacts on hydrological processes and the hydraulic behavior of the river system. To address these concerns, this research utilizes an integrated modeling approach, combining the HEC-HMS and HEC-RAS software tools, to assess changes in flow rates and simulate their effects on river channel hydraulics. The study employs a comprehensive

methodology, integrating various data sources such as land use data, precipitation records, and streamflow measurements. HEC-HMS is employed to simulate the hydrologic response of the Bear Creek Watershed under different urbanization and development scenarios, generating flow rates that reflect the altered surface conditions. These flow rates are then utilized as boundary conditions for subsequent 1D/2D simulations in HEC-RAS, allowing for a detailed analysis of the hydraulic behavior of the river channel. The findings of this research shed light on the impact of urbanization and development on flow regime characteristics within the Bear Creek Watershed. Parameters such as peak flows, flow duration curves, and flood routing are analyzed to understand the changes in hydrological patterns resulting from land use alterations. Furthermore, the implications on river channel hydraulics, including water levels, velocities, and shear stresses, are assessed to gain insights into the potential effects on flood risks, sediment transport, and channel stability. By utilizing the integrated modeling capabilities of HEC-HMS and HEC-RAS, this research provides a comprehensive understanding of the complex interactions between urbanization, development, and the hydrological behavior of the Bear Creek Watershed. The outcomes of this study can inform decision-making processes for local authorities, land developers, and environmental managers, facilitating sustainable land use planning and watershed management practices. Overall, this thesis contributes to the knowledge base surrounding the Bear Creek Watershed and serves as a valuable resource for understanding the implications of urbanization and development on flow regime and river channel hydraulics. The integrated modeling approach presented in this research can be applied to other watersheds facing similar challenges, promoting informed decision-making and sustainable development practices in urbanized are

TABLE OF CONTENTS

LIST OF FIGURES

LIST OF TABLES

CHAPTER 1 INTRODUCTION

Flooding and soil erosion extensively affect our agricultural land, water quality and infrastructure posing great environmental challenges. In urban areas, these issues damage exponentially due to human activities like urbanization, land use changes and industrialization [1]. One research conducted an exploratory analysis on the effects of urbanization on water resources. They investigated the impacts of urban development on water quantity and quality, highlighting the challenges faced in managing water resources in urban areas [2] . The study emphasized the need for sustainable urban planning strategies to mitigate the adverse effects of urbanization on water resources. Prasood [3] studied the effects of urbanization on water resources in a tropical river basin in South India. They examined the changes in land use and land cover due to urbanization and their implications for water resources. The research highlighted the importance of monitoring and managing water resources in rapidly urbanizing regions to ensure their sustainable use. Urbanization in Ijebuland, southwestern Nigeria, was investigated by researchers. The study assessed the impacts of urban expansion on land and water resources in the region. It emphasized the need for effective land and water management strategies to address the challenges posed by urbanization and ensure the sustainable use of resources [4].

It is a necessity to understand effect of urbanization and development on river channel hydraulics and flow regime for environmental management and sustainable development. Crop and forest cover play a significant role in determining dynamics of the flow within the river channel. Research by Eckermann, Hunt, and Kinoshita [5] highlights the influence of vegetation and canopy cover change on river channel hydraulics. The results devised by them point out the importance of vegetation changes throughout a watershed. Urbanization and land use changes

significantly affect basin hydrology, as demonstrated by studies conducted in various regions. The Malir Basin, Karachi, Pakistan, industrialization and increase in the urban topography has led to changes in stormwater generation patterns, streamflow characteristics and risk of flooding [6] [7]. This highlights the need for comprehensive assessments to understand the complex relationships between land-use changes and river system dynamics [8]. Floodplain mapping and management are crucial in urban catchments to minimize the impact of floods. Utilizing the HEC-RAS modeling approach, Rangari, Sridhar, Umamahesh, and Patel [9] conducted a case study in Hyderabad City to explore floodplain mapping and management in an urban context. Their efforts provide insights into the application of HEC-RAS for flood analysis and management. HEC HMS and HEC-RAS have proven to be effective rainfall to runoff simulator and modelling tools to understand hydrologic processes and to model flood events. In Tabuk, Saudi Arabia, Alsubeai and Burckhard [10] employed rainfall-runoff simulation and the HEC-HMS and HEC-RAS models to study flood events. This study gives a great insight into understanding hydrologic processes in urban watersheds.

Digital Elevation Models (DEMs) have become invaluable in floodplain mapping and analysis. Nagarajan et al. [11] reviewed the use of DEMs in floodplain mapping, employing tools such as HEC-HMS, HEC-RAS, and ArcGIS. Their comprehensive review emphasizes the significance of DEM-based floodplain mapping in conjunction with modeling tools for accurate flood risk assessment. Combining HEC-HMS and HEC-RAS provides a greater depth of understanding and provides invaluable information; the two software uses a variety of methods to predict flow and depth inundation. This integration has been explored in various studies by researchers in the field [12][13]. Their research puts into light the essence of integrating modelling tools for understanding floodplain dynamics. They emphasize effects of change in historical land

use on the flow regime or the increase or decrease of surface runoff from development point of view studied using coupled 1D/2D HEC-RAS-HEC-HMS hydrological modeling. Ainskin [14] focused on tools for managing hydrologic alteration on a regional scale. The research aimed to estimate changes in flow characteristics in ungauged sites, where direct data measurements are limited. The study highlighted the significance of modeling approaches, such as the Soil Conservation Service Curve Number (SCS-CN), Artificial Neural Network (ANN), and HEC-HMS, in understanding and managing hydrological alterations. Such research sheds light on the long-term impacts of land-use changes on flood dynamics in river basins [15]. Understanding the vulnerability of culverts, bridge and hydraulic superstructures to high intensity discharge flood events is crucial for ensuring infrastructure resilience. Alsubeai [16] conducted a study to identify and analyze inundated bridge superstructures in high-velocity flood events. Their findings contribute to the understanding of bridge vulnerability and provide crucial information for infrastructure resilience planning. Addressing the challenges careful drainage during flood events, Pervaiz [17] conducted a feasibility study of submerged floating crossings. Such studies emphasize on the essence of such innovative infrastructure solutions for ensuring connectivity and minimizing disruptions caused by flooding. To discuss a few innovative ideas to enhance hydrologic data, the utilization of remote sensing techniques has also played a significant role in understanding urban hydrological processes. A study employed small unmanned aerial vehicles to capture small-scale surface temperature and vegetation changes to understand variations across diverse urban land uses [18]. Their study highlighted the influence of urban heat island effects on hydrological processes, underscoring the importance of remote sensing techniques in urban hydrological research. The field of hydrologic and hydraulic modelling requires field data inputs and new technologies that capture morphological, geological and climate information. In data-

sparse regions, merging satellite rainfall estimates has been explored to improve rainfall estimation accuracy. Ahmad [19] conducted a study on merging satellite rainfall estimates in the Indus basin, addressing the challenges posed by data scarcity. This research contributes to enhancing rainfall estimation techniques in areas with limited ground-based observations. Bhattacharya and Ahmad [20] proposed a K nearest neighbor approach for merging satellite rainfall estimates from diverse sources in sparsely gauged basins. Their study contributes to improving rainfall estimation accuracy in areas with limited ground-based observations. Understanding the petrophysical properties of geological rocks encountered in carbon storage and utilization is crucial for hydraulic processes. Hu, Wang, Zhang, Zhao, Iltaf, Liu, and Fukatsu [21] investigated the petrophysical properties of representative geological rocks, enhancing our understanding of rock properties related to carbon storage and their potential implications for hydraulic processes. The importance of coupling hydrologic and hydraulic models to model floodplain has become essential [22]. By integrating models such as HEC-HMS and HEC-RAS, coupled with precipitation runoff modeling, researchers have been able to simulate rainfall-runoff processes and evaluate floodplain inundation maps. Research studied the effects of urbanization on water resources in a tropical river basin in South India. They examined the changes in land use and land cover due to urbanization and their implications for water resources [23]. The research highlighted the importance of monitoring and managing water resources in rapidly urbanizing regions to ensure their sustainable use.

One of the key advancements in flood inundation modeling is the utilization of a coupled 1D/2D hydrodynamic model, which combines the capabilities of the HEC-HMS and HEC-RAS models. Research papers [24], [25], and [26] highlight the effectiveness of this modeling approach in assessing and analyzing flooding scenarios, providing valuable insights into the dynamics of flood events and their impact on the environment. The development of HEC-HMS and HEC-RAS

models for urban floodplain mapping and flood damage reduction in Brownsville, Texas, was conducted by researchers. The study focused on utilizing these models to assess flood risks, map floodplains, and implement measures for flood damage reduction. The research demonstrated the effectiveness of HEC-HMS and HEC-RAS in flood analysis and management [27].

The research conducted by [28] on the Khazir River in the Middle East—Northern Iraq shows the application of the HEC-RAS and HEC-HMS models in flood analysis. By integrating rainfall-runoff simulation with hydraulic modeling, the researchers were able to evaluate the river's behavior during flood events and assess the potential impacts on agricultural land, water quality, and infrastructure.

A study showcases multiple scenario analyses of Huangpu River flooding using a coupled 1D/2D flood inundation model. By considering both one-dimensional river flow and two-dimensional overland flow, the study provided a comprehensive assessment of flood risk under different hydrological and hydraulic conditions [29]. This approach allows for a more accurate representation of the river hydraulics and flood dynamics, enabling better flood forecasting and risk management.

Additionally, [30] presents a case study of the Baeksan flood event in Korea, utilizing the HEC-RAS 1D/2D coupling simulation. The study demonstrates the practical application of this modeling approach and its ability to capture the complex interactions between river channels and floodplains. The outcomes of this research contribute significant insights into floodplain mapping, flood risk assessment, and erosion management, further emphasizing the importance of utilizing coupled 1D/2D models in flood inundation studies. By leveraging the capabilities of the HEC-HMS and HEC-RAS models in a coupled 1D/2D configuration, researchers can achieve a more comprehensive understanding of flood dynamics and their consequences. This modeling approach

enables the simulation of rainfall-runoff processes, river hydraulics, and floodplain inundation, providing major outcomes about flooding and erosion characteristics. The integration of 1D/2D modeling with HEC-HMS allows for a better representation of the hydrological response, while the incorporation of HEC-RAS facilitates a detailed analysis of river flow and flood extents. These advancements in flood inundation modeling, as demonstrated by the research papers cited, offer significant potential for improving flood risk assessment, mitigation strategies, and urban planning in flood-prone areas. Moreover, one emerging area of research focuses on the impacts of vegetation and canopy cover changes on river channel hydraulics [31]. Halwatura and Najim (2013) developed an HEC-HMS model for runoff simulation in a tropical catchment. Their study demonstrated the applicability of the HEC-HMS model in estimating runoff in regions with limited data availability. The research highlighted the potential of HEC-HMS as a tool for hydrological analysis and flood forecasting [26].

In addition to these research advancements, the evaluation of ice loads on bridges using deterministic and probabilistic approaches has gained attention [10]. With the increasing frequency of extreme weather events, it is crucial to assess the structural integrity of bridges under ice loading conditions. By integrating deterministic and probabilistic methodologies, researchers have been able to provide insights into the potential impacts of ice loads on bridge structures, facilitating informed decision-making in bridge design and maintenance [10]. incorporating new ideas from recent research papers, such as coupling hydrological and hydraulic models for floodplain inundation mapping, studying the effects of vegetation and canopy cover changes on river hydraulics, and evaluating ice loads on bridges, holds great potential for advancing our understanding of urban hydrological processes. These research findings contribute to the development of more accurate flood analysis techniques, improved floodplain mapping, and

enhanced urban planning strategies. [29] analyzed the future flooding and risk assessment using the HEC-HMS and HEC-RAS models in the Babai River Basin. The study utilized these models to simulate runoff and predict flood inundation under climate change scenarios. The research provided insights into the potential impacts of climate change on flooding and highlighted the importance of utilizing modeling tools for flood risk assessment. [30] conducted a study on flood inundation mapping in an ungauged basin. They utilized modeling approaches, including HEC-HMS and HEC-RAS, to predict flood travel time and determine the extent of inundation. The research emphasized the significance of accurate floodplain mapping for effective flood management [30]. The evaluation of one-dimensional and two-dimensional HEC-RAS models for predicting flood travel time and inundation area in a flood warning system was carried out by researchers. The study compared the performance of both modeling approaches in terms of accuracy and applicability. The research highlighted the importance of selecting the appropriate modeling approach based on specific flood forecasting and management needs [31]. By implementing these innovative approaches, we can address the challenges posed by urbanization, soil erosion, and flood inundation, leading to more sustainable and resilient urban environments. By integrating the findings and methodologies from these diverse research papers, this study aims to address the impact of urbanization and development on river channel flow regimes and hydraulics. The research motivation stems from the need to develop sustainable urban planning strategies, effective flood management measures, and erosion control techniques to mitigate the adverse impacts of soil erosion and flood inundation in urban areas. Through these efforts, this study will contribute to the advancement of knowledge and the development of strategies to ensure the sustainable coexistence of urban areas and river systems.

In summary, these research papers contribute to the understanding of the impact of urbanization and development on water resources. They highlight the challenges faced in managing water quantity and quality in urban areas and emphasize the need for sustainable urban planning strategies. The studies also demonstrate the use of modeling tools such as HEC-HMS and HEC-RAS in assessing hydrological alterations, simulating runoff, mapping floodplains, and predicting flood inundation. Furthermore, they emphasize the importance of accurate floodplain mapping and the need for effective flood management strategies in urban catchments.

The novelty of the research can be attributed to efforts for a combined hydrologic and hydraulic model with HEC-HMS and HEC-RAS 1D/2D simulations for a region located adjacent to the Dallas-Fort Worth International Airport (Airport). Analyzing small impacts like imperviousness change or land cover change can help us identify flood inundation and encroachment from a highly urbanized location.

The thesis aims to model urbanization and development impact over a short period of time and focuses on the Big Bear Creek channel that is situated in a fast-growing urban region. It aims to understand flood and inundation change for the 5 years (2017-2022). These locations being within the DFW airport region can help us identify implications of airport activity over a river channel.

Study Area

Bear Creek Watershed is in the northern part of Texas as shown in **Figure 1** and one of the most significant urbanized locations in the area. The watershed due to its increasing population has consistent source of clean water, provisions for flood control, and recreation. In this section, we will discuss various aspects of the Bear Creek Watershed, including its topography, population, urbanization, land use, land cover, and the DFW airport and its influence on the region in general.

The Big Bear Creek watershed covers an area of approximately 84 square miles (USGS Geological survey, the map data delivery). The study area has been selected as it adjacent to the Airport and we can assess the direct impact of an airport on a natural channel also the watershed is a rapidly developing area such as the DFW metroplex, which is growing with increase in population and urbanization.

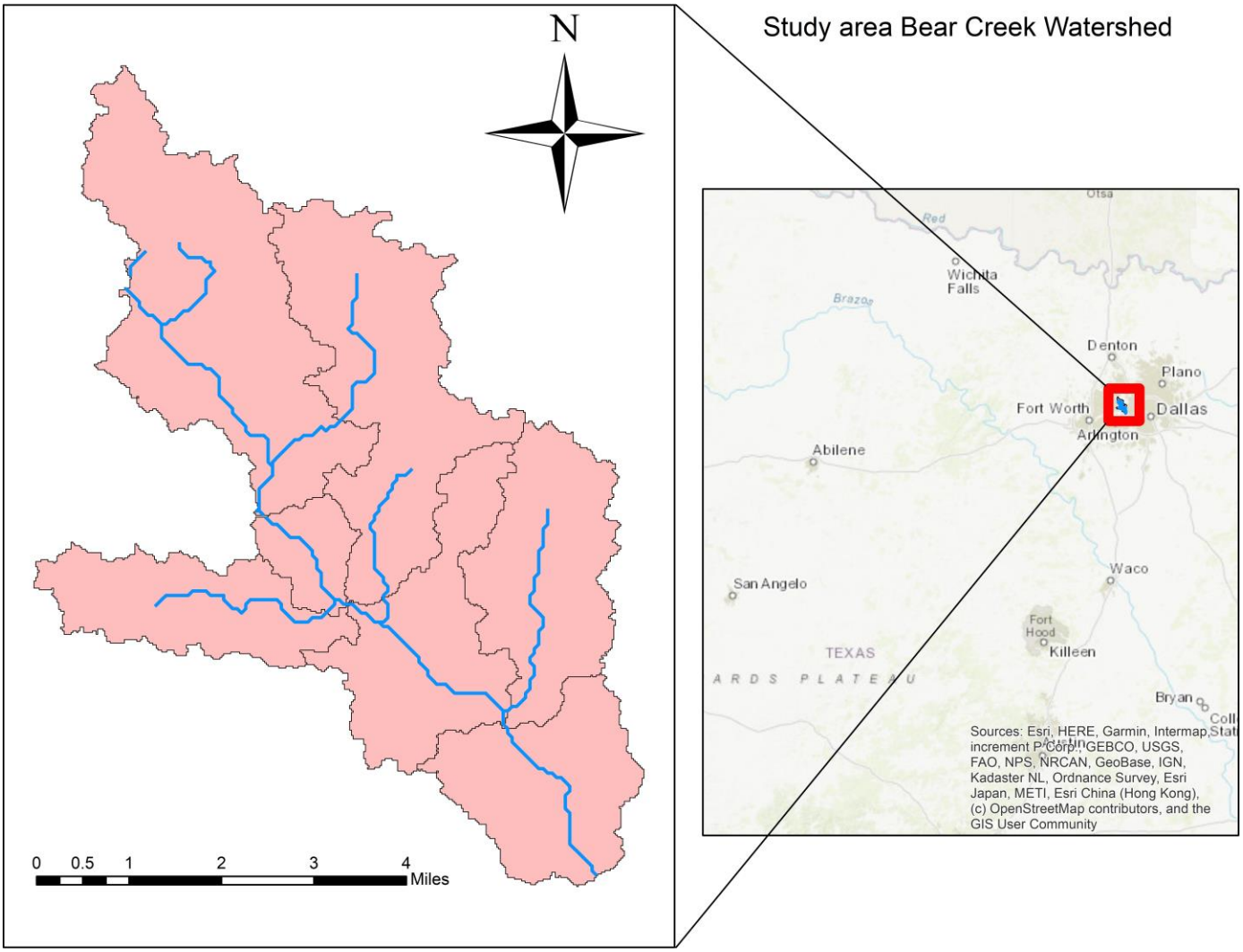

Figure 1 Study Area Bear Creek Watershed.

Bear Creek watershed is characterized by a mixture of rolling hills, steep slopes, and flat areas (US Geological survey National geospatial program, topographic maps). The topography of the area influences the flow of water within the watershed. The highest elevation in the watershed is approximately 862.861 feet, while the lowest elevation is around 348 feet (3 GEP Digital Elevation Model 1m file). The Bear Creek Watershed is home to a diverse population, including urban and rural residents. The population of the Dallas Fort Worth metroplex (DFW) area which is the major contributing region to Bear Creek channel has been increasing steadily over the years, and it is projected to continue growing. According to the United Nations world population prospects, the population of the was approximately 100,000 in 1953, and it is projected to reach 6.6 million by 2040. The urbanization of the watershed has had a significant impact on the environment. As the population has grown, so has the demand for housing, commercial development, and infrastructure.

The rapid urbanization of the area has led to the conversion of natural land cover to impervious surfaces, such as roads, parking lots, and buildings. The increase in impervious surfaces has led to an increase in stormwater runoff, which can cause flooding and erosion. The land use and land cover of the Bear Creek Watershed have changed significantly over the years. The area was originally covered by prairie grasses and forests, but much of this natural land cover has been replaced by agriculture, urban development, and transportation infrastructure. The development of transportation infrastructure, such as highways and airports, has also had a significant impact on the land use of the watershed. A majority part of the Dallas-Fort Worth International Airport (Airport) is located within the Bear Creek Watershed and is one of the busiest airports in the world. The airport covers an area of approximately 27 square miles and serves more than 69 million passengers annually. The airport has had a significant impact on the land use and

land cover of the watershed. The construction and operation of the airport have led to the conversion of natural land cover to impervious surfaces, such as runways, taxiways, and parking lots. The airport has also led to the development of supporting infrastructure, such as highways and rail lines. The increase in impervious surfaces has led to an increase in stormwater runoff, which can cause flooding and erosion.

The Bear Creek Watershed is home to two main channels-the Big Bear Creek and Little Bear Creek. The Big Bear Creek flows through the cities of Keller and Fort Worth, while Little Bear Creek runs through the cities of Euless and Hurst. Both channels play a vital role in maintaining the ecological balance of the watershed. The Big Bear Creek is a large, perennial stream that originates in the northern part of Tarrant County and flows southward for approximately 28 miles before joining the West Fork of the Trinity River. The channel is characterized by deep pools, riffles, and runs, and provides habitat for a variety of aquatic species, including fish, insects, and amphibians. Little Bear Creek, on the other hand, is a smaller, intermittent stream that flows for approximately 10 miles before joining the Trinity River. The channel is characterized by a shallow gradient, and its flow is dependent on rainfall events. Despite its smaller size, Little Bear Creek provides important habitat for several aquatic species, including the endangered Texas blind salamander. Both channels have experienced changes in their hydrology due to urbanization and development in the watershed. The construction of impervious surfaces, such as roads and buildings, has increased the volume and velocity of stormwater runoff, which can lead to erosion and sedimentation in the channels. In addition, the alteration of natural land cover has led to changes in the water quality and temperature of the streams, which can have adverse effects on aquatic species. Efforts have been made to mitigate the impacts of urbanization on the Big Bear Creek and Little Bear Creek. The development of stormwater management

practices, such as detention ponds and green infrastructure, can help to reduce the volume and velocity of stormwater runoff, which can help to prevent erosion and sedimentation in the channels. In addition, efforts to restore natural land cover and improve water quality can help to create a more sustainable and resilient watershed.

Figure 2 Main Bear Creek channel

In this thesis, we focus on the Bear Creek main channel, which is downstream from the urban area that has undergone significant land use changes, urbanization, and industrialization. These development activities can lead to changes in the hydrology of the stream and exacerbate soil erosion and flooding, potentially causing significant damage to infrastructure and property

downstream. Some recent site visits conducted across the channel show bank erosion and debris accumulation in the channel shown in **Figures 2 and 3.**

Figure 3 Site visit, Bear Creek main channel

We aim to develop a flood depth and inundation model using the HEC-RAS software to simulate the influence of urbanization, land use changes, and airport activities like development of supporting infrastructure and conversion of vegetated and forest areas to urbanized regions on flooding and soil erosion in the main Bear Creek channel. To develop an accurate flood inundation

erosion model, it is important to understand the factors that contribute to flooding and soil erosion in urban areas. One major factor is land use changes. In many urban areas, land use changes can lead to increased impervious surfaces, such as roads and buildings, which can alter the hydrology of streams and rivers and lead to increased soil erosion and flooding. Additionally, human activities such as construction and development can also disturb the soil, making it more susceptible to erosion. Industrial activities like construction of supporting infrastructure, manufacturing unit water disposal and other associated with airports can have a significant impact on the hydrology of streams and rivers, altering the flow regime and increasing the risk of flood and soil erosion. In the case of the main Bear Creek channel, the nearby airport could be a significant contributor to high flood depths at the downstream location of the channel. To model flood inundation and soil erosion accurately in the main Bear Creek channel, we will use the HEC-RAS software. HEC-RAS (Hydraulic Engineering Center's River Analysis System) is a widely used software package for hydrologic and hydraulic modeling that can simulate the flow and sediment transport in rivers and streams. Using HEC-RAS, we will develop a hydraulic model that can predict the impact of urbanization, land use changes, and airport activities on flooding in the main Bear Creek channel. The model will further be used to capture the soil erosion throughout the channel, but it has not been added to this report as it requires more analysis.

The use of ArcGIS proved to be an invaluable tool throughout our research. Its geospatial data processing capabilities enabled us to manipulate and analyze various geographical and environmental data relevant to our study area. Additionally, we employed Arc-Hydro, an extension specifically designed for basin delineation, to assist in accurately defining the boundaries of the basins under investigation. This delineation process is vital as it allows us to establish the specific areas from which water flows into a particular point of interest. The seamless integration of these

software tools provided us with a comprehensive and robust framework for conducting our research. By combining the hydrologic modeling capabilities of HEC-HMS, the hydraulic analysis capabilities of HEC- RAS, and the geospatial data processing features of ArcGIS, we were able to achieve a comprehensive understanding of the water flow dynamics within our study area. Through these combined efforts, we gained valuable insights into the behavior of water within our study area, which will contribute to improved flood management strategies and hydraulic structure design.

CHAPTER 2 METHODOLOGY

The methodology employed in this study aimed to assess the impact of `urbanization and development on the river flow regime. The study utilized flow and stage data obtained from the USGS gauge located at Bear Ck, Shady Grove Rd, Grand Prairie, TX – 0804956950 as shown in **Figure 4.** 2017 and 2022 have been selected for modelling scenarios due to factors – The gauge data for comparison is available from 2015 onwards. The rainfall from 2022 which has 8.01 in of total accumulation and had caused major water clogging within the DFW area, the channel flow regime from such rainfall is an interesting observation that can help us understand core areas which may require water resource management solutions. 2017 was selected as it had 35 inches of total accumulation for the entire year which was the lowest total accumulation in the decade. 2017 was a hot year with less rainfall and so it was selected for modelling.

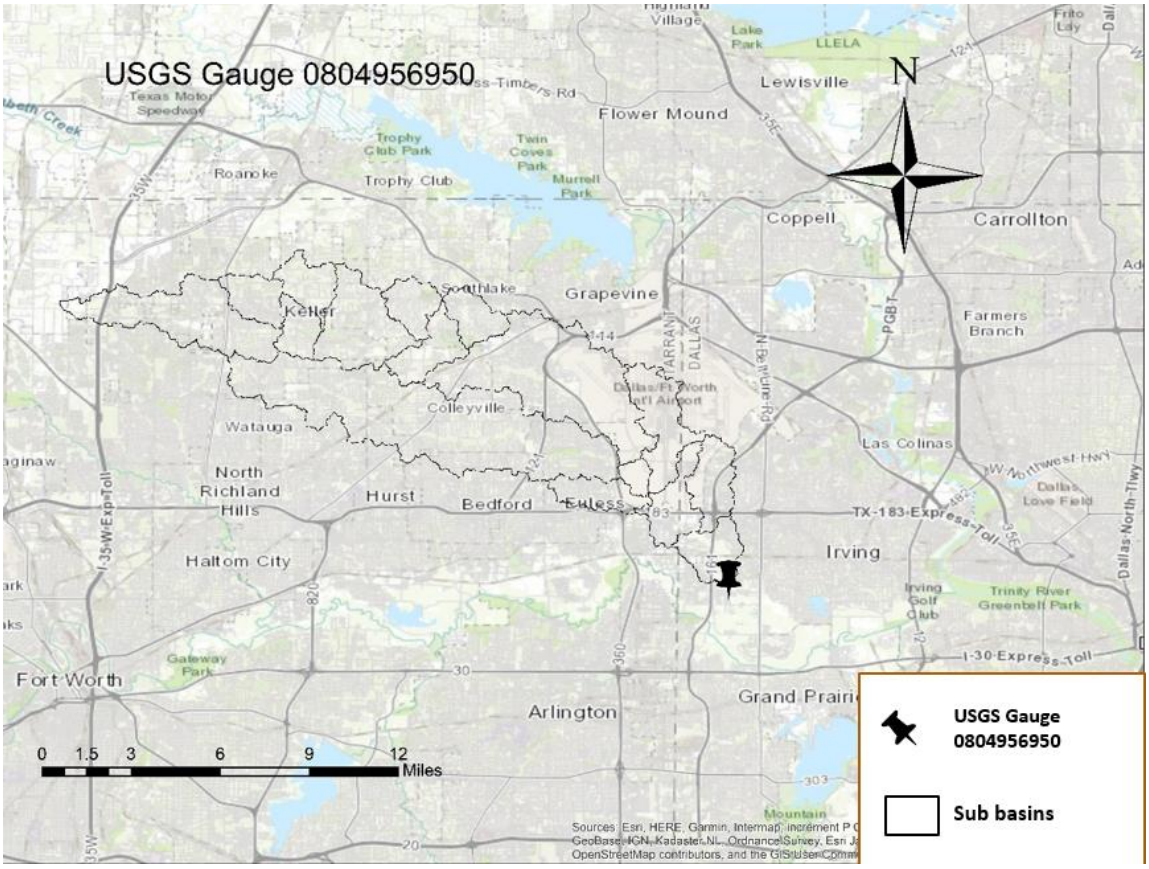

Figure 4 USGS Gauge 0804956950

This gauge served as the downstream boundary control point for both the HMS (Hydrologic Engineering Center's Hydrologic Modeling System) and HEC-RAS (Hydrologic Engineering Center's River Analysis System) models.

To evaluate the effects of urbanization, the study focused on two different years, namely 2017 and 2022. For each year, the two rainfalls with the highest total accumulation were selected for analysis. The observed flow data from the gauge was used to calibrate the HMS model separately for each year.

In the HMS model, the infiltration process was modeled using initial and constant loss parameters. The GSSURGO (Gridded soil survey geographic database) from NRCS (Natural Resources Conservation Services) soil data provided soil type information used to calculate the

constant rate, while the NLCD (National Land Cover Database) imperviousness data assigned imperviousness values to the model. Basin average calculations were performed on ArcGIS to obtain parameter values for each basin.

The Muskingum-Cunge method was implemented to model routing in reaches within the HMS model. Relevant data from the 1D steady flow HEC-RAS model of the city of Grapevine was gathered to fill the parameters for the Muskingum-Cunge method. The remaining parameters were directly taken from the CDC HMS model, including the SCS (Soil Conservation Service) Unit hydrograph transform method and the recession constant baseflow method.

After careful calibration and matching of the simulated flow with the observed flow at the gauge location, the data was extended to the HEC-RAS model to simulate the rainfall events and determine the depth and inundation boundary within the Bear Creek channel. For the HEC-RAS 1D/2D coupled simulations, the 3GEP 1m DEM (Digital Elevation Model) file was clipped to include only the study area. The 1D steady flow HEC-RAS model from the city of Grapevine provided the cross-sections for the main Bear Creek channel, while the 3GEP 1m DEM file served as the base for modeling the 2D flow areas. The 2D flow areas were combined with the 1D cross-sections using lateral structures.

The model was then simulated using the same rainfall events for both 2017 and 2022 and further calibrated to match the stage measurements at the most downstream cross-section.

By implementing this methodology, the study aimed to analyze the impact of urbanization and development on river channel hydraulics and map the flood inundation boundary within the Bear Creek watershed. **Figure 5** shows a concise workflow methodology to find the answer to our research.

Figure 5 Methodology workflow

Data and Software

HEC-HMS

HEC-HMS, which stands for Hydrologic Modeling System, is a software tool developed by the U.S. Army Corps of Engineers' Hydrologic Engineering Center (HEC) [33]. It is specifically designed to model and analyze hydrologic processes in watersheds. HEC-HMS provides a comprehensive platform for constructing hydrologic models, simulating rainfall-runoff processes, and evaluating the behavior of water within a watershed. The primary use of HEC-HMS is to simulate and predict the response of watersheds to various precipitation events. It allows users to input meteorological data, such as rainfall and temperature, and analyze how these inputs interact with the watershed's characteristics, including topography, soil types, land use, and vegetation. HEC-HMS uses various methods to simulate the hydrologic processes, such as rainfall excess, evapotranspiration, snowmelt, infiltration, and runoff generation.

Initial Constant Loss method

HEC-HMS offers several methods for rainfall-runoff modeling. One widely used method is the Initial and Constant Loss method. This method considers two components: the initial abstraction, which represents the water retained on the land surface before runoff begins, and the constant loss, which represents the ongoing losses due to infiltration, evaporation, and other processes. By estimating these components, the Initial and Constant Loss method helps to predict the volume and timing of runoff generated from a rainfall event.

$$TotalLoss = InitialLoss + (ConstantLoss * Rainfall)$$

where:

Total Loss is the cumulative amount of rainfall lost before runoff generation.

Initial Loss is the amount of rainfall that is lost at the beginning of the storm event.

Constant Loss is a fraction or coefficient representing the ongoing loss of rainfall as the storm event progresses.

Rainfall is the total amount of rainfall received.

In the context of imperviousness, it is used in the initial and constant loss method to represent the proportion of the catchment area that is covered by impermeable surfaces such as roads, buildings, and pavements. Impervious surfaces do not allow water to infiltrate into the soil and can significantly affect the hydrologic response of a catchment. The imperviousness value is assigned to the catchment or sub-catchment areas in the hydrologic model. It is used to estimate the portion of rainfall that directly becomes surface runoff without infiltration. Higher imperviousness values indicate a greater amount of runoff generated from the rainfall. The imperviousness value is typically obtained from land cover datasets, such as the NLCD (National Land Cover Database), which provide information on the land cover types and their corresponding imperviousness percentages.

Muskingum-Cunge method

Another commonly used method in HEC-HMS is the Muskingum-Cunge routing. This routing method is employed to analyze the flow of water in rivers and channels. It considers parameters such as reach length, channel slope, channel rough- ness, and storage characteristics to simulate the movement of water through a river reach. By applying the Muskingum-Cunge routing

method, HEC-HMS enables users to assess flow velocities, water levels, and flow hydrographs along river channels.

The Muskingum-Cunge routing equation can be expressed as follows:

$$Q(t) = (1 - K) * Q(t - t) + \left(\frac{K}{2}\right) * \left(S(t) + S(t - t)\right) + \left(\frac{t}{2 * Tc}\right) * \left(\frac{dS(t)}{dt} - \frac{dS(t - t)}{dt}\right)$$

where:

Q(t) is the outflow discharge at time t.

Q(t-t) is the previous time step's outflow discharge at time t-t.

K is the storage coefficient, representing the proportion of flow that remains in the reach at each time step. It ranges from 0 to 1, with higher values indicating greater storage and slower flow.

S(t) is the channel storage at time t.

S(t-t) is the previous time step's channel storage at time t-t.

Tc is the travel time or routing time parameter, representing the time it takes for water to travel through the reach.

t is the time step interval.

dS(t)/dt and dS(t-t)/dt are the rates of change of channel storage at time t and t-t, respectively.

SCS Unit hydrograph method

The Soil Conservation Service (SCS) unit hydrograph is a widely used method for estimating the runoff hydrograph resulting from a rainfall event. It assumes that the excess rainfall from a storm is uniformly distributed over the watershed and that the runoff response is linear and time-invariant. The SCS unit hydrograph is particularly useful for small to medium-sized watersheds.

The SCS unit hydrograph can be described by the following formula:

$$Q(t) = (P - Ia) * (U * S) * (1 - e^{(-\frac{t}{T})})$$

where:

Q(t) is the runoff discharge at time t.

P is the rainfall intensity in inches per unit time.

Ia is the initial abstraction, which represents the amount of rainfall that is retained or absorbed by the watershed before runoff begins.

U is the unit hydrograph peak discharge per unit of excess rainfall.

S is the unit hydrograph storage coefficient, representing the fraction of excess rainfall that becomes direct runoff.

e is the base of the natural logarithm (approximately 2.71828). t is the time since the start of the rainfall event.

T is the time of concentration, which represents the time it takes for the

Run off to travel from the farthest point in the watershed to the outlet.

The SCS unit hydrograph assumes that the excess rainfall is converted into direct runoff with a certain lag time and that the shape of the resulting hydrograph follows a specific pattern. The U-S curve represents the relationship between the peak discharge and the total volume of excess rainfall. The SCS unit hydrograph method is commonly used for hydrological modeling and design of hydraulic structures. It provides a simplified representation of the runoff response in a watershed, allowing engineers and hydrologists to estimate the peak flows and runoff volumes associated with different storm events. However, it is important to note that the SCS unit hydrograph method has certain limitations and assumptions, and its applicability may vary depending on the characteristics of the watershed and the storm event being analyzed.

Recession Baseflow method

Additionally, HEC-HMS incorporates the recession baseflow method. This method is employed to estimate the baseflow component of streamflow during dry periods when there is minimal or no rainfall. It utilizes recession analysis to separate the baseflow component from the total streamflow, providing insights into the groundwater contribution to streamflow.

The formula for the recession baseflow method can be expressed as:

$$Q(t) = Qb * e(-a * t)$$

where:

$Q(t)$ is the streamflow at time t.

Qb is the baseflow, which is the streamflow sustained by groundwater discharge.

a is the recession constant, representing the rate at which baseflow depletion occurs.

e is the base of the natural logarithm (approximately 2.71828) and t is the time since the start of the recession period.

The recession baseflow method assumes that baseflow depletion occurs at a constant rate, represented by the recession constant a. The exponential decay function captures the gradual decrease in streamflow during dry periods, reflecting the slow response of groundwater systems. In summary, HEC-HMS is a versatile software tool for hydrologic modeling and analysis. Its uses include simulating rainfall-runoff processes, predicting watershed response to precipitation events, and evaluating the behavior of water within a watershed. The software employs various methods, such as the Initial and Constant Loss method, Muskingum-Cunge routing, Snyder unit hydrograph transform, and recession baseflow method, to facilitate accurate and comprehensive hydrologic modeling and analysis.

HEC-RAS (Hydrologic Engineering Center's River Analysis System)

HEC-RAS, short for Hydrologic Engineering Center's River Analysis System, is a widely used software developed by the U.S. Army Corps of Engineers [34]. It serves as a powerful tool for hydraulic modeling and analysis of river systems, channels, and floodplains. HEC-RAS offers a comprehensive set of features that enable engineers, hydrologists, and researchers to simulate and study the flow of water in rivers and evaluate the associated hydraulic conditions. The software allows users to input topographic and geometric data of the river system, including cross-sectional profiles, channel roughness, and bridge or culvert structures. One of the primary uses of HEC-RAS is the analysis and prediction of river flow parameters. velocities, and discharges at various cross-sections along the river. This information is crucial for understanding the potential impacts of flooding, designing hydraulic structures, and assessing flood risk in a given area. HEC-RAS also offers capabilities for unsteady flow analysis, which allows users to evaluate the changing flow conditions over time. This is particularly useful for predicting and studying flood events, as it considers variations in flow rates, river stages, and the interaction between inflows and outflows at different locations along the river system. Furthermore, HEC-RAS supports the analysis of bridge and culvert hydraulics. The software can model the flow through these structures and assess factors such as backwater effects, flow velocities, and potential scour at the bridge piers. This information helps engineers in designing and evaluating the hydraulic performance of bridges and culverts. Additionally, HEC-RAS integrates with other software tools, such as HEC-HMS and GIS platforms, to enhance its capabilities. It can receive input from HEC-HMS hydrologic models, allowing for a more comprehensive analysis of the entire hydrologic cycle. Integration with GIS platforms facilitates the import and visualization of geospatial data, aiding in the accurate representation of the river system and its surroundings. In summary, HEC-RAS is a powerful

hydraulic modeling software used for analyzing and predicting the behavior of river systems. Its features enable users to simulate flow, estimate water levels, velocities, and discharges, evaluate flood risk, and design hydraulic structures. HEC-RAS plays a crucial role in flood management, hydraulic engineering, and the assessment of water resources in riverine environments.

The diffusion wave equation is a mathematical equation used to describe the movement of water in open channels during unsteady flow conditions. It is a simplified form of the Saint-Venant equations, which are commonly used in hydraulic modeling. Below each dynamic fluid movement equations are discussed which have been used to model flow from separate rainfalls onto the overland and through the main river channel eventually.

The diffusion wave equation can be expressed as:

$$dQ/dt + a * dA/dx = 0$$

where:

dQ/dt represents the partial derivative of the flow rate with respect to time, which represents the rate of change of flow over time.

a is the wave celerity or wave speed parameter, which relates to the characteristics of the channel and the flow.

dA/dx represents the partial derivative of the cross-sectional area with respect to the longitudinal distance x, which represents the rate of change of the channel cross-sectional area along the channel length.

The diffusion wave equation describes the movement of water in an open channel by considering the changes in flow rate and channel cross-sectional area. It accounts for the effects of dispersion and attenuation of flow waves as they propagate through the channel. The wave celerity parameter a represents the speed at which disturbances or waves travel through the channel. It

depends on the channel geometry and the hydraulic properties of the flow. The value of a is typically determined using empirical relationships or hydraulic principles based on the channel characteristics. The diffusion wave equation is often used in hydraulic modeling to simulate unsteady flow conditions and predict water levels, flow velocities, and other hydraulic parameters in open channels. It provides a simplified representation of the complex dynamics of flow propagation and attenuation. It is important to note that the diffusion wave equation is an approximation and may not capture all the complexities of flow behavior in all situations. It is most accurate for gradually varying channels and subcritical flow conditions. For more complex flow situations, such as rapidly varying or supercritical flows, more advanced models and equations may be required.

Arc-GIS and Arc-Hydro

ArcGIS is a widely used Geographic Information System (GIS) software developed by Esri. It provides a comprehensive platform for managing, analyzing, and visualizing geospatial data. ArcGIS offers a wide range of tools and functionalities that enable users to work with various types of spatial data, such as maps, satellite imagery, and geospatial databases. One of the primary uses of ArcGIS is geospatial data processing [36]. It allows users to import, manipulate, and analyze different types of geospatial data, including vector data (points, lines, polygons) and raster data (gridded data such as satellite imagery or elevation models). With ArcGIS, users can perform geoprocessing tasks such as data conversion, projection, spatial analysis, and overlay operations to gain valuable insights and make informed decisions.

Arc Hydro is an extension for ArcGIS specifically designed for hydrologic analysis and water resources management. It provides a suite of tools and models to support tasks such as

watershed delineation, stream network generation, flow di- rection and accumulation calculations, and flow path analysis. Arc Hydro greatly simplifies the process of hydrologic modeling and analysis within the ArcGIS environment. The Raster Calculator tool in ArcGIS allows users to perform mathematical operations and analyses on raster datasets. It provides a powerful toolset for combining, manipulating, and deriving new raster layers from existing ones. Users can perform operations such as arithmetic calculations, logical operations, conditional statements, and mathematical functions to create customized raster layers that suit their specific analysis requirements. ArcGIS also offers various tools for plotting and visualizing geospatial data. Users can create maps with multiple layers, apply symbology to represent different attributes, and customize the appearance of map elements. ArcGIS provides options for thematic mapping, labeling, and symbolization to effectively communicate spatial patterns and relationships. Additionally, users can generate graphs, charts, and histograms to visually analyze attribute data associated with spatial features.

HEC-Metvue

HEC-MetVue is a software developed by the U.S. Army Corps of Engineers' Hydrologic Engineering Center (HEC) that serves as a graphical user interface (GUI) tool for accessing meteorological data and generating inputs for hydrologic modeling applications such as HEC-RAS and HEC-HMS [35]. HEC-MetVue provides users with capabilities to download radar rainfall data and utilize GIS-based shapefiles to create gridded precipitation data for HEC-RAS and basin average precipitation for HEC-HMS. One of the key functionalities of HEC-MetVue is the ability to access and download radar rainfall data. Radar data is particularly valuable for hydrologic modeling as it provides high-resolution spatial rainfall information. HEC-MetVue allows users to

connect to radar data sources and retrieve radar precipitation data for a specific area or basin of interest. This radar data can then be used to generate inputs for hydrologic models. HEC-MetVue also integrates GIS capabilities by enabling users to utilize GIS-based shapefiles. Shapefiles are a common format for storing geographic data, and HEC-MetVue leverages this format to form gridded precipitation data for HEC-RAS and basin average precipitation for HEC-HMS. Users can input shapefiles that define the boundaries and attributes of specific geographic features, such as watersheds or sub-basins. HEC-MetVue utilizes these shapefiles to extract relevant meteorological data and generate gridded or averaged precipitation data for hydrologic modeling purposes. By combining radar rainfall data and GIS-based shapefiles, HEC-MetVue allows users to create spatially distributed precipitation inputs for HEC-RAS and basin average precipitation inputs for HEC-HMS. These inputs are crucial for accurately representing the spatial distribution of precipitation within a watershed or river basin, enabling more precise hydrologic modeling and analysis.

GSSURGO Soil data (Gridded soil survey geographic database)

GSSURGO, which stands for Gridded Soil Survey Geographic Database, is a comprehensive dataset developed by the Natural Resources Conservation Service (NRCS) that provides detailed information about soil properties and characteristics across the United States [37]. The GSSURGO data is derived from traditional soil survey maps, which are created through extensive fieldwork and laboratory analysis conducted by soil scientists. It includes attributes such as soil texture, organic matter content, soil depth, soil drainage class, soil pH, and other relevant soil properties.

One of the key features of GSSURGO is its gridded format, which means that the soil information is organized into a grid system covering the entire country. This gridding allows for easier integration and analysis of soil information with other geospatial datasets, making it a valuable resource for various applications.

The GSSURGO data has numerous practical uses. In agriculture, it helps farmers and land managers make informed decisions regarding crop selection, irrigation management, and nutrient application. The detailed soil characteristics aid in identifying suiTable areas for specific crops, understanding soil water holding capacity, and assessing soil fertility.

In engineering and construction projects, GSSURGO data plays a crucial role in site selection, foundation design, and erosion control. Engineers can assess the stability and load-bearing capacity of the soil, identify potential hazards like sinkholes or expansive soils, and develop appropriate erosion prevention strategies.

The dataset also supports environmental planning and natural resource management initiatives. It assists in identifying sensitive areas for conservation efforts, mapping wetlands, assessing soil erosion risk, and guiding land-use planning decisions. GSSURGO data is particularly useful for modeling hydrological processes, predicting runoff, and understanding the impacts of land management practices on water quality.

Moreover, researchers and scientists utilize GSSURGO data for a wide range of studies and analysis. It serves as a valuable resource for analyzing soil patterns, con- ducting soil carbon assessments, studying soil-plant relationships, and investigating the impacts of climate change on soil properties.

Stage IV Radar Rainfall

Stage IV radar rainfall is a type of precipitation estimation method that utilizes weather radar data to estimate rainfall amounts and intensity [38]. It is known as" Stage IV" because it is the fourth generation of radar-based precipitation estimation techniques developed by the National Weather Service (NWS) in the United States. Stage IV radar rainfall combines information from multiple weather radars located within a particular region to create a composite radar image. This composite image provides a more accurate representation of the spatial distribution and intensity of rainfall over a given area. The radar data is processed and calibrated using algorithms to convert radar reflectivity values into estimates of rainfall rates.

The Stage IV radar rainfall data is typically available on a high-resolution grid, covering a specific geographic region. The grid cells represent small areas within the region, and each cell contains an estimated rainfall value. This gridded data allows for a more detailed analysis of precipitation patterns and enables hydrologists and meteorologists to better understand the spatial distribution of rainfall.

Stage IV radar rainfall is widely used for various applications, including flood forecasting, water resource management, and weather analysis. Hydrologists use the data to monitor and forecast river and streamflow, assess the potential for flooding, and make decisions regarding water release from reservoirs. It is particularly valuable in areas where rain gauges are sparsely distributed or where ground-based observations may be limited.

The Stage IV radar rainfall data is also used in weather analysis and forecasting. Meteorologists utilize it to track and monitor storms, identify areas of heavy rainfall, and issue timely warnings for severe weather events such as flash floods. The high spatial and temporal resolution of the data aids in understanding the evolution and movement of weather systems.

Furthermore, Stage IV radar rainfall data is often integrated into hydrological models and systems for improved runoff and flood forecasting. By incorporating the radar-derived precipitation estimates, these models can provide more accurate simulations of river flow, inundation, and other hydrological processes.

3 GEP 1m Digital Elevation Model

The 3GEP 1m Digital Elevation Model (DEM) refers to a high-resolution digital representation of the Earth's surface, specifically the elevation data, with a grid cell size of 1 meter. It is a dataset that provides detailed information about the topography of a given area, including the elevation, slope, and aspect [39].

The 3GEP 1m DEM is created using advanced remote sensing techniques, such as Light Detection and Ranging (LiDAR) technology. LiDAR sensors collect precise elevation measurements by emitting laser pulses and measuring the time it takes for the pulses to return after bouncing off the Earth's surface. These elevation measurements are then processed and interpolated to generate a continuous surface representing the topography.

The high resolution of the 3GEP 1m DEM makes it valuable for various ap- plications, including terrain analysis, hydrological modeling, land use planning, and environmental assessment. It allows for the identification of subtle landforms, the delineation of drainage networks, and the characterization of terrain features.

In hydrological modeling, the 3GEP 1m DEM provides essential input for analyzing water flow, determining catchment boundaries, and estimating runoff patterns. It aids in the identification of potential flood-prone areas, the design of drainage systems, and the assessment of water resource availability.

The 3GEP 1m DEM also supports terrain analysis, allowing for the calculation of slope and aspect, which are crucial for understanding land surface characteristics and processes. It facilitates studies related to landform classification, land cover mapping, and slope stability analysis.

Additionally, the high-resolution 3GEP 1m DEM serves as a foundation for other geospatial analyses and visualizations. It can be used as a base layer for creating 3D terrain models, generating contour maps, and conducting watershed analyses

Methods

Rainfall

In the analysis conducted for the Bear Creek watershed, the rainfall data utilized for the HEC-Metvue model and HEC-RAS simulations was based on basin average rainfall. The rainfall data was obtained from the Rain on Mesh 4km x 4km grid. The process involved overlaying the Stage IV rainfall data over the sub basin shapefile in HEC-Metvue and applying basin average calculations over the shapefile. This approach allowed for the determination of total rainfall accumulation in each sub basin within the watershed. 2017 and 2022 rainfalls were selected for analysis

Figures 6, 7, 8, and 9 in the analysis showcase the total rainfall accumulation over the sub basins in the Bear Creek watershed. These Figures highlight the highest total accumulation of rainfall observed in the respective years. The choice of these rainfalls was based on their significant accumulation compared to other years.

In particular, the year 2017 was relatively hotter and experienced lower rainfall compared to other years. In contrast, the year 2022 witnessed one of the largest rainfalls with a total accumulation of 8.01 inches. This information provides valuable insights into the rainfall patterns and extremes observed in the Bear Creek watershed during these specific years.

By adopting this methodology and considering the selected rainfalls, a comprehensive analysis of the rainfall characteristics and their impact on the watershed can be conducted

Table 1 Rainfall duration and total amount accumulation

Rainfall Duration	Total Accumulation (in.)
06/23/2017-06/26/2017	3.46
12/17/2017-12/20/2017	2.66
08/20/2022-08/22/2022	8.01
11/02/2022-11/05/2022	2.52

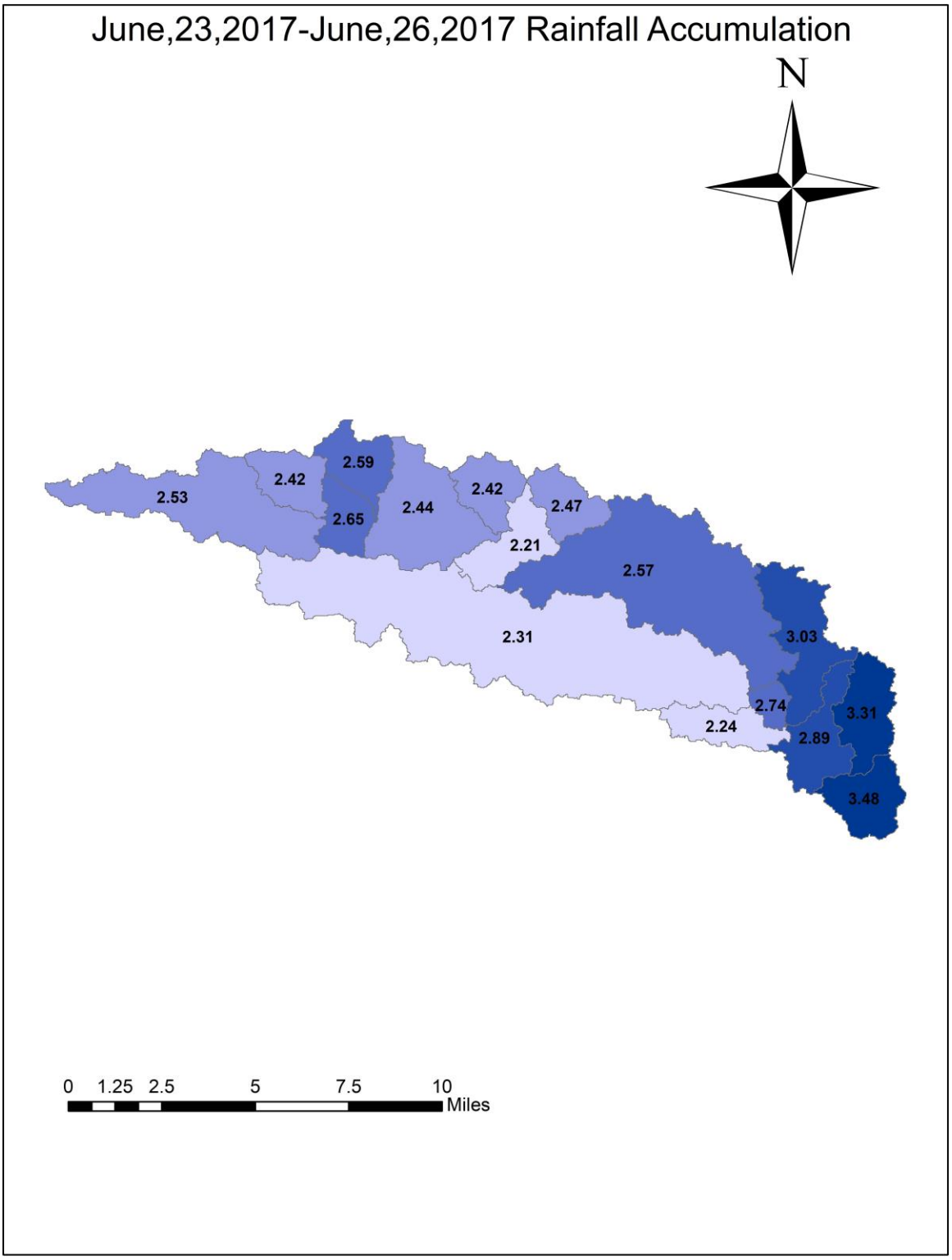

Figure 6 Rainfall Accumulation June, 2017

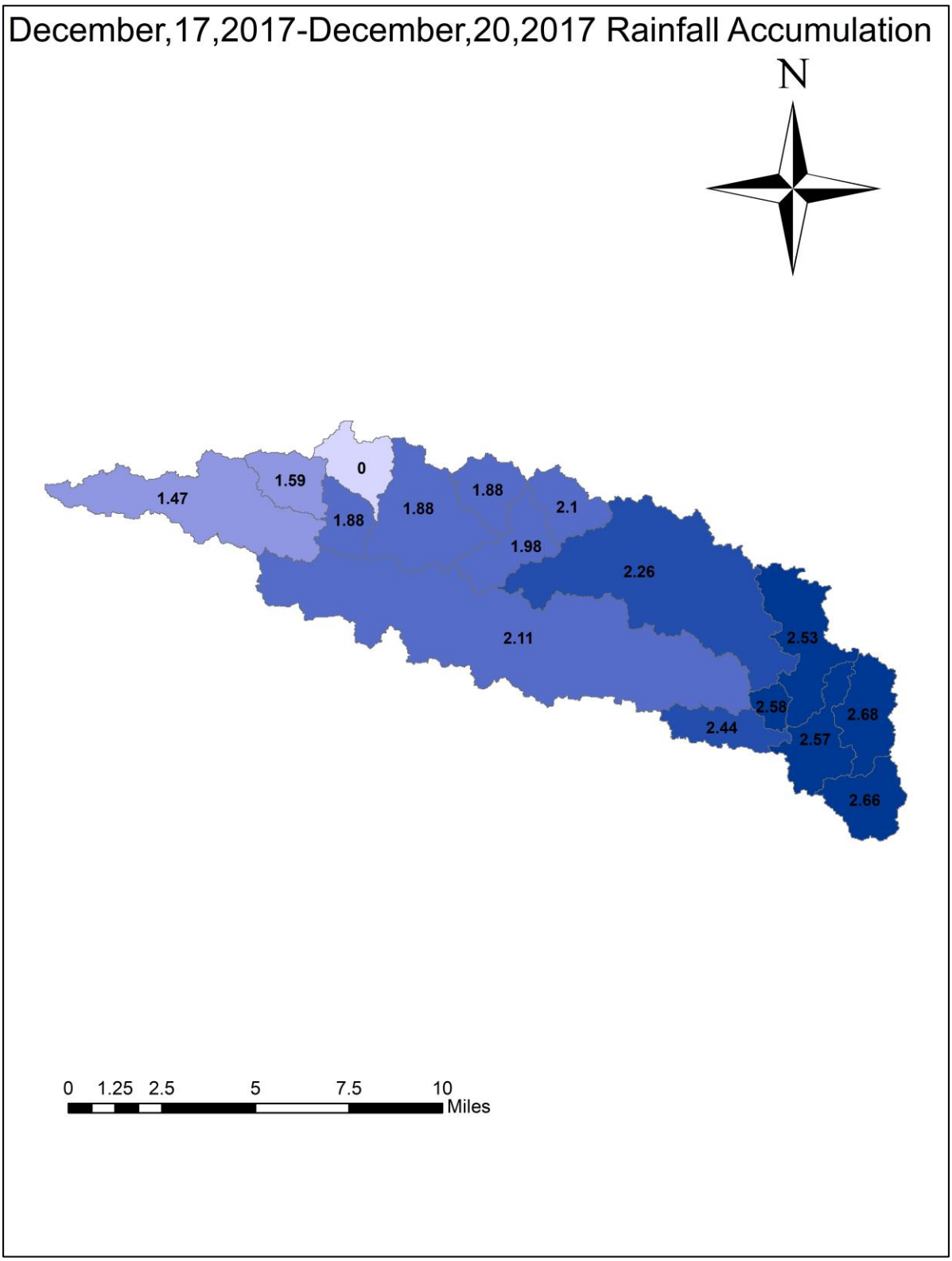

Figure 7 Rainfall Accumulation December, 2017

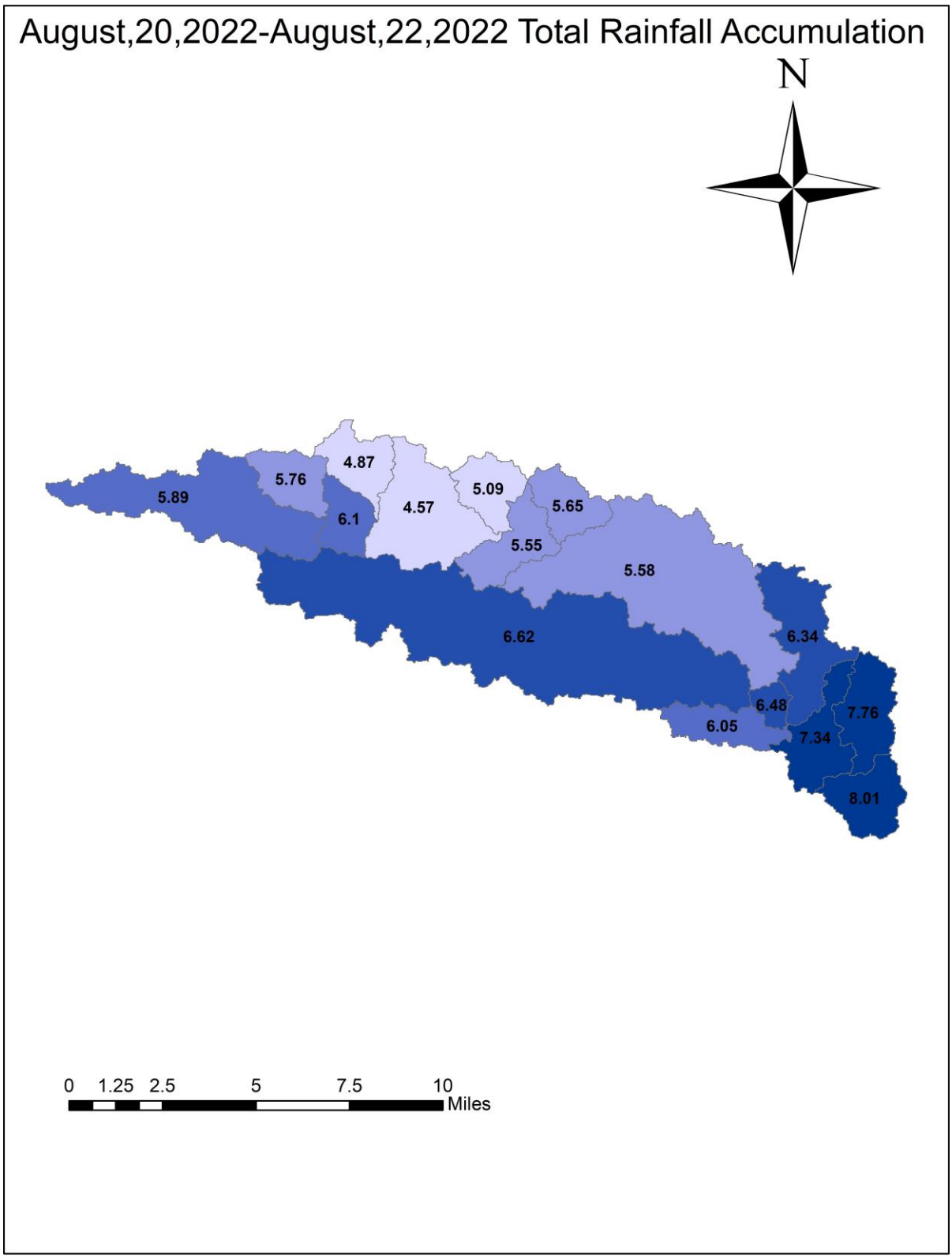

Figure 8 Rainfall Accumulation August, 2022

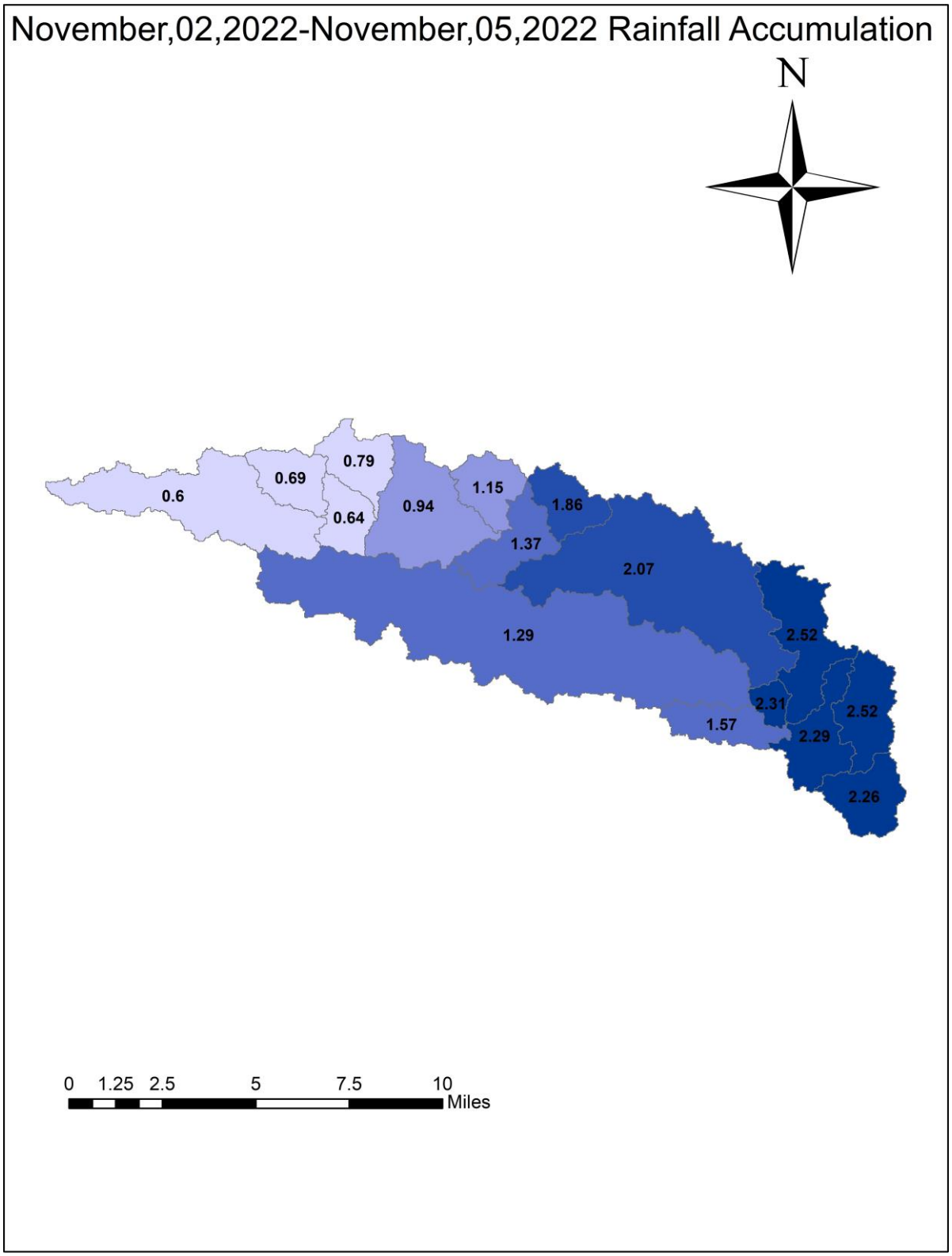

cFigure 9 Rainfall Accumulation, November 2022

HEC-HMS modelling

This section provides information on the implementation method of HEC-HMS model. The model uses physics and probabilistic methods to match runoff generated from specific rainfall events in 2017 and 2022. Stepwise method for creating an HMS model using different parameters is mentioned below.

Data Collection:

1. Use of Arc-hydro to delineate sub-basins from 3GEP DEM file. as shown in **Figure 10**. Basin names has been assigned as shown in **Figure 11**

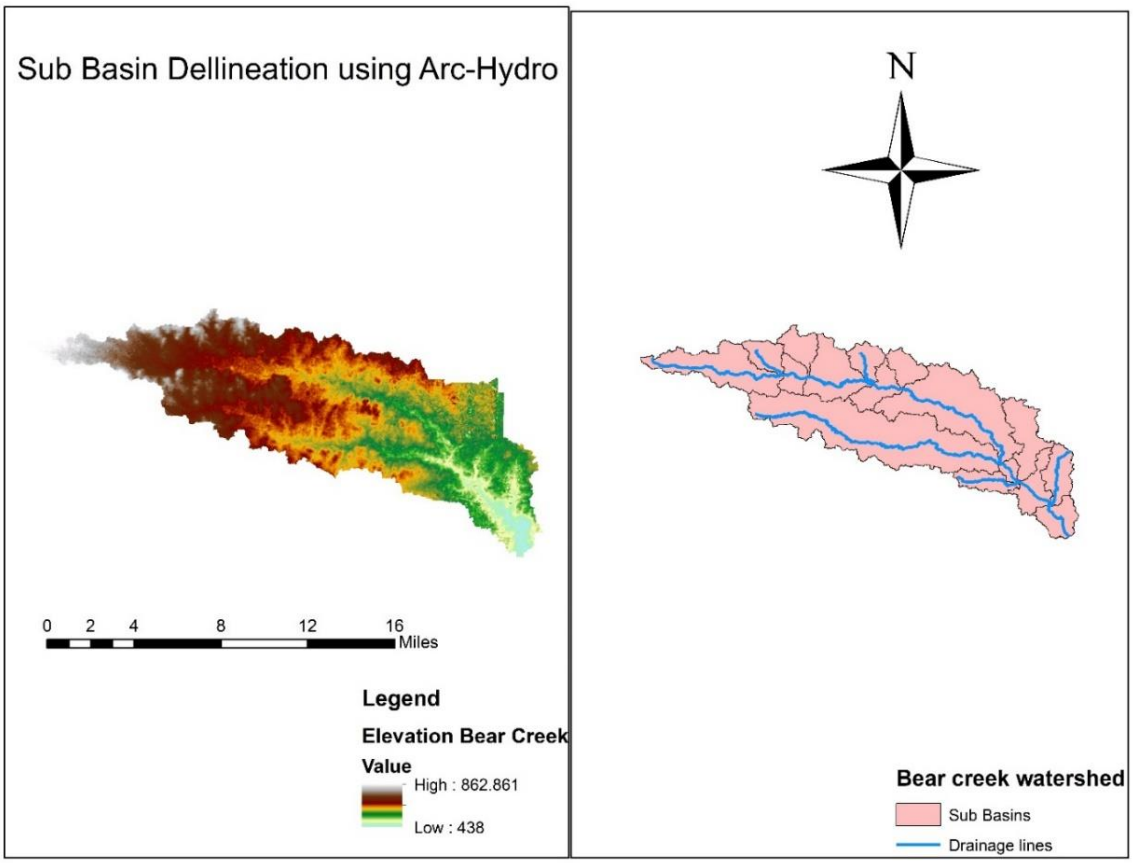

Figure 10 Sub basin delineation using Arc hydro

2. Rainfall has been downloaded from Stage IV radar rainfall from the file transfer protocol software. The rainfalls summarized in the rainfall section have been used for the model. Basin average has been implemented using HEC-Metvue as shown in **Figures 6,7,8,9.**
3. Obtain GGSURGO soil data, which provides information about soil properties such as texture, drainage, and organic matter content.
4. Acquire NLCD imperviousness data, which identifies the percentage of impervious surfaces in the study area.
5. Zonal statistics in ArcGIS is to find basin average for each basin in the Bear Creek watershed shapefile for all parameters applied.
6. SCS unit hydrograph transform method and recession constant method parameters have been directly taken from the CDC HEC-HMS model. Values used for SCS unit hydrograph transform parameters and recession constant parameters are summarized in **Tables 2,3 and 4.**

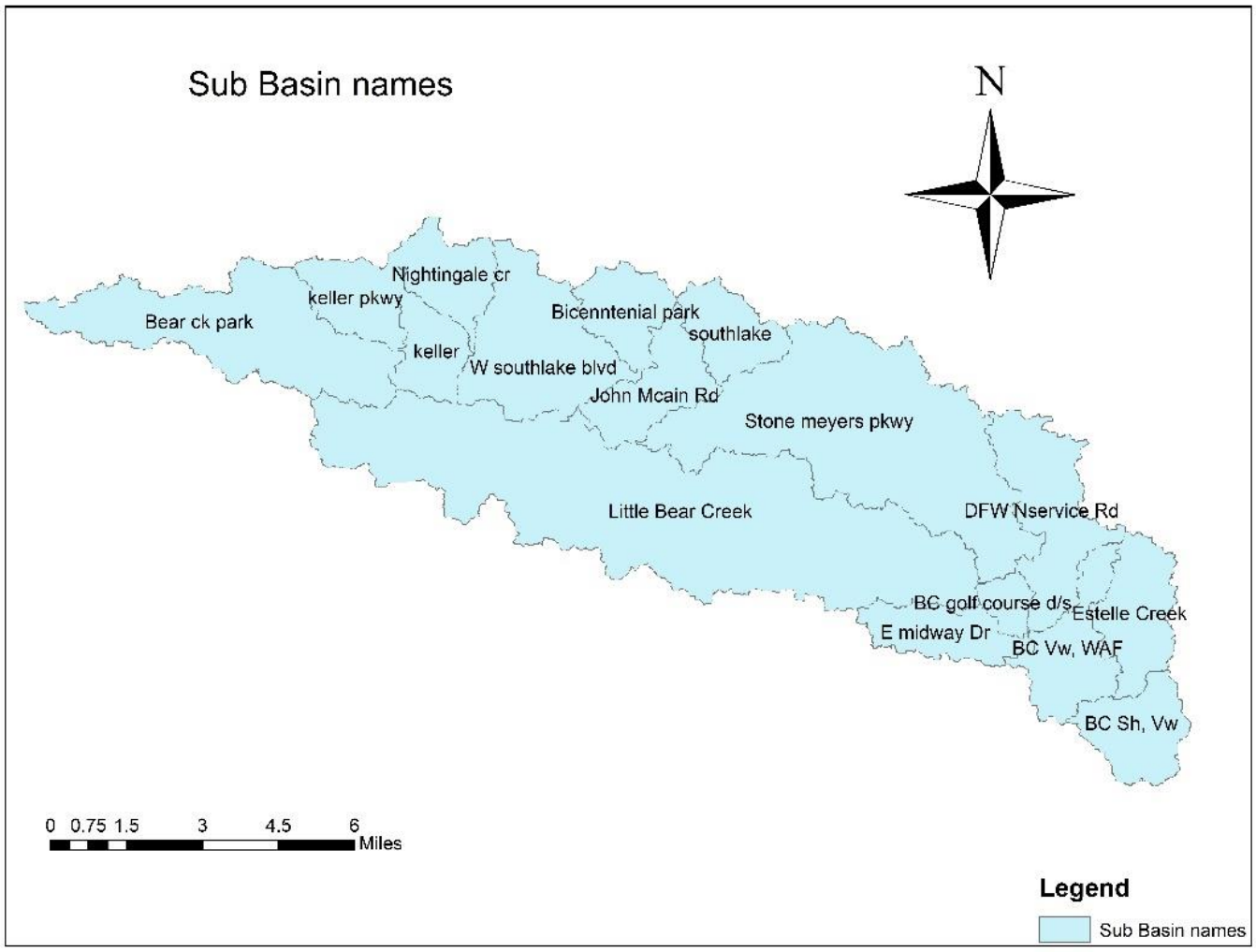

Figure 11 Basin Nomenclature

Table 2 SCS unit hydrograph transform parameters

Sub Basin	Lag-time (min)
Bear Ck park	13.5373
Keller pkwy	11.7123
Nigthingale cr	8.3091
Keller	7.9165
W southlake blvd	8.3424
Bicenntenial park	8.6089
John mcain rd	7.4072
South lake	8.5902
Stone meyers pkwy	9.3843
Little Bear Creek	11.2171
DFW Nservice Rd	8.17435
E midway dr.	8.71354
BC golf course d/s	8.18087
Estelle Creek	8.10014
BC Vw, WAF	7.1993

Table 3 Recession constant parameters 1

Sub basin	Initial Type	Initial Discharge (cfs/mi2)
Bear Ck park	Discharge Per Area	0.02
keller pkwy	Discharge Per Area	0.02
Nigthingale cr	Discharge Per Area	0.02
Keller	Discharge Per Area	0.02
W southlake blvd	Discharge Per Area	0.02
Bicenntenial park	Discharge Per Area	0.02
John mcain rd	Discharge Per Area	0.02
South lake	Discharge Per Area	0.02
Stone meyers pkwy	Discharge Per Area	0.02
Little Bear Creek	Discharge Per Area	0.02
DFW Nservice Rd	Discharge Per Area	0.02
E midway dr.	Discharge Per Area	0.02
BC golf course d/s	Discharge Per Area	0.02
Estelle Creek	Discharge Per Area	0.02
BC Vw, WAF	Discharge Per Area	0.02
BC Sh, Vw	Discharge Per Area	0.01

Table 4 Recession constant parameters 2

Subbasin	Recession constant	Threshold type	Ratio to peak
keller pkwy	0.54	Ratio to Peak	0.02
Nightingale cr	0.54	Ratio to Peak	0.02
Bicenntenial park	0.54	Ratio to Peak	0.02
southlake	0.54	Ratio to Peak	0.02
keller	0.54	Ratio to Peak	0.02
Bear ck park	0.54	Ratio to Peak	0.02
W southlake blvd	0.54	Ratio to Peak	0.01
John Mcain Rd	0.54	Ratio to Peak	0.02
Stone meyers pkwy	0.54	Ratio to Peak	0.02

Little Bear Creek	0.54	Ratio to Peak	0.02
DFW Nservice Rd	0.54	Ratio to Peak	0.02
BC golf course d/s	0.54	Ratio to Peak	0.02
E midway Dr	0.54	Ratio to Peak	0.02
Estelle Creek	0.54	Ratio to Peak	0.02
BC Vw, WAF	0.54	Ratio to Peak	0.02
BC Sh, Vw	0.58	Ratio to Peak	0.02

7. Initial and Constant Loss Parameter:

   Utilize GGSURGO soil data to determine the initial abstraction and constant loss values based on the soil characteristics. A basin average is generated using zonal statistics on Arc-GIS, as shown in **Figure 12 and 13** while constant rate is also calculated similarly using pixel weights of each soil type, constant rate is shown in **Figure 14** and is kept constant throughout the 2 scenarios.

8. Incorporate NLCD imperviousness using zonal statistics, as shown in **Figure 15.**

9. Muskingum-Cunge Routing Parameter:

   Identify the main river channel within the study area and divide it into reach segments. Segmentation of river reach has been accomplished using cross sectional data available to us from the 1d steady flow HEC-RAS model of City of Grapevine. The file contains cross section data for a major portion of the main bear creek channel except the most downstream and the most upstream location. The image of the the entire cross section data is shared in the Appendix A section in Figure. The cross-sectional data is available to us and hence the

associated geometries can be applied to the HMS reaches. All geometrical parameters are copied and reaches are defined in HEC-HMS. Input these channel properties into the HEC-HMS model and assign appropriate Muskingum-Cunge routing parameters derived from the HEC-RAS 1D steady flow file to each reach segment

TableTable 5 Muskingum-Cunge Reach length

Reach	Length (FT)
Reach-1	20171
Reach-2	9148
Reach-3	31391
Reach-4	14905
Reach-5	20426
Reach-6	24224.7
Reach-7	11989.5
Reach-8	8133
Reach-9	7876.5
Reach-10	9394.21

Table

Table 6 Muskingum Cunge reach parameters

Reach	Slope	Manning's n	Width	side slope	Invert
Reach-1	0.00072	0.03	110	0.5	12
Reach-2	0.00032	0.025	105	0.5	12
Reach-3	0.00016	0.03	100	0.5	12
Reach-4	0.00019	0.035	100	0.5	12
Reach-5	0.00049	0.03	65	0.5	10
Reach-6	0.00073	0.03	75	0.5	10
Reach-7	0.00019	0.045	150	0.3	10
Reach-8	0.00027	0.04	64	0.5	6
Reach-9	0.00018	0.04	75	0.5	7
Reach-10	0.0091	0.04	77	0.5	8

10. Calibrate the Muskingum-Cunge parameters using observed flow data, considering the effects of soil properties and imperviousness on the routing process. the parameters are set as per the above methodology and are summarized in **Table 5 and 6**

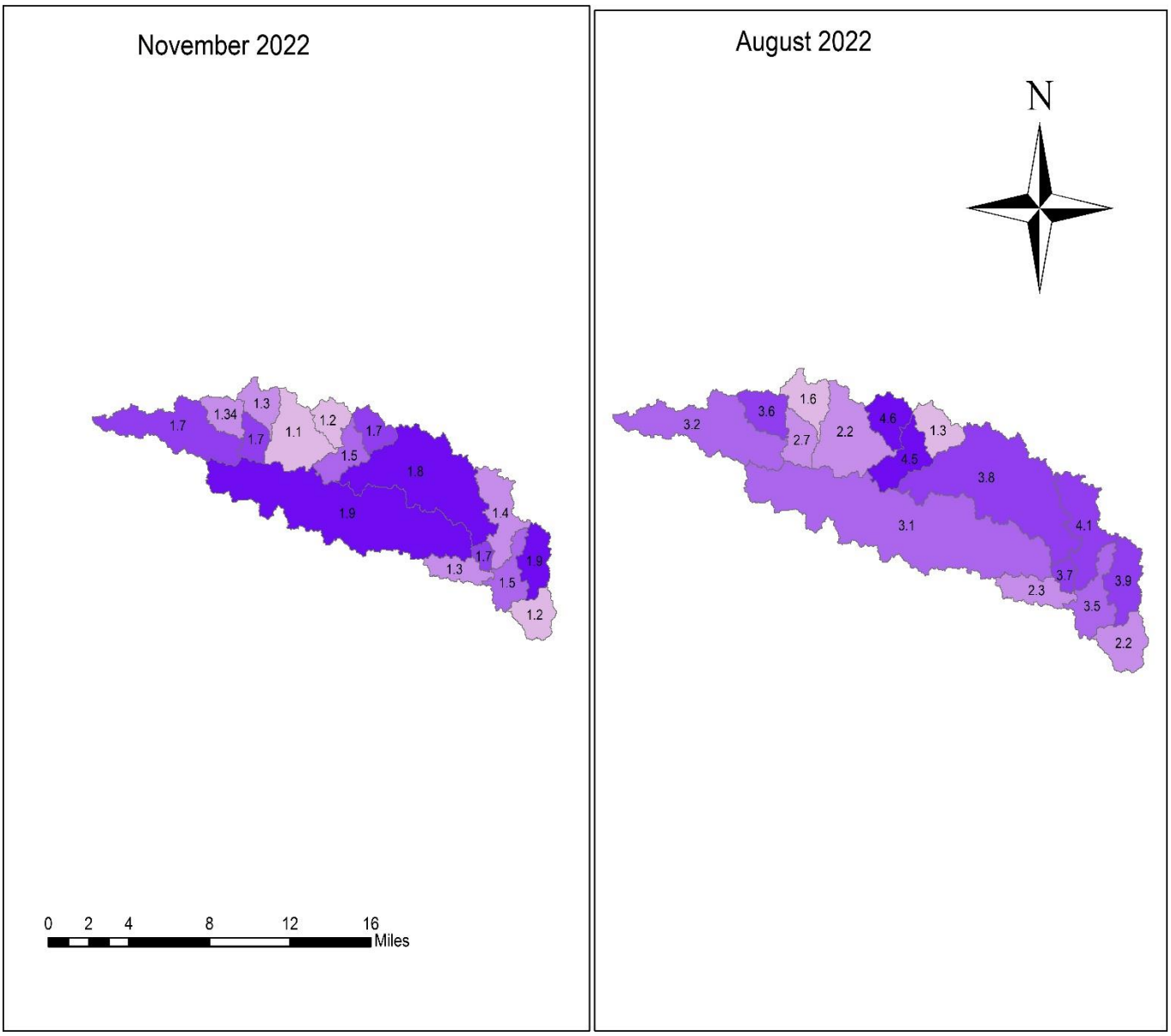

Figure 12 Initial Abstraction 2022

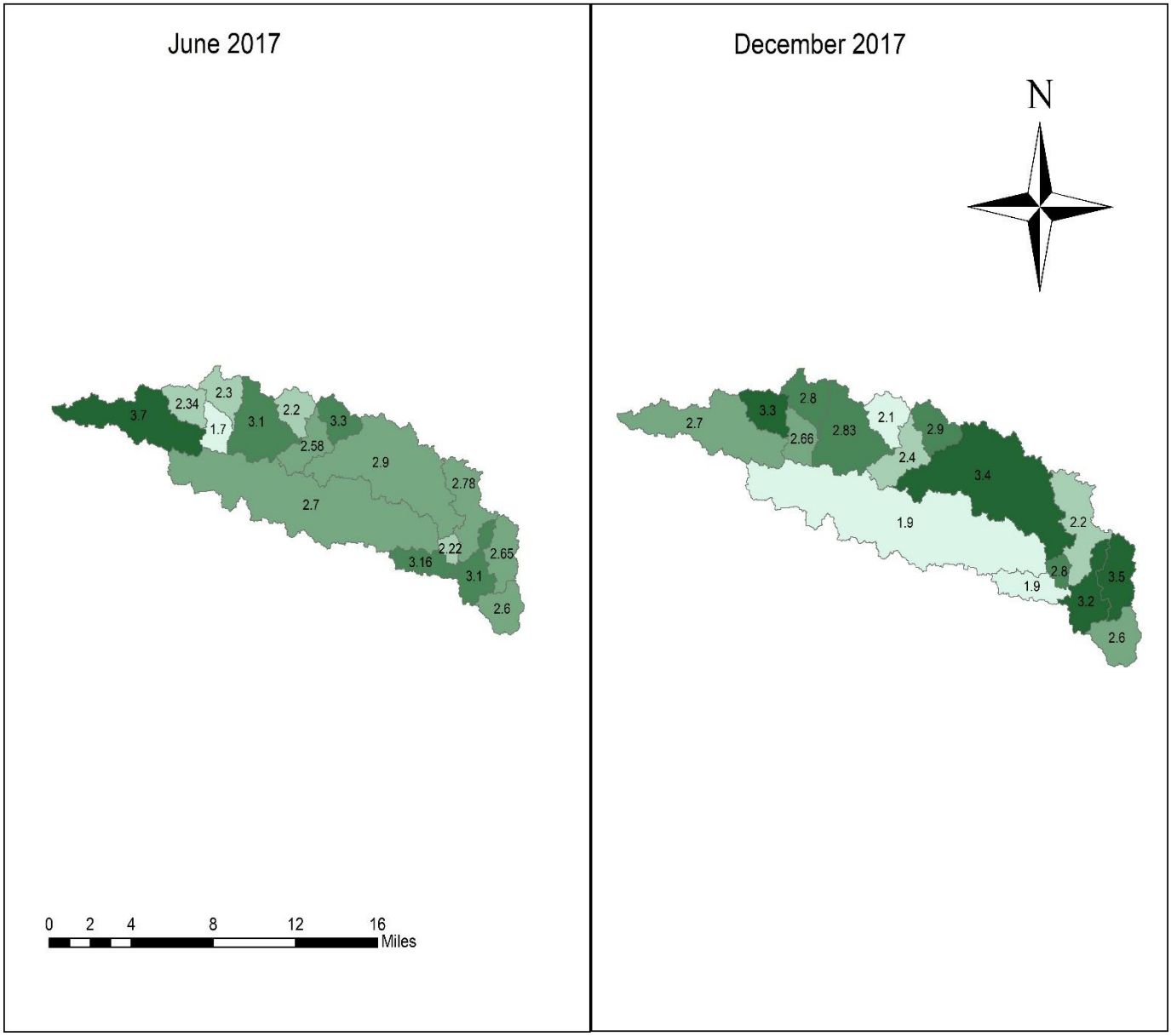

Figure 13 Initial Abstraction 2017

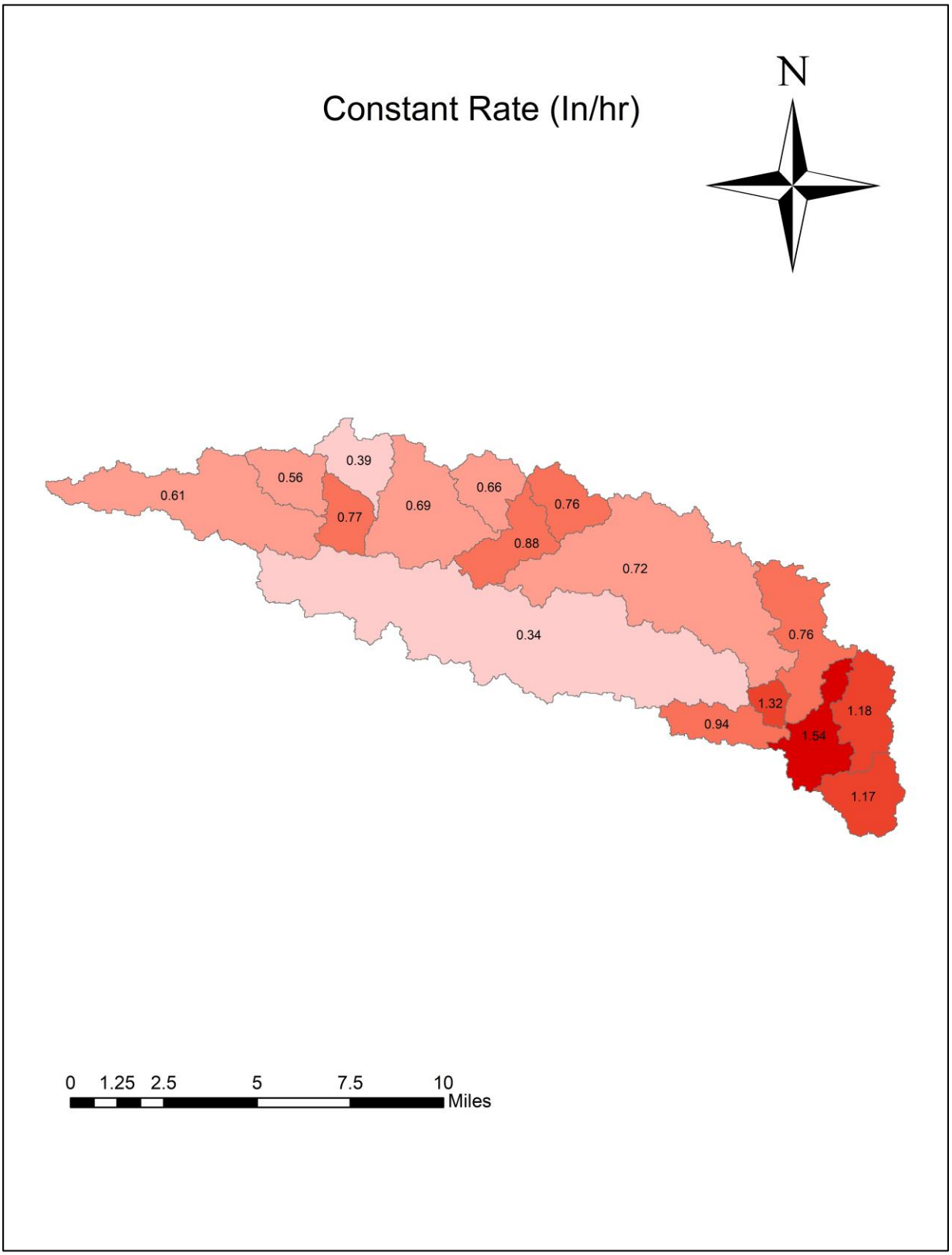

Figure 14 Constant Rate

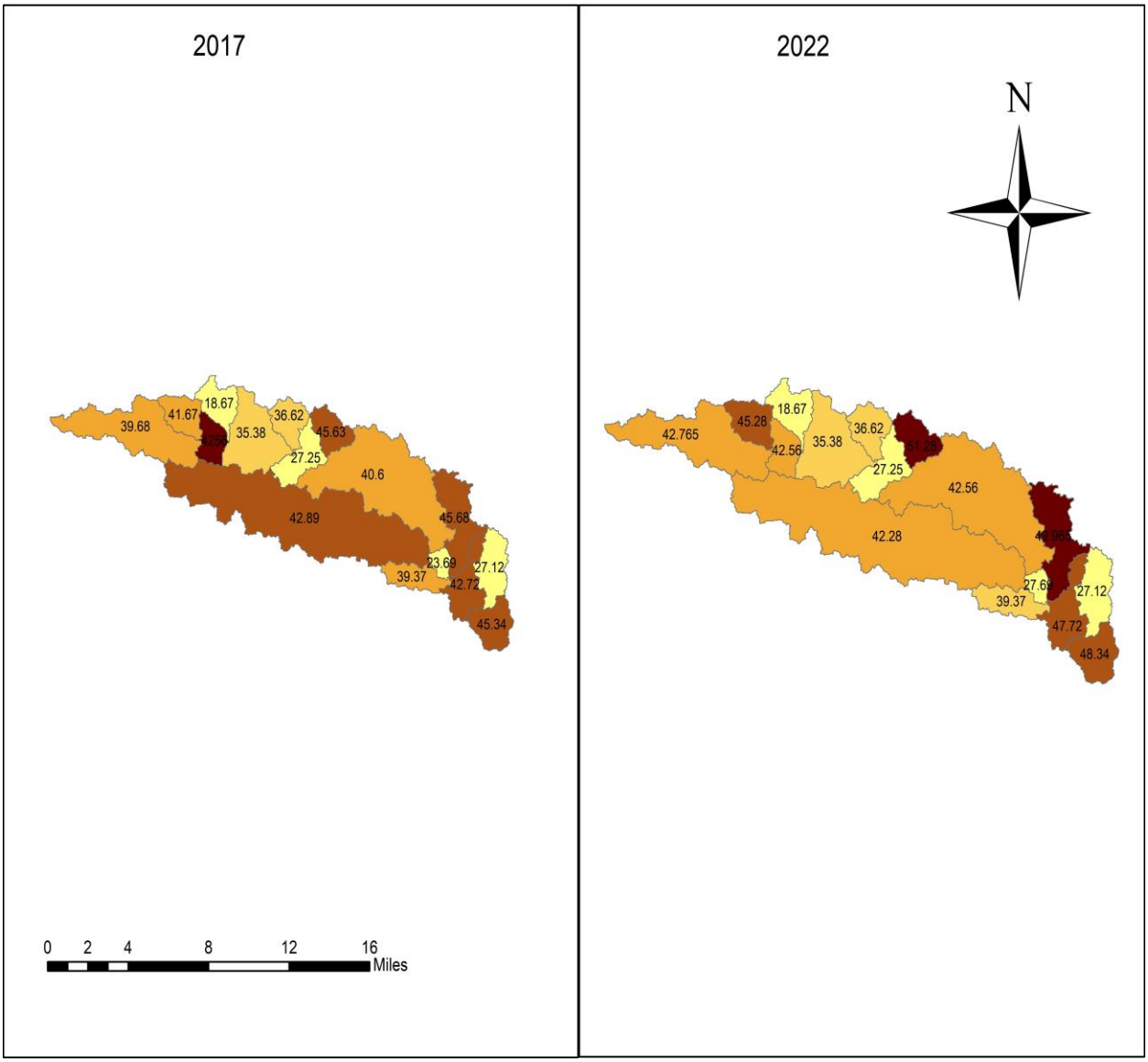

Figure 15 *Imperviousness 2017 and 2022*

A final model is made using the above methodology. **Figure 16** shows the final model image and **Table 7** summarizes the model configuration

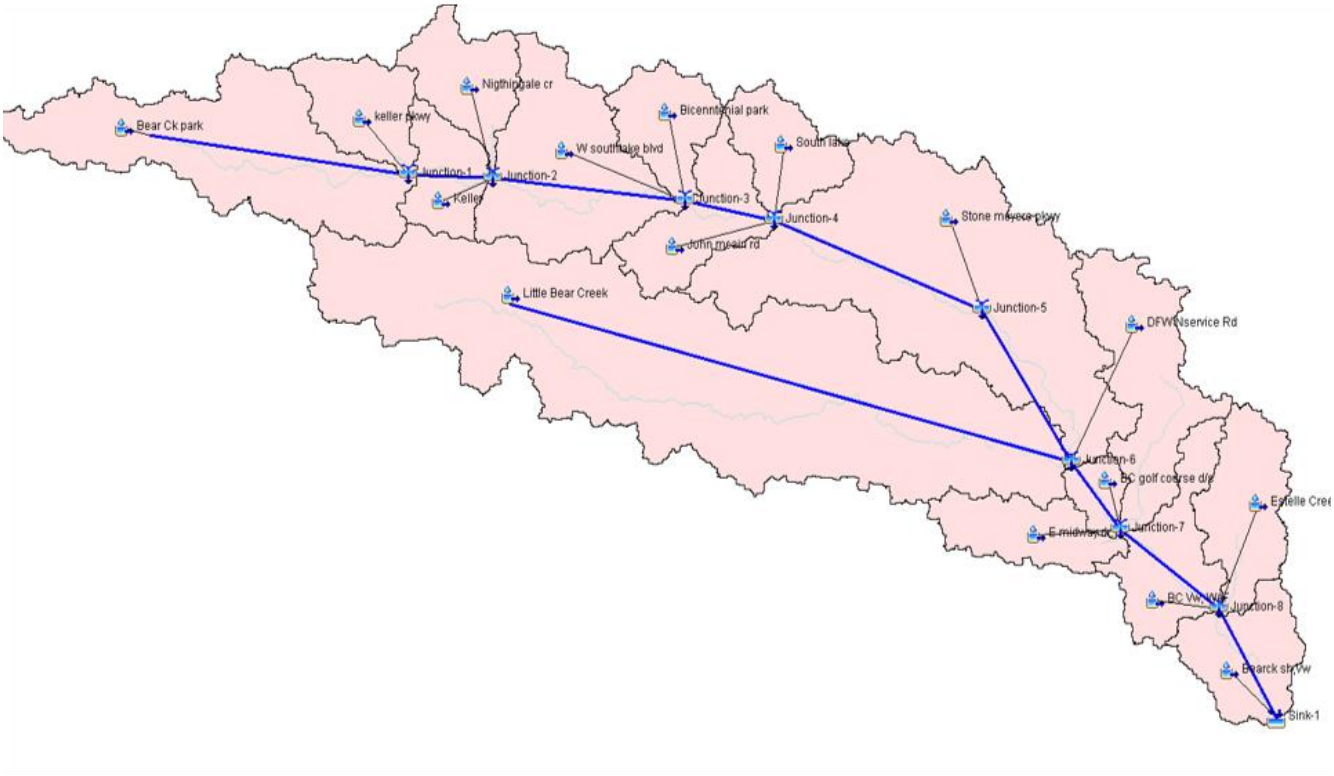

Figure 16 *Final HMS model*

Table 7 HEC-HMS model configuration

Model Configuration	
Sub basins	16
Junctions	8
Sink	1
Reaches	10

11. Model Evaluation and Calibration:

    Evaluate the performance of the HEC-HMS model by comparing the simulated results with observed streamflow data. Adjust the model parameters iteratively, considering the influences of initial abstraction to improve the agreement between simulated and observed hydrographs. Validate the calibrated model by using an independent set of observed streamflow data from USGS gauge 0804956950.

    Refine the model parameters as necessary to enhance the accuracy and reliability of the HMS model.

    Results of calibration are mentioned in the results section.

HEC-RAS modelling

1. To create a HEC-RAS 1D/2D model using a 1D cross-section steady flow file from city of Grapevine, NLCD imperviousness data, and GSSURGO soil data to model infiltration, the following steps were implemented
2. Gather the necessary data: The 1D cross-section steady flow file was taken from the City of Grapevine 1D HEC-Ras steady flow simulations **Figure 17** shows the cross-section file with its geo-referenced location, The cross sections that will be used to model are clipped from the original file. The cross-section details have been added to the Appendix A in the last section. To model infiltration and surface roughness NLCD imperviousness data and GSSURGO soil data for the study area are added as RAS layers on the RAS mapper. The steady flow file contains detailed information about geometry of each cross section and

roughness coefficients. NLCD imperviousness data provides information about land cover types and their associate runoff characteristics, while GSSURGO soil data offers soil properties relevant to infiltration modeling.

3. 2D flow areas have been defined for the study area adjoining the 1D reach given in Table 8 and then connected using lateral structures, details of which are summarized in **Table 9.**
4. The 1D cross section has been extended till the gauge location (USGS 0806954950) to match the observed stage from the gauge with the simulated stage data. The last cross section from the 1D steady flow file is the cross section 38462 while 2 extra cross sections have been added to extend the cross sections namely 33313 and 27811 till the gauge location to match the stage.
5. Incorporated the NLCD imperviousness data by directly importing data into HEC-RAS. This can be done by assigning each land cover type a corresponding Manning's roughness coefficient that represents its runoff characteristics. Modify the roughness coefficients for the corresponding 2D flow area based on the land cover types present in the vicinity of the cross-section. The 2D flow areas have not been modelled accurately due to data redundancy and only serve the purpose of modelling inundation boundary.
6. Integrate the GSSURGO soil data into the model to simulate infiltration. Since Initial and deficit loss has been used, HEC-RAS provides options to incorporate soil properties, such as hydraulic conductivity and initial and maximum loss to model infiltration. Assign the appropriate soil properties to each area within the model domain based on the corresponding soil types from the GSSURGO data.
7. Infiltration and manning's roughness for the 2D are not accurate representatives of the real-world values and hence are not included in the report. Though use of the 2D flow areas

will be essential to model sediment transport from the 2D flow areas into the channel.

8. 2D flow areas are defined across the model domain that are tied to the 1D cross section using lateral structure a weir flow coefficient of 0.2, width of weir 2ft and 10ft of distance from head water location are input into the model geometry.
9. The final model as shown in **Figure 19** is made ready and 4 rainfalls, 2 from 2022 and 2 from 2017 simulations are run to make a running model. **Figure 18** shows the locations the input hydrographs as boundary conditions
10. Calibrate and validate the model: After setting up the model, it is essential to calibrate and validate it using observed data. To compare observed data, we have used stage data from USGS gauge 0804956950.
11. Perform simulations: Once the model is calibrated and validated, the model is used to simulate 100-year rainfall to analyze the effect of urbanization and development

Table 8 2D flow area HEC RAS Model

TableHEC-RAS

2D Flow Area	Manning’n	Area sqft
Airport	0.025	6385.15
Lilbc	0.045	5078.01
Emidway Dr.	0.05	6327.72
klu	0.05	4799.45
Leftdownstream	0.06	5394.1
Right downstream	0.06	5046.85

Table 9 Weir stations and length HEC-RAS model

2D Flow Area	River station	Length (ft)
Airport	74100	745.39
	69000	2845.1
	64000	1151.69
	61000	1575.69
	58710	951.46
	48200	1934.54
Lilbc	74000	1463.56
	71420	1073.71
	70305	1310.7
	67500	1442.78
Emidway Dr.	54800	1740.29
	50900	1932.3
	48300	1934.54
klu	42400	1000.45
Leftdownstream	37010	10396.3
Rightdownstream	37000	10056.7

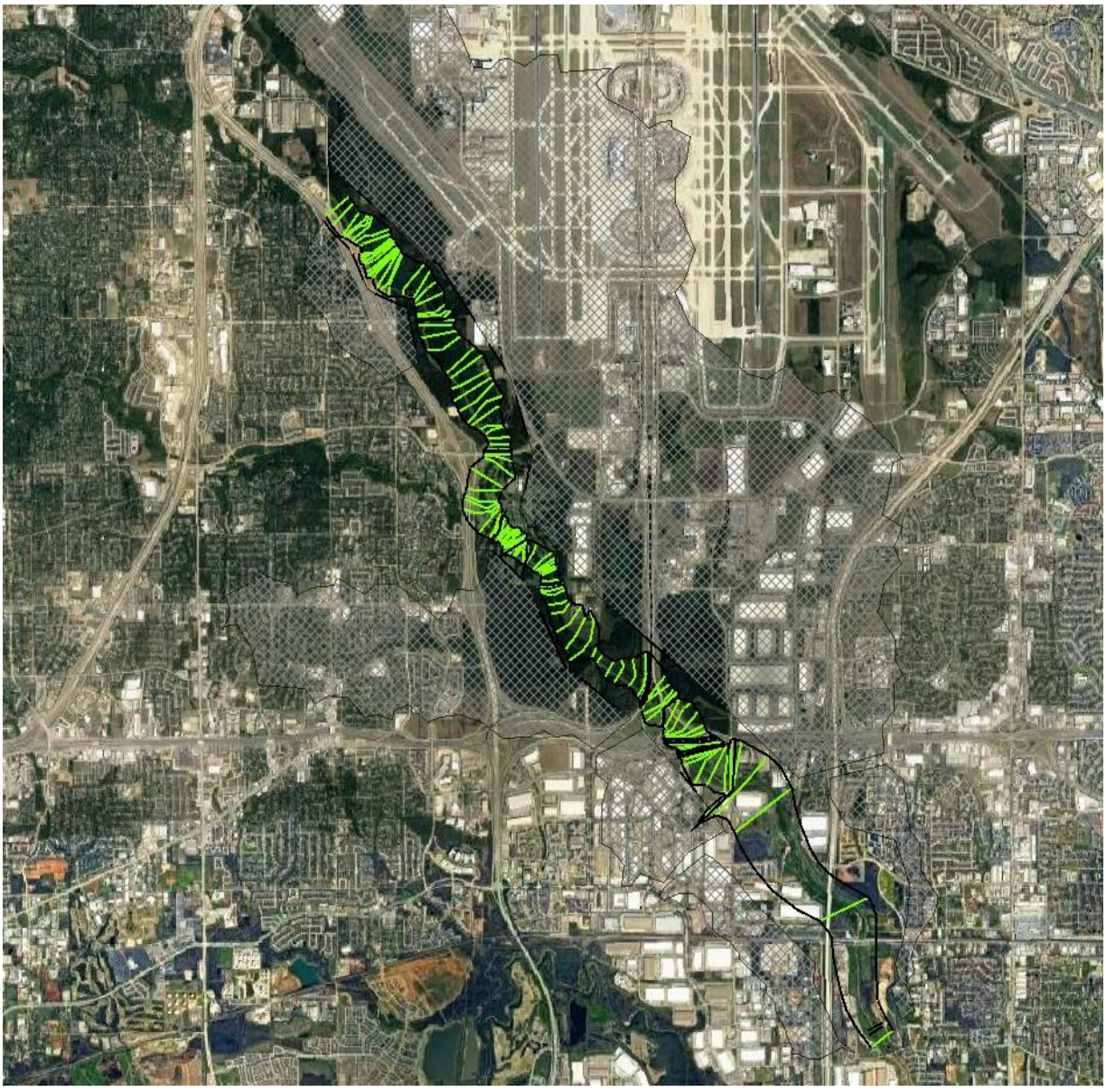

Figure 17 HEC-RAS 1D city of Grapevine steady flow model

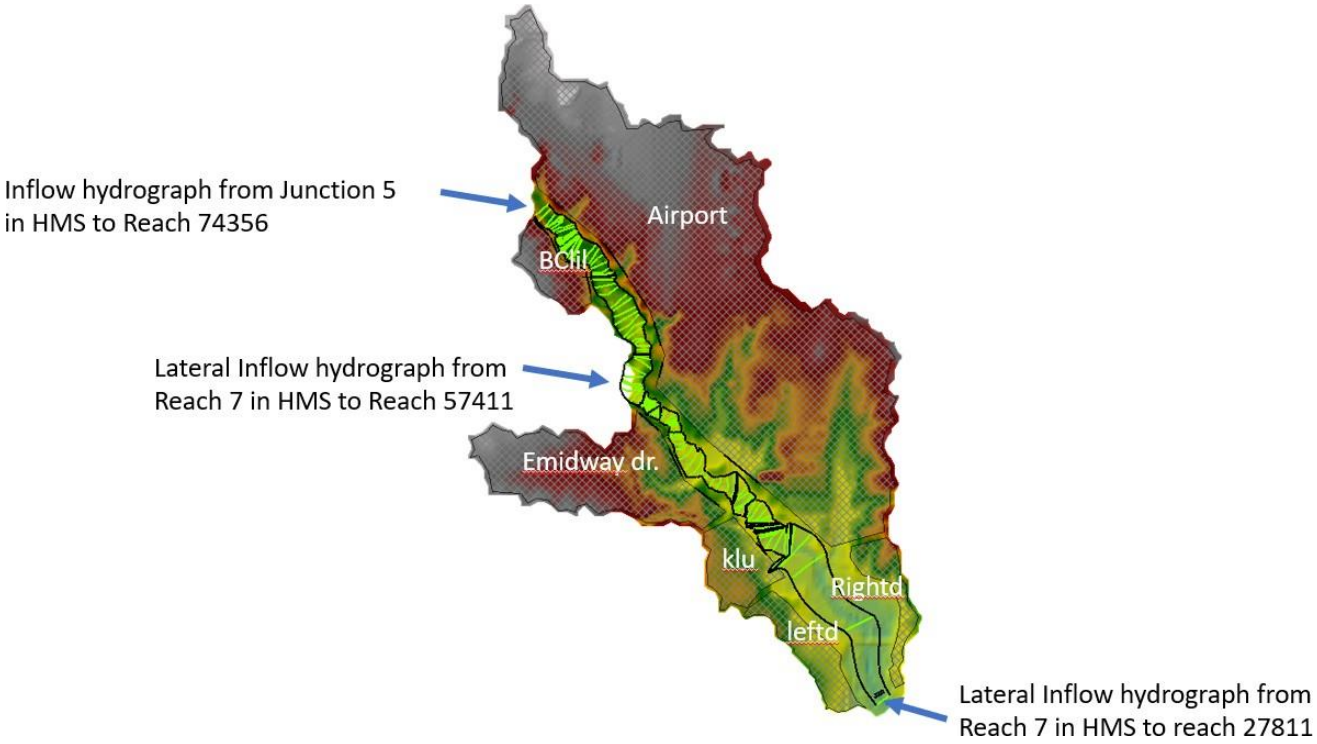

Figure 18 Flow Hydrograph input locations

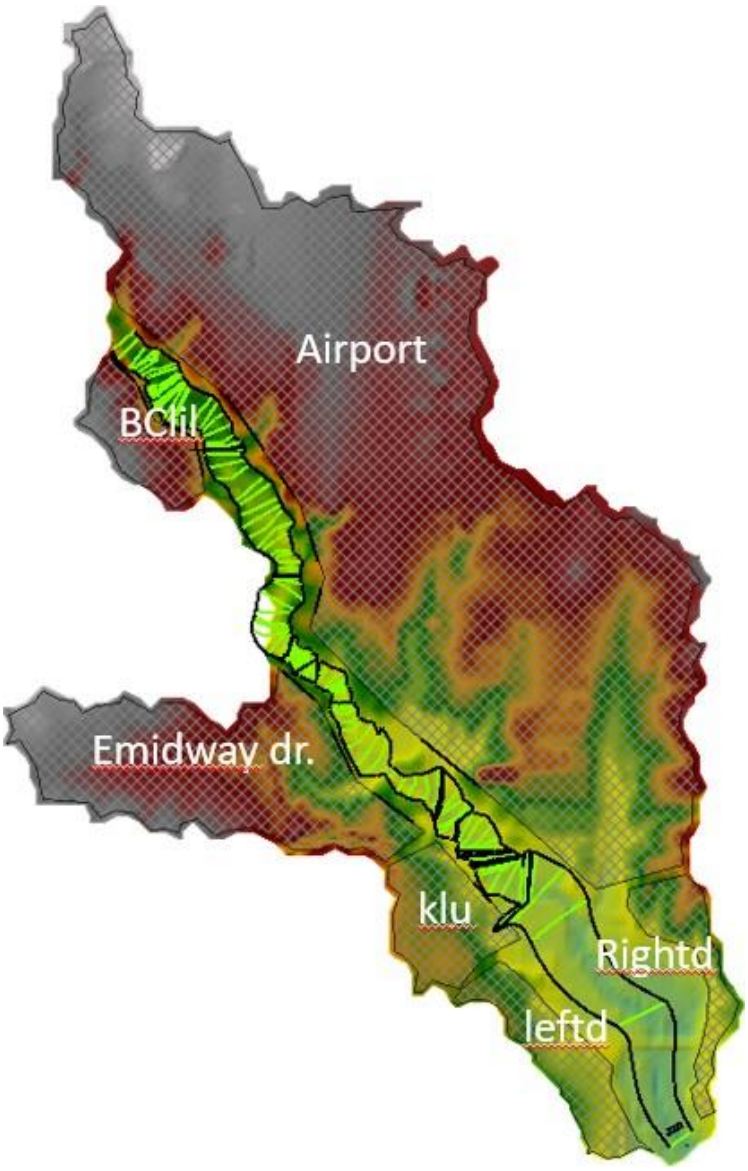

Figure 19 Final HEC-RAS model

CHAPTER 3 RESULTS

The workflow depicted in **Figure 20** outlines the sequence of steps followed to summarize the findings. The initial phase involves the calibration of the HEC-HMS model using rainfall data from August 2022, which is then validated using November 2022 rainfall data. Similarly, for the 2017 scenario, the HEC-HMS model is calibrated using December rainfall data and validated using June rainfall data.

After the meticulous calibration and validation processes, the resulting flow rate time series are utilized as input for the HEC-RAS model, serving as both inflow and outflow hydrographs. The stage at the gauge location is compared, and the HEC-RAS model is subsequently calibrated and validated for the corresponding rainfalls.

Subsequently, the HEC-HMS models are employed to simulate the 100-year, 24-hour rainfall events. The resulting outputs are used to compare the stage at three locations: one upstream, one midstream, and one downstream. This comparison allows for a comprehensive assessment of the impact of urbanization and development on the river's water levels at various sections along its course.

By following this workflow, the study aims to provide valuable insights into the effects of urbanization and development on river channel hydraulics, enabling a better understanding of the associated flood risk and inundation patterns.

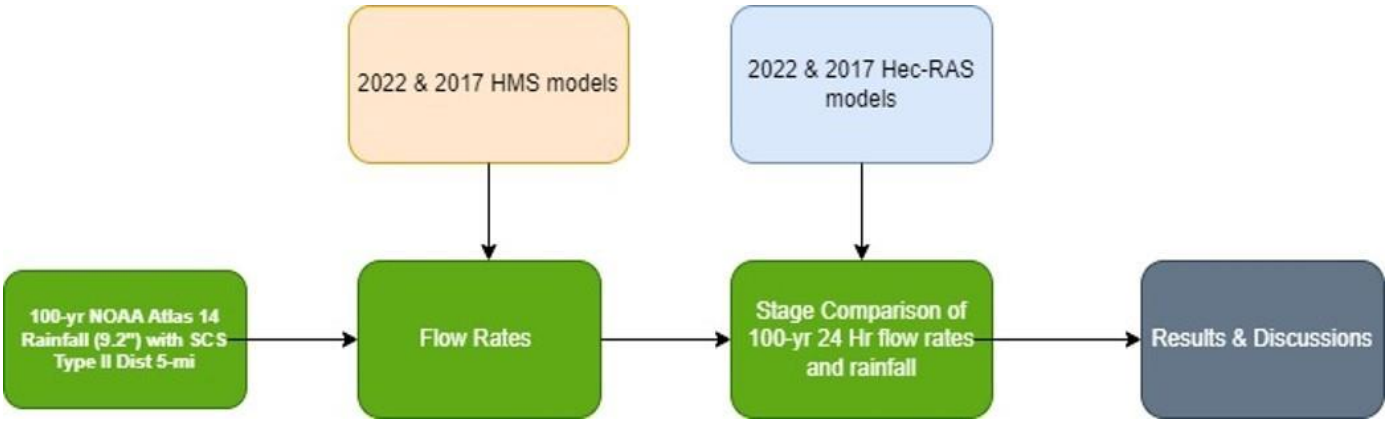

Figure 20 Results Workflow

HMS Results

The HMS results show good correlation with the observed flows. The methodology incorporated have produced results for each rainfall and can be further input into the HEC-RAS model, Figures 21,22,23 & 24 show the comparison of simulated vs observed flows with data taken from USGS gauge 0806950495. The simulated and observed volume comparison has been summarized in **Table 10**, time of peak for observed and simulated peak is summarized in Table 11 and the observed and simulated model efficiency is summarized in Table 12. Further 100-year 24-hour rainfall taken from the NOAA atlas website is also input into the model and the hydrographs at the gauge location are compared in **Figure 24** and the maximum flow rates with total rainfall are summarized in Table 13.

Table 10 Simulated vs observed volume

Rainfall Time	Simulated Volume (in)	Observed Volume (in)
June, 2017	0.87	0.72
December, 2017	0.78	0.7
August, 2022	1.78	1.69
November, 2022	0.68	0.74

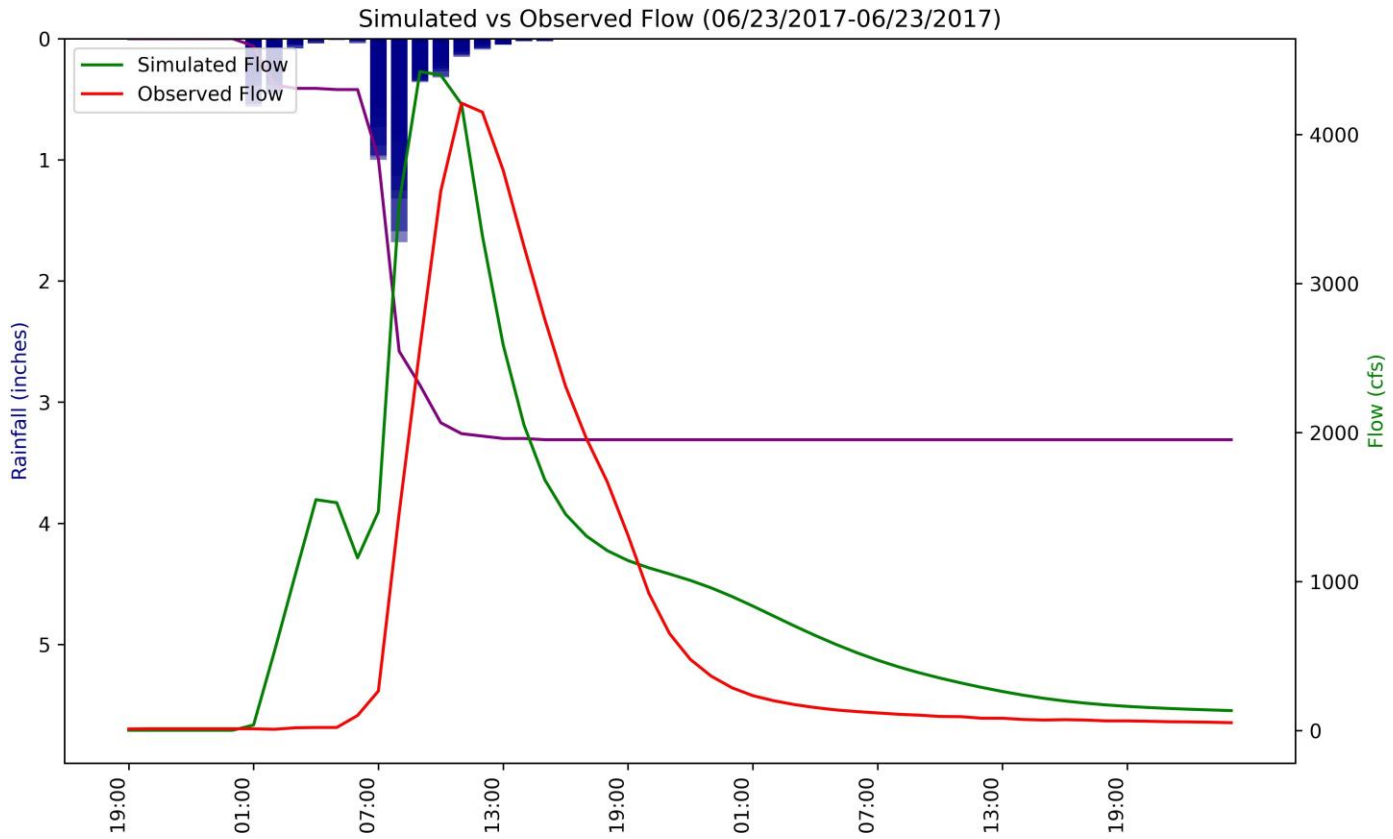

Figure 21 Simulated vs Observed flow, June rainfall, 3.46 in

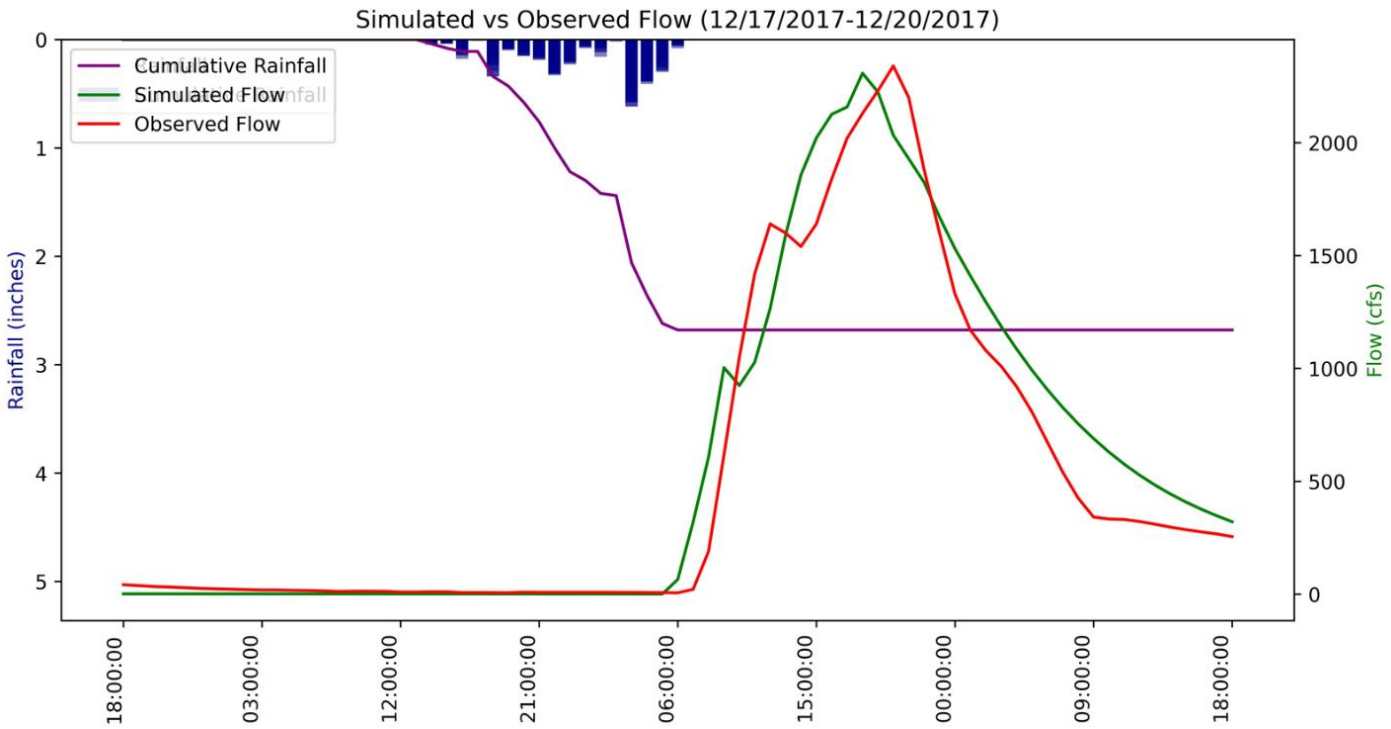

Figure 22 Simulated vs observed, December rainfall, 2.66 in

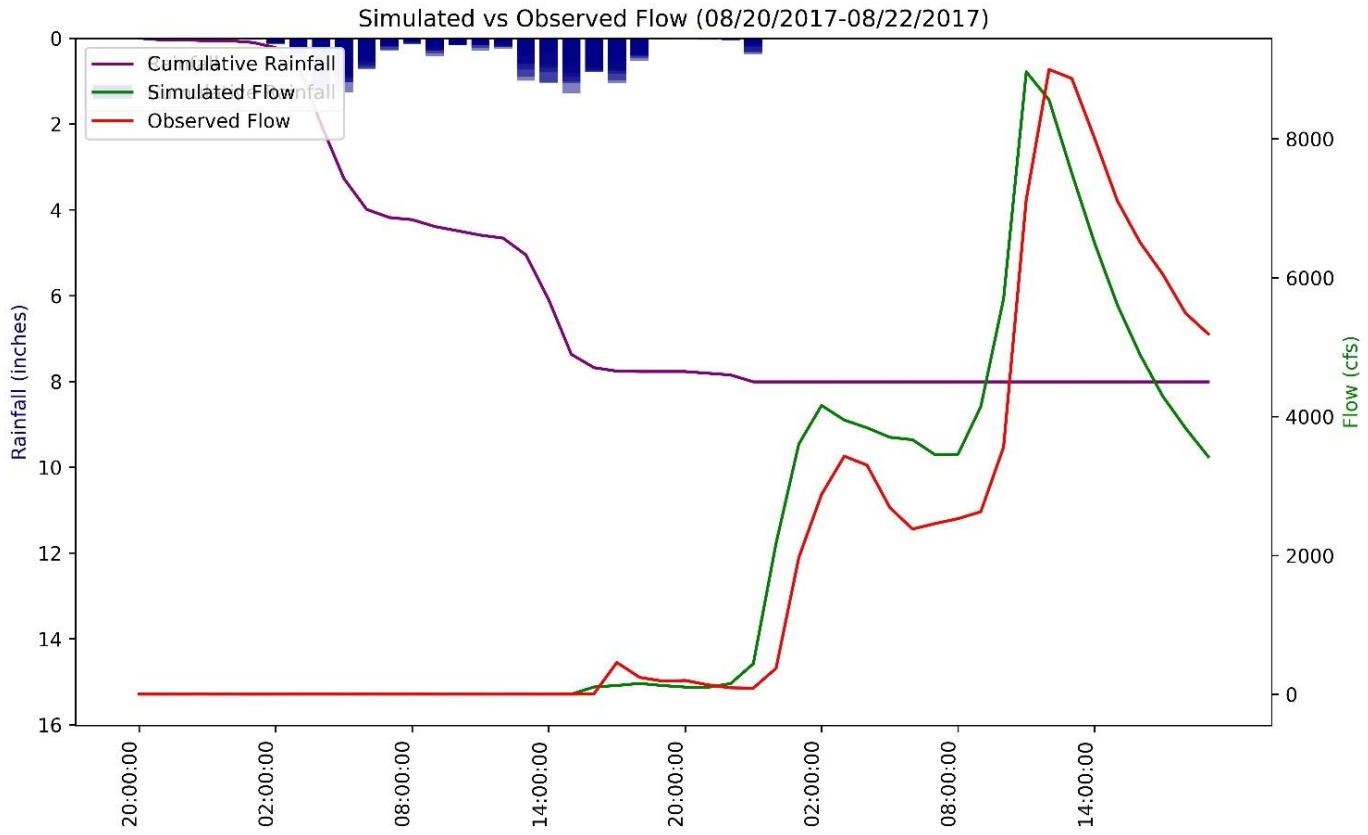

Figure 23 Simulated vs observed, August Rainfall, 8.01 in

Table 11 Simulated vs observed peak timing

Rainfall Time	Simulated time of Peak	Observed Time of peak	Delay (hr.)
June, 2017	10:00	11:00	1
December, 2017	18:00	20:00	2
August, 2022	11:00	12:00	1
November, 2022	17:00	19:00	2

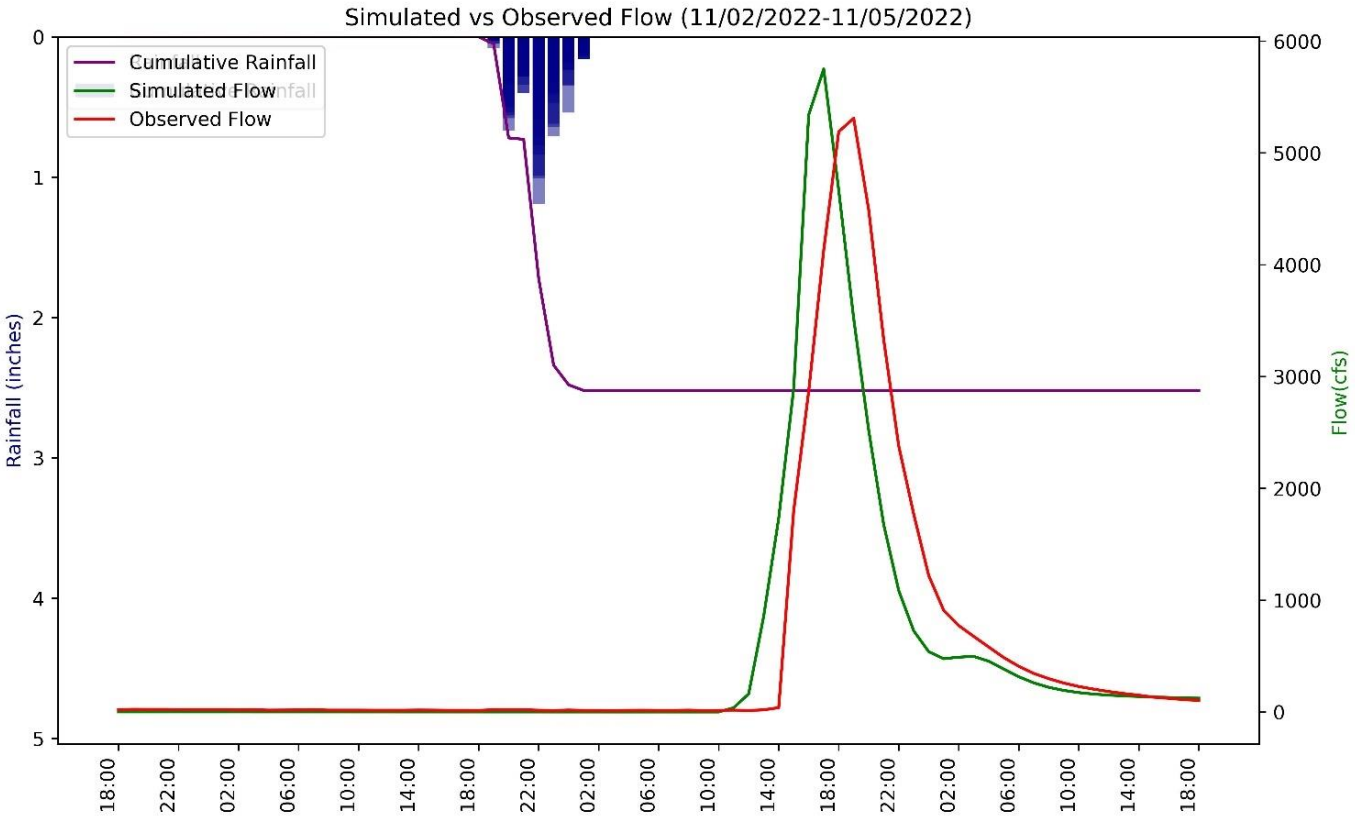

Figure 24 Simulated vs Observed, November Rainfall 2.52 in.

Table 12 HEC-HMS model efficiency

Rainfall Time	Simulated Peak flow (cfs)	Observed Peak flow (cfs)	Total Rainfall (in.)	NSE
June, 2017	4398.5	4210	3.46	0.756
December, 2017	2307	2340	2.66	0.941
August, 2022	8965.8	9000	8.01	0.886
November, 2022	5750.7	5310	2.52	0.796

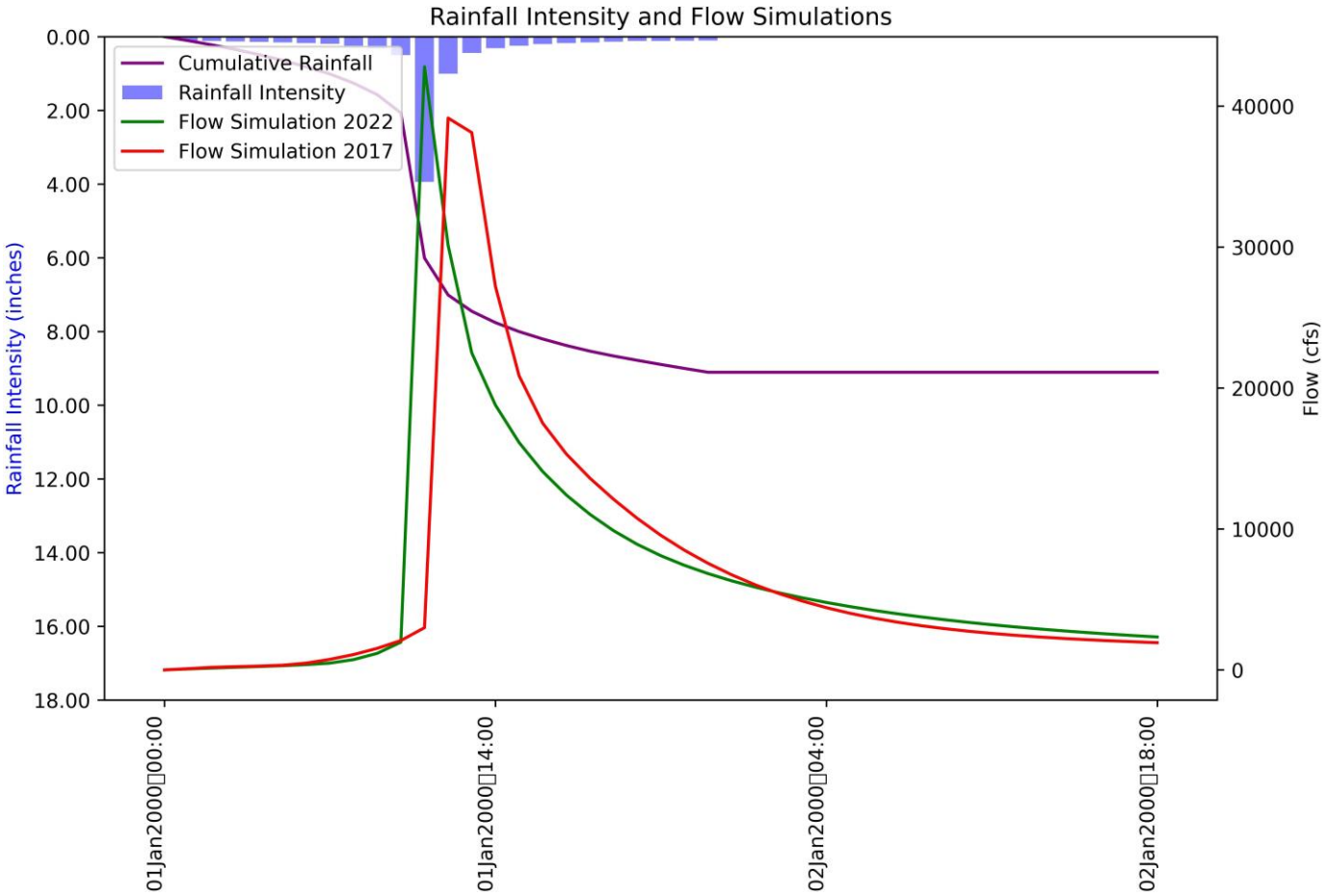

Figure 25 100 year 24 hr rainfall input results of HMS model 2017 and 2022

Table 13 100 year 24 hr HMS model simulations

Bains Model	Max flow (cfs)	Rainfall Acc. (in)
2017	39154.9	9.2
2022	42786.7	9.2

HEC-RAS Results

The HMS model produces flow rates at locations that previously did not have any data available. These flow rates are input boundary conditions to the HEC-RAS model. The flow boundary conditions are input at three locations in the HEC-RAS model, Junction-5 is corresponding to cross section 74356, Outflow from Reach 7 is input as lateral inflow at cross section 57411 and finally the downstream Sink-1 corresponds to cross section 27811 in HEC-RAS where the outflow boundary condition is given as input as shown in **Figure 26**. The locations of the input boundary condition are selected based on overlaying the HMS model on the HEC-RAS geometry file and conducting Arc-hydro analysis to find the upstream location drainage area.

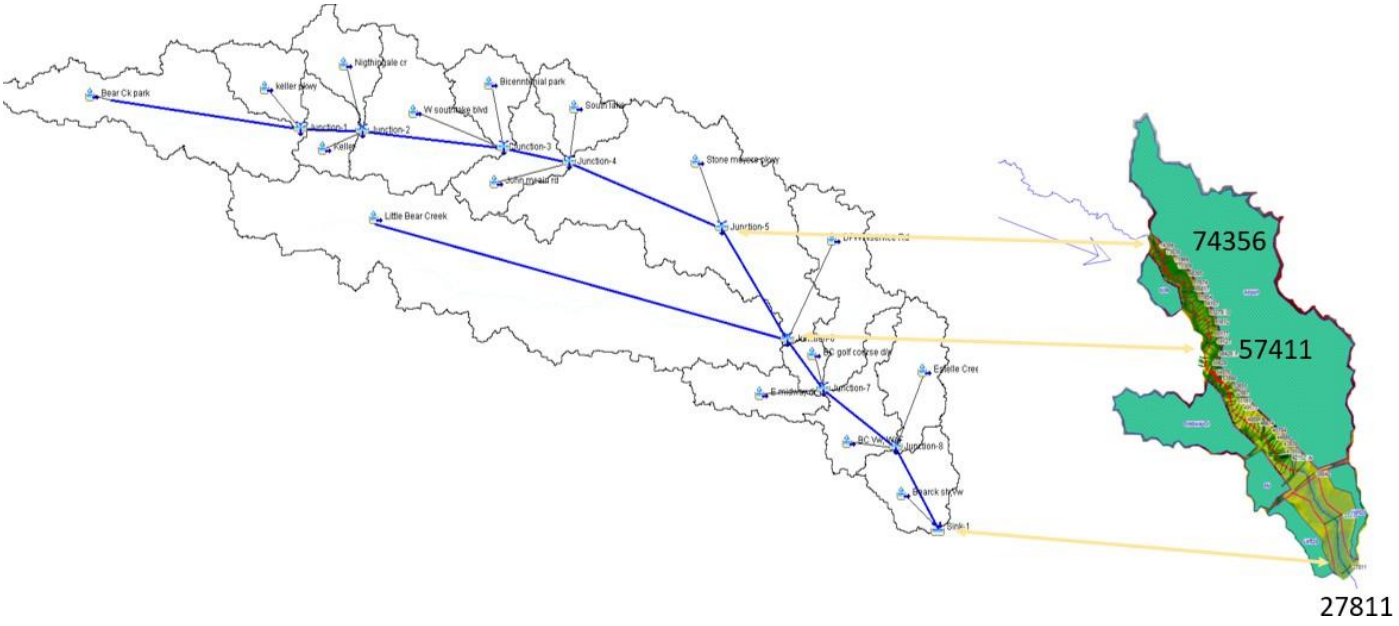

Figure 26 HMS to RAS corresponding locations for hydrograph input

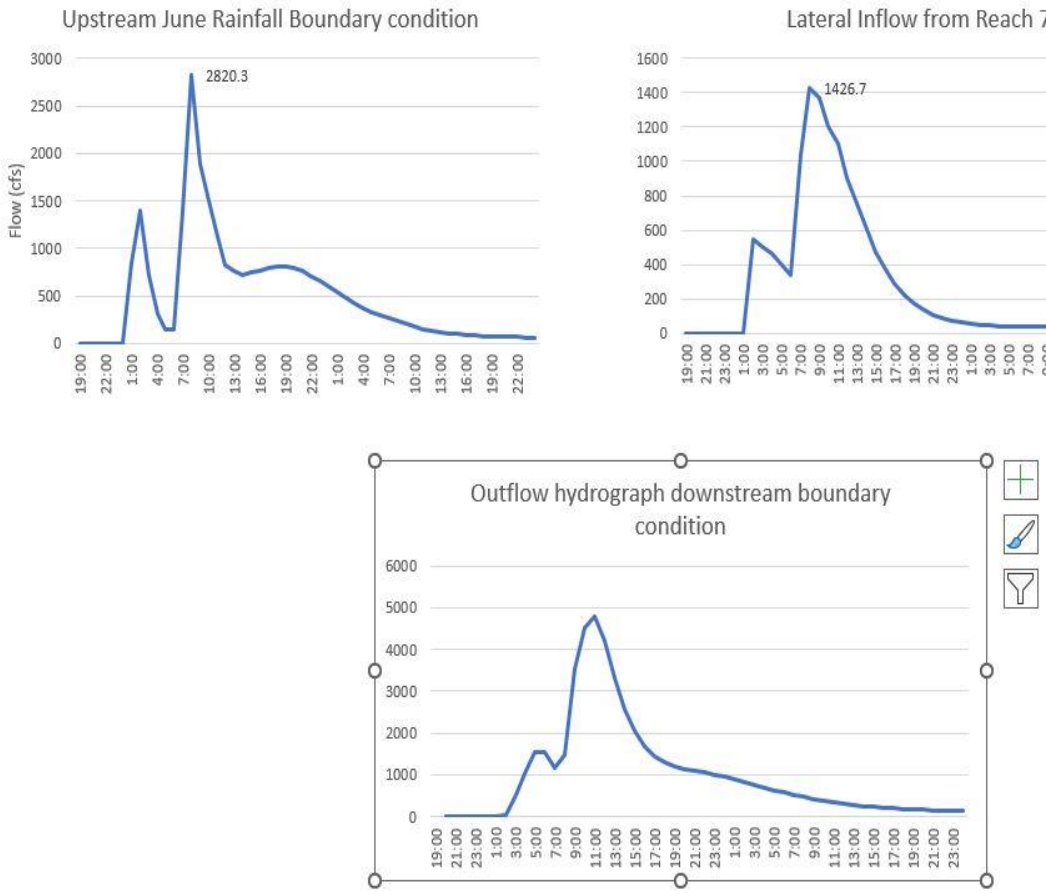

Figure 27 Flow hydrograph input for June rainfall

Figure 27 shows the flow hydrograph boundary conditions input into the HEC-RAS model for June 2017 rainfall

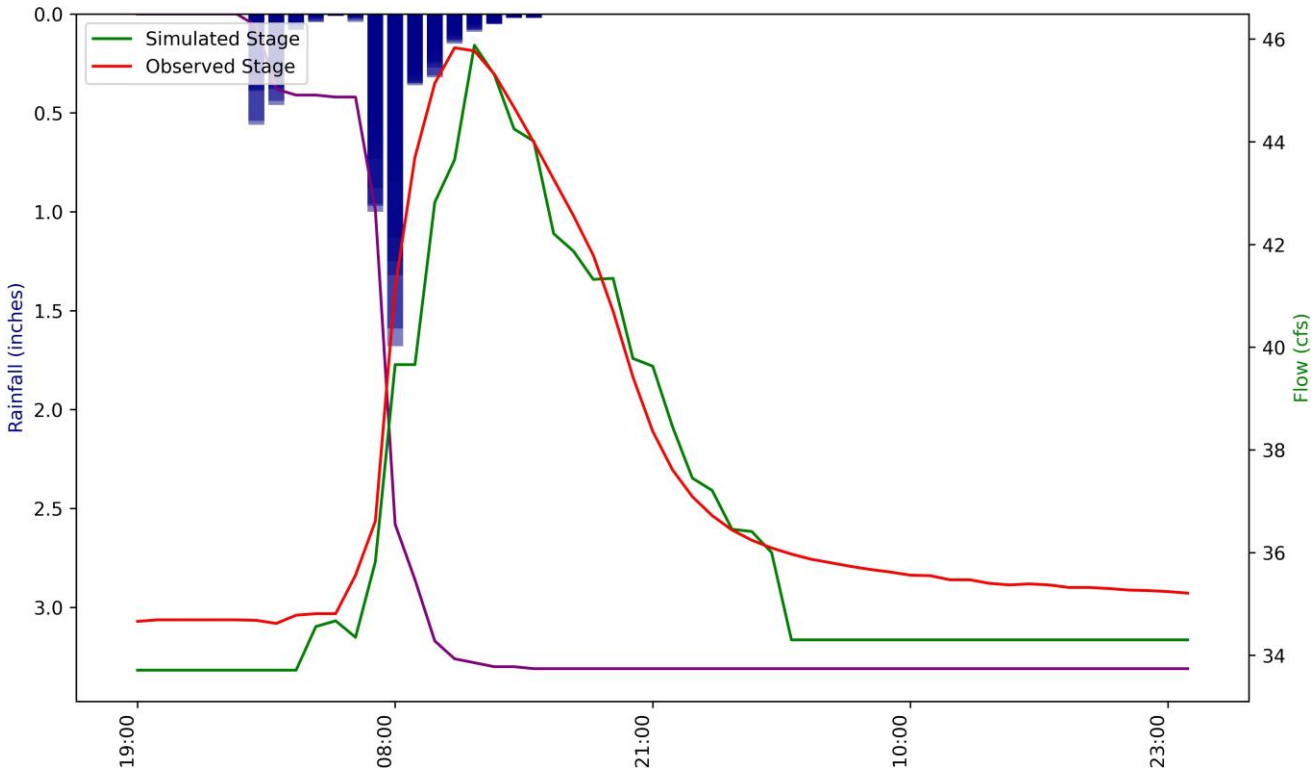

Figure 28 Simulated vs observed stage, June rainfall

Figure 28 shows the stage comparison between simulated and observed data for June, 2017 rainfall. The model shows a good correlation with observed data

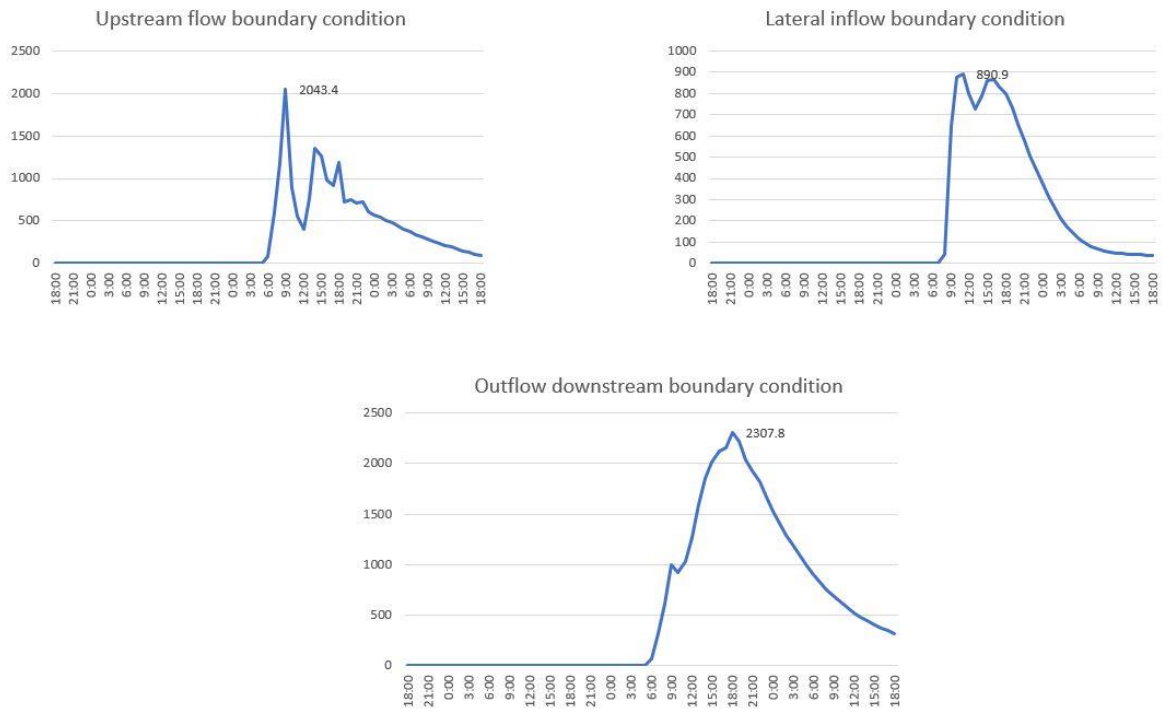

Figure 29 Simulated vs observed stage, December rainfall

Figure 29 shows the flow hydrograph boundary conditions input into the HEC-RAS model for December, 2017 rainfall

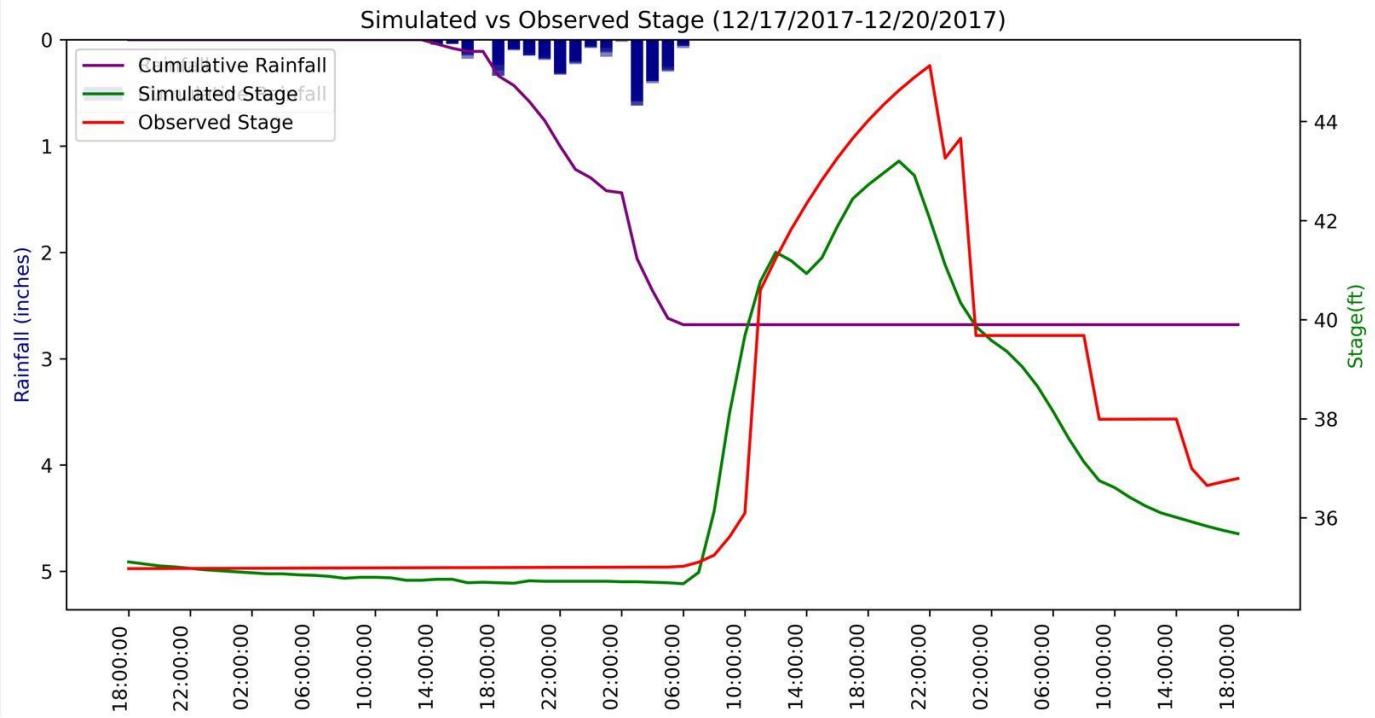

Figure 30 Simulated vs observed stage, December rainfall

Figure 30 shows the stage comparison between simulated and observed data for December, 2017 rainfall. The model shows a good correlation with observed data

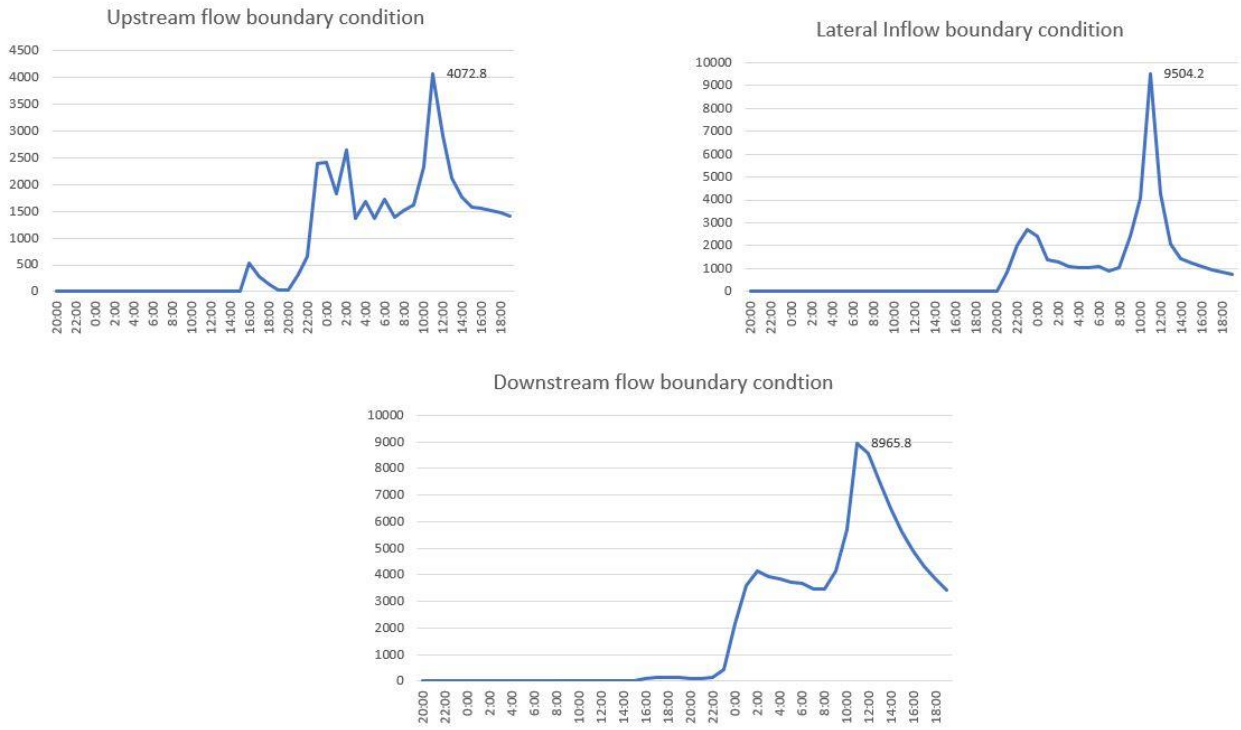

Figure 31 Flow hydrograph input August rainfall

Figure 31 shows the flow hydrograph boundary conditions input into the HEC-RAS model for August, 2022 rainfall.

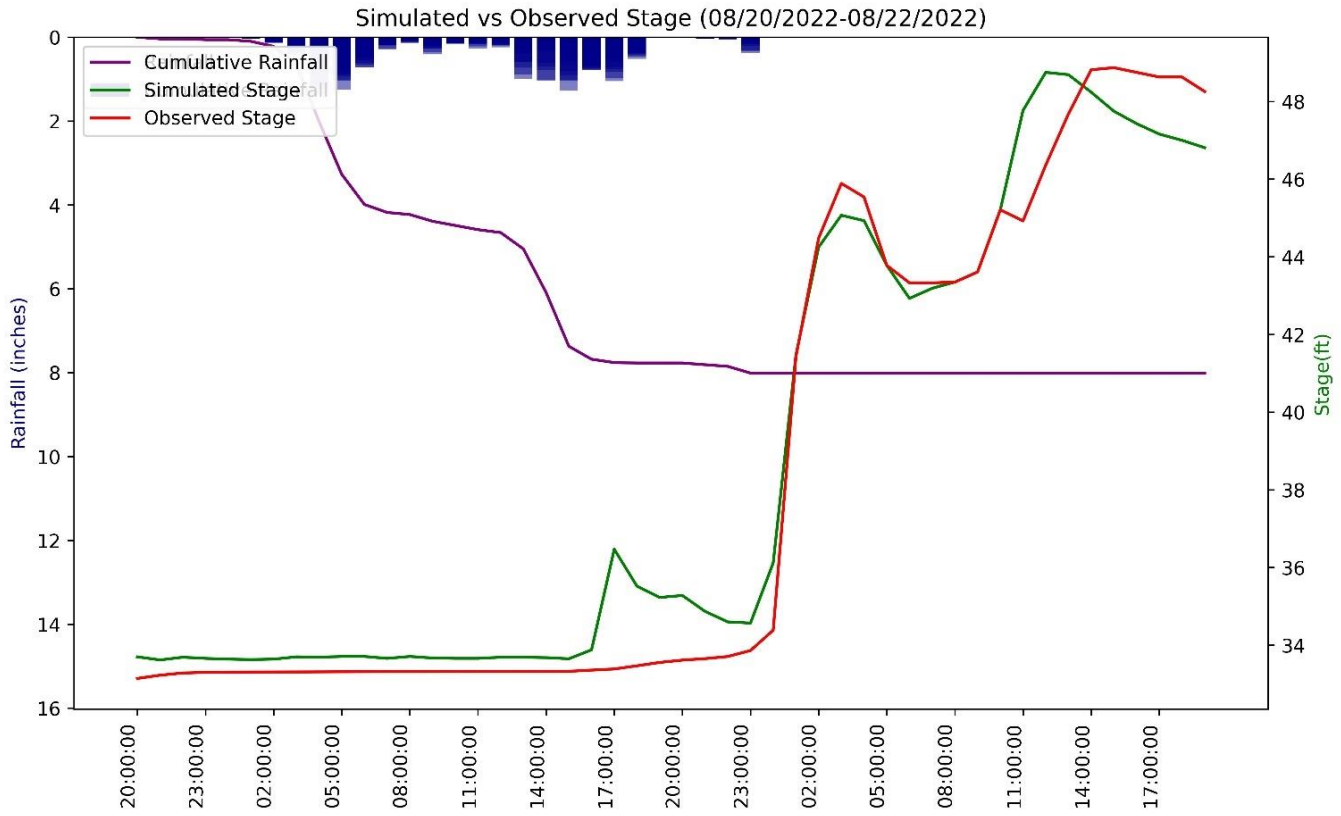

Figure 32 Simulated vs observed stage August rainfall

Figure 32 shows the stage comparison between simulated and observed data for August, 2022 rainfall. The model shows a good correlation with observed d

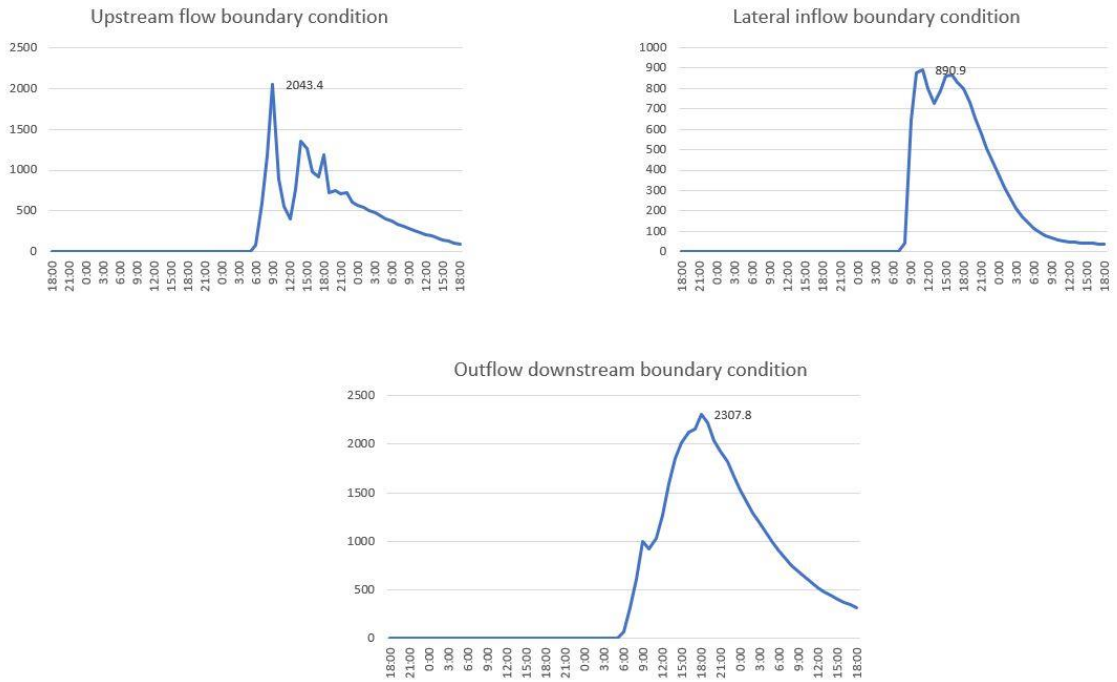

Figure 33 Flow hydrograph input November rainfall

Figure 33 shows the flow hydrograph boundary conditions input into the HEC-RAS model for November, 2022 rainfall.

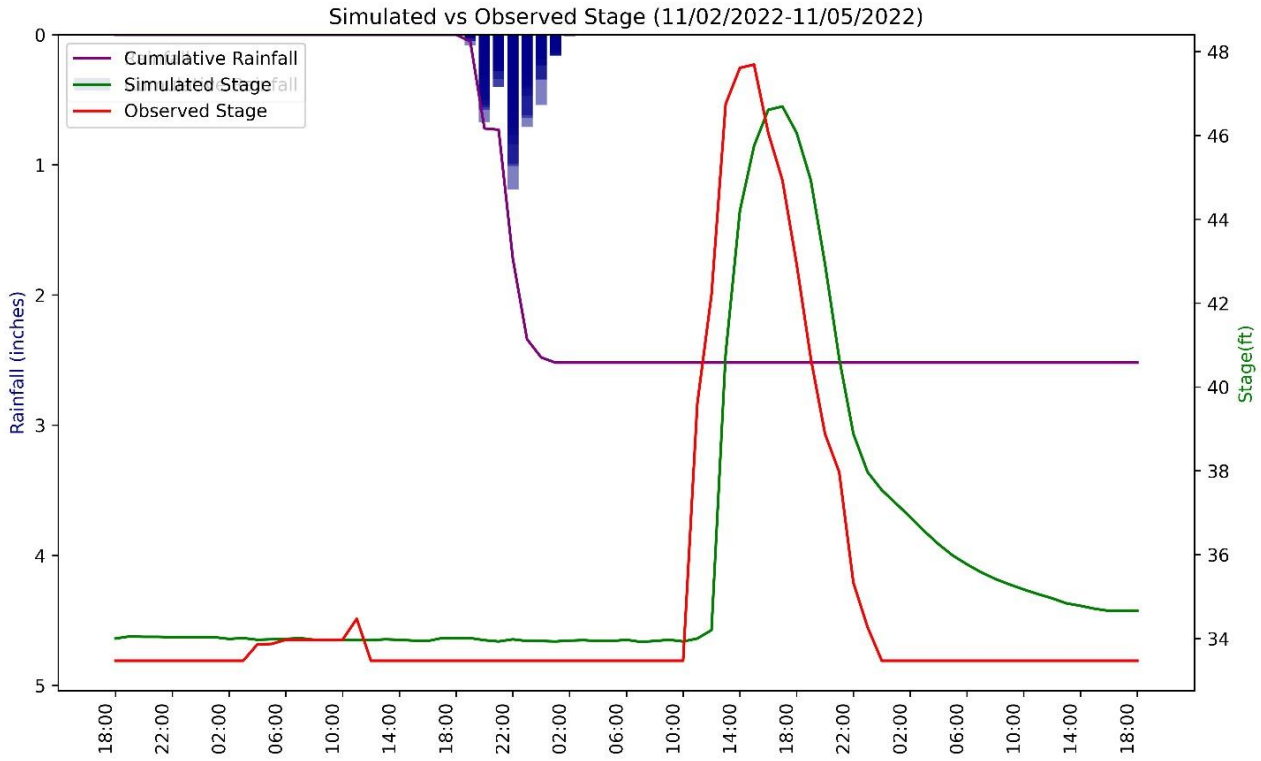

Figure 34 Simulated vs observed stage November rainfall

Figure 34 shows the stage comparison between simulated and observed data for November, 2020 rainfall. The model shows a good correlation with observed data.

Table14 summarizes the above results and shows the model efficiency for the HEC-RAS models. The maximum simulated and observed stage is compared. The maximum water surface elevations are compared for one upstream, one midstream and one downstream for each rainfall at the time step of maximum elevation in **Figure 35, 36, and 37**. The inundation boundaries are compared for 2017 and 2022 in **Figures 38 and 39**

Table 14 HEC-RAS model efficiency and 100 year 24 Hr simulations output

Rainfall Event	Maximum simulated Stage (ft)	Maximum observed Stage (ft)	NSE
June, 2017	45.88	45.83	0.92
December 2017	45.127	42.91	0.81
August, 2017	48.81	48.75	0.96
November, 2017	47.69	46.69	0.92
100-yr 24 hr 2017	60.39 ft		
100-yr 24 hr 2022	63.7 ft		

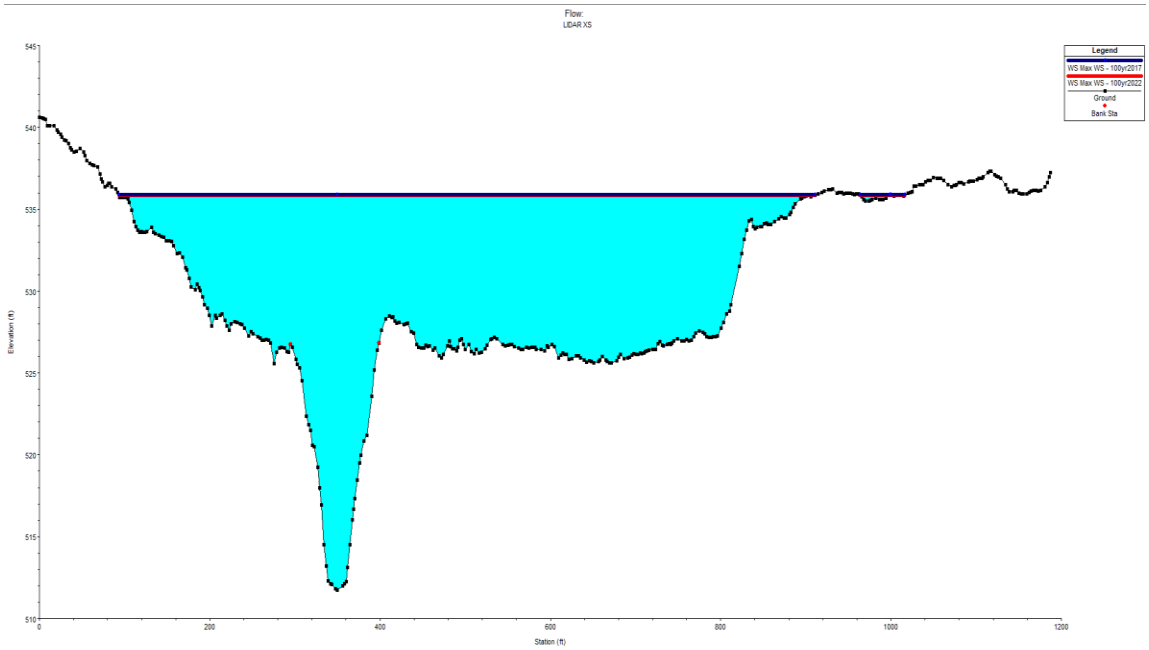

Figure 35 Maximum Water surface elevation comparison all rainfalls at X's 74356

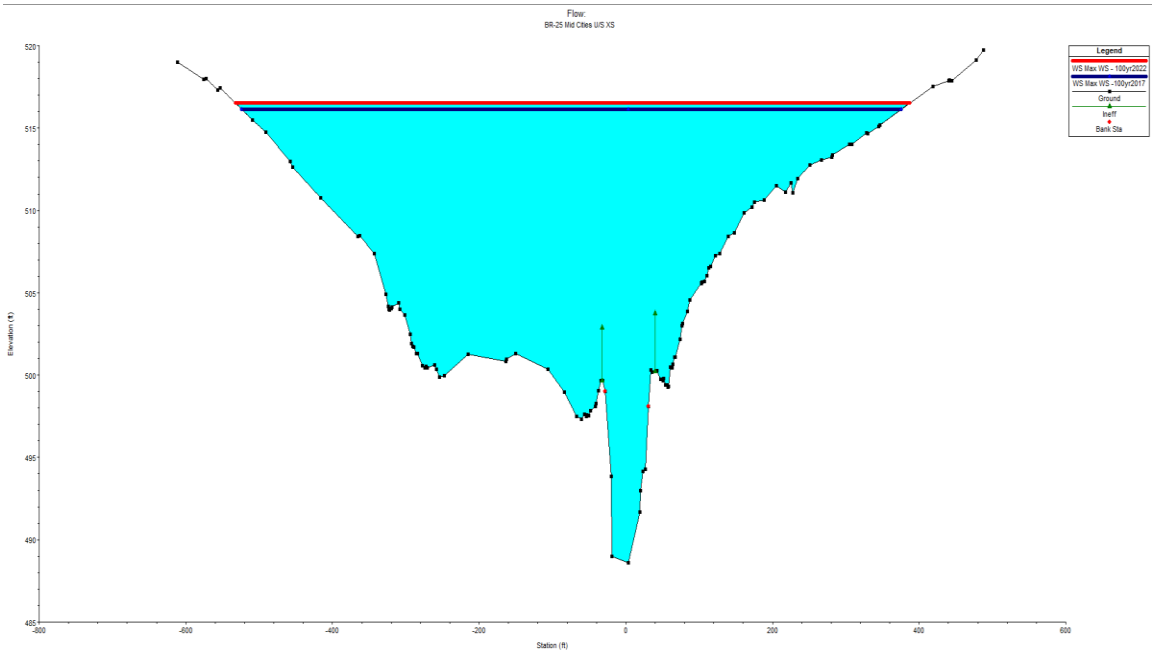

Figure 36 Maximum water surface elevation comparison for all rainfalls at X's 58858

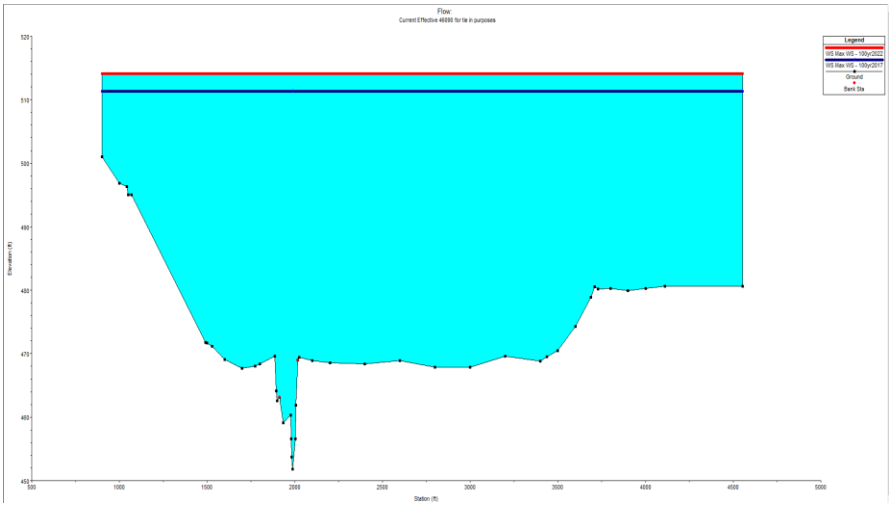

Figure 37 Maximum water surface elevation comparison for all rainfalls at X's 38642

The flood inundation boundaries show slight variation in encroachment in the channel with the 100-year rainfall as input as in Figures 38 and 39. The difference in area encroached is 500 sq ft. The difference is highlighted with the boxes marked in both Figures. The elevation in the reaches shows very high elevation change specially for the most downstream cross section.

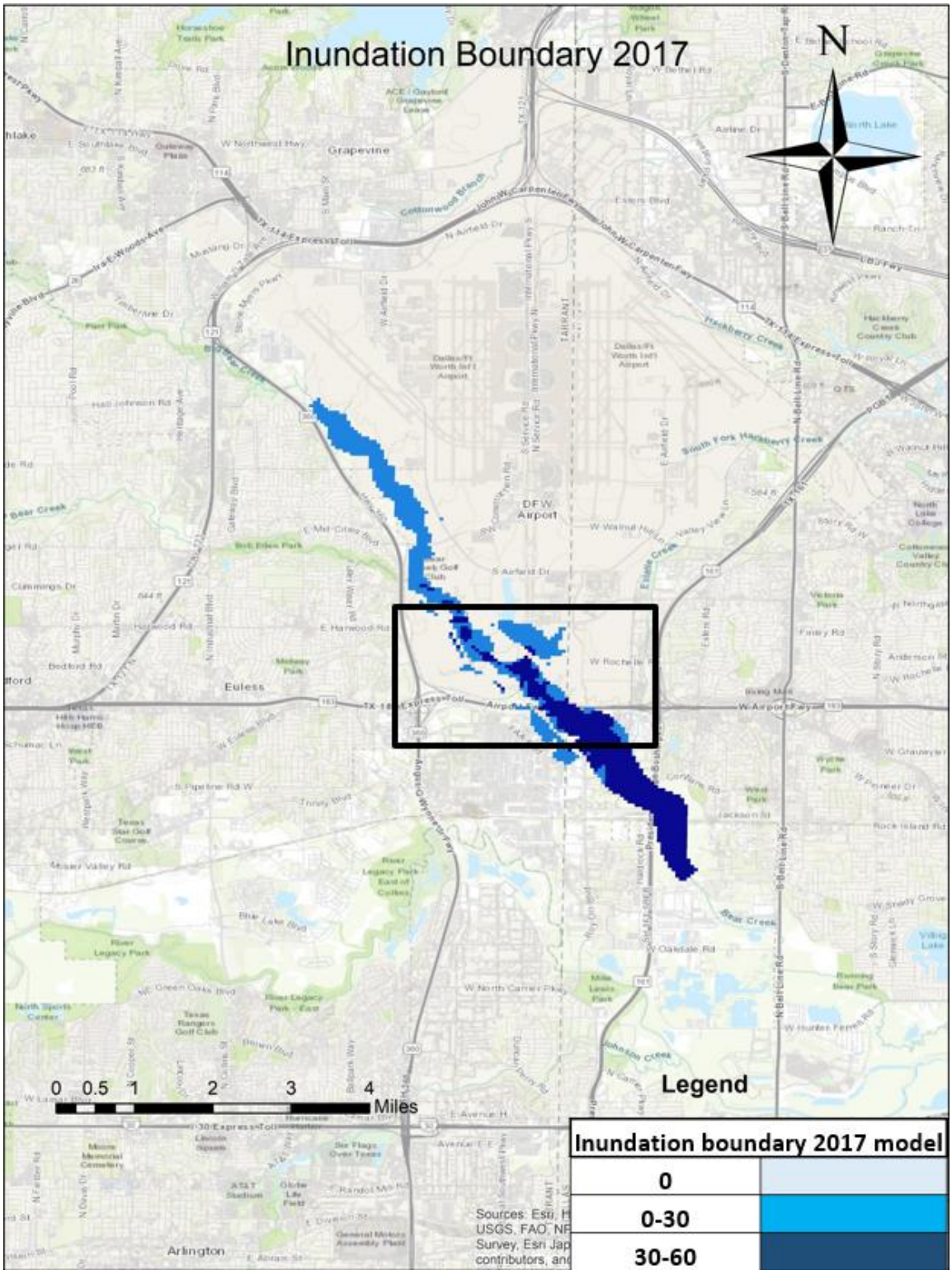

Figure 38 Inundation boundary 100 year 24 hr rainfall 2017 model

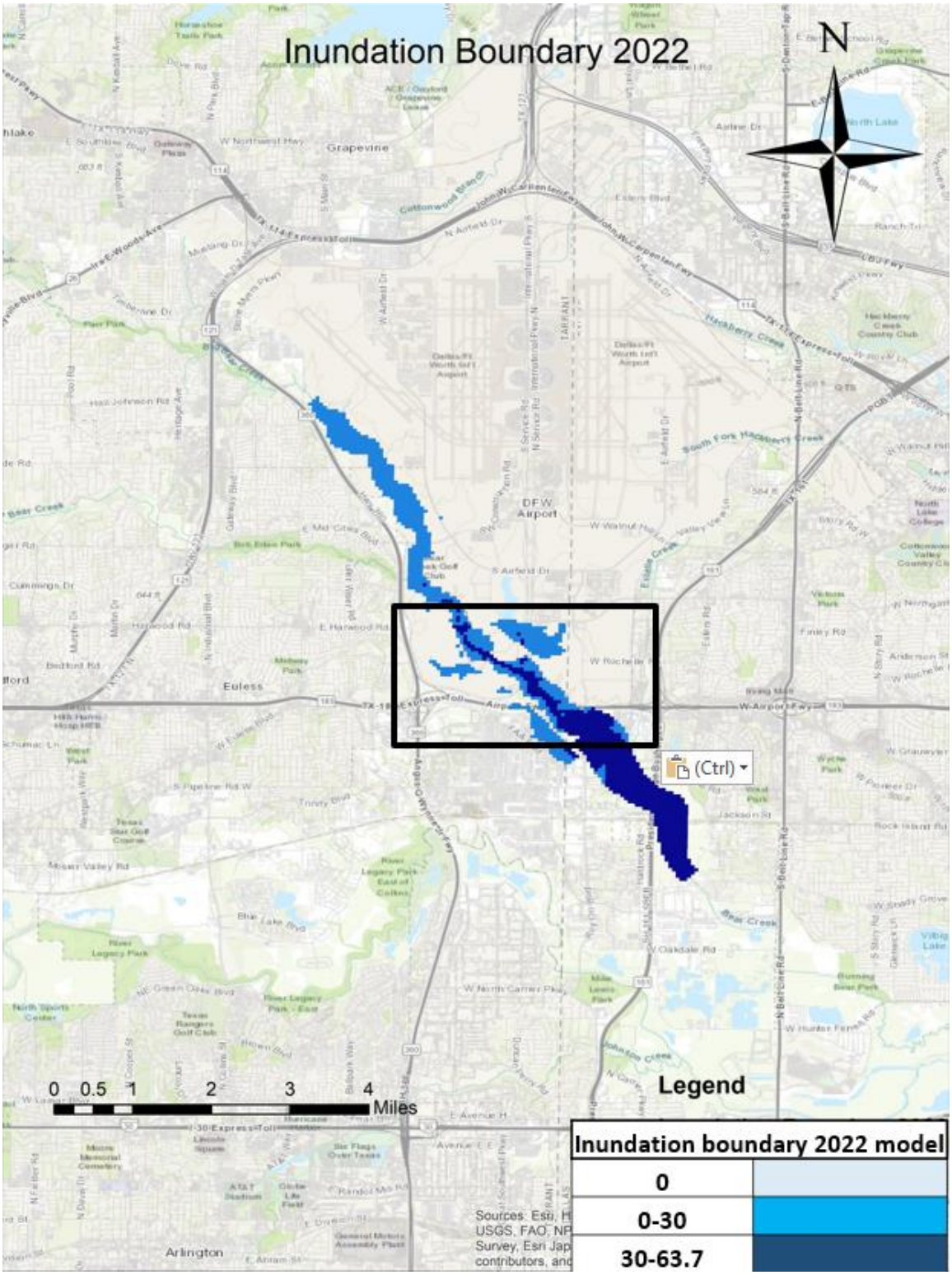

Figure 39 Inundation boundary 100-year 24 hr 2022 model

CHAPTER 4 DISCUSSIONS

The simulations conducted using the integrated HEC-HMS and HEC-RAS modeling approach have generated valuable data that provides insights into the real-world scenario of the Bear Creek Watershed. By analyzing the simulated flow regime and river channel hydraulics for different years, this research highlights the potential implications for flood management, water resources planning, and ecological sustainability in the watershed. The section is divided into two parts major findings and project limitations.

Major findings

In the HEC-HMS model, the characterization of each basin relies on the NLCD imperviousness data and GSSURGO soil type data to accurately model infiltration. The unique characteristics of each basin, including imperviousness and antecedent conditions, play a crucial role in determining the flow rates. Notably, the Estelle Creek sub basin, which encompasses the airport region, exhibits the highest changes in imperviousness between the two analyzed years. The simulated results from the HEC-HMS model exhibit a strong correlation with the observed data, indicating and increase in flow rates over the past five years. This rise in flow rates can be attributed to changes in land usage, which likely led to a decrease in roughness and infiltration, consequently, causing larger volumes of stormwater to flow into the reach. The airport region, with its increased imperviousness, emerges as a significant contributing factor to the heightened flow rates. Similarly, the HEC-RAS model utilizes the flow rates obtained from the HEC-HMS simulation as input values. After careful calibration, a 100-year, 24-hour rainfall analysis is conducted. The observed data and the HEC-RAS results exhibit a high correlation, suggesting the reliability of the simulated data. Downstream, there is a considerable increase in water surface

elevation, with a difference of 3 feet between the two analyzed years. This elevation difference highlights the impact of increasing urbanization, which may have contributed to the rise in water surface elevations. To calibrate the HEC-RAS simulated data, modifications are made to the reach length and Manning's n roughness. In the 2017 model, the roughness upstream is kept low, and slight adjustments are made to the channel length. Conversely, for the 2022 model, the roughness upstream is increased, indicating potential vegetation growth that has resulted in higher roughness and, consequently, higher storage time.

This prolonged storage time causes the flow to reach the gauge location later. The findings from this study, as discussed above, shed light on the impact of land usage changes, imperviousness, and vegetation growth on the flow rates and water surface elevations within the Bear Creek watershed. The strong correlation between the simulated and observed data underscores the reliability of the models and their effectiveness in simulating and analyzing hydrological processes.

The modelling effort supports the hypothesis of increased stage and flow from 2017 to 2022 but over estimates the elevation for the 100-year rainfalls.

Project Limitations

Despite the strong alignment of our results with the initial hypothesis, it is important to acknowledge certain limitations that affect the accuracy and representation of our findings. One limitation lies in the HMS model's use of basin averages for each parameter. While this approach provides a broad understanding of the basin's characteristics, it may not capture the minute variations in actual conditions. Incorporating actual spatial data would likely enhance the model's accuracy and improve the representation of the real-world conditions. Another limitation relates

to the 2D flow areas in HEC-RAS. Due to the lack of comprehensive data, these areas are not accurately modeled in our analysis. Further efforts could be directed towards improving the modeling of these areas to increase efficiency in terms of matching flows from overbank locations. By incorporating more detailed data and refining the 2D flow areas, we can achieve a more comprehensive understanding of the flow dynamics.

Furthermore, the lack of complete bathymetry for the 1D steady flow file introduces limitations in accuracy. The absence of detailed cross-sectional data near the gauge location necessitates the manual setting of the cross section based on information available approximately 9000 feet upstream. This approximation may introduce uncertainties and impact the precision of the results. Obtaining a complete and more detailed bathymetry dataset, particularly in the vicinity of the gauge location, would enhance the accuracy of the analysis and provide a more robust representation of the flow characteristics. Despite these limitations, the current analysis provides valuable insights into the impact of land usage changes, imperviousness, and vegetation growth on flow rates and water surface elevations.

The model input of 100-year 24-hour rainfall of 9.2in over a 24 hr. period on all basins for HEC-HMS model and similarly for 2d flow areas in HEC-RAS model may not be ideal to the nature of rainfalls, since storms move across the region distributing rainfall in a spatially varied manner. Recognizing these limitations highlights opportunities for future research and improvements in data availability, modeling techniques, and analysis methods. By addressing these limitations, we can further refine our understanding of the hydrological processes in the Bear Creek watershed and improve the accuracy of our predictions and simulations.

CHAPTER 5 CONCLUSION

In conclusion, our study utilized the HEC-HMS and HEC-RAS models to analyze the impact of land usage changes, imperviousness, and vegetation growth on flow rates and water surface elevations in the Bear Creek watershed. The results of our analysis align well with our initial hypothesis, indicating that these factors significantly influence the hydrological dynamics in the watershed.

The HEC-HMS model, despite its limitations in using basin averages for parameter representation, demonstrated a strong correlation between the simulated and observed data. This suggests that the model captures the overall trends and patterns of flow rates in the watershed. However, incorporating actual spatial data would improve the accuracy and representativeness of the model.

Similarly, the HEC-RAS model exhibited a high level of agreement between the simulated and observed data, indicating that it effectively captures the impact of changing land usage on water surface elevations. Calibration of the model, including adjustments to reach length and roughness coefficients, allowed for a better representation of the flow dynamics. However, limitations related to incomplete bathymetry and 2D flow area modeling must be addressed to enhance the accuracy of the results.

While our findings support the hypothesis that changes in imperviousness and vegetation growth contribute to increased flow rates and water surface elevations, it is important to acknowledge the limitations of our study. These limitations include the use of basin averages, incomplete bathymetry data, and simplified modeling of 2D flow areas. Addressing these limitations through the incorporation of actual spatial data, improved bathymetry datasets, and

refined modeling techniques would provide a more comprehensive understanding of the hydrological processes in the watershed.

Despite these limitations, our study provides valuable insights into the complex interactions between land usage changes and hydrological dynamics. The strong correlation between the simulated and observed data validates the importance of considering these factors in watershed management and flood mitigation strategies. Future research should focus on refining modeling techniques, incorporating more detailed data, and addressing the limitations identified in this study to improve the accuracy and applicability of hydrological models in similar watersheds.

Overall, our study contributes to the understanding of the hydrological processes in the Bear Creek watershed and emphasizes the need for further research and improvements to accurately simulate and predict flow rates and water surface elevations in changing environmental conditions.

APPENDIX A

HEC-RAS 1D cross section Manning's n original file

River Station	Frctn (n/K)	LOB	Channel Bed	ROB	n #4	n #5	n #6
81536	n	0.07	0.05	0.08			
81094	n	0.08	0.05	0.08			
80525	n	0.08	0.05	0.08			
80231	n	0.09	0.05	0.08			
79934 CONFLUENCE OF TR	n	0.09	0.05	0.08			
79584	n	0.07	0.05	0.08			
79410 L	n	0.07	0.05	0.07			
79058	n	0.07	0.05	0.07			
78923	n	0.07	0.05	0.07			
78908 WALKBRIDGE	Bridge						
78893	n	0.07	0.045	0.07			
78250	n	0.07	0.05	0.07			
77876 K	n	0.07	0.05	0.07			
77339	n	0.08	0.05	0.07			

77252 STATE HIGHWAY 36	Bridge						
77163	n	0.06	0.045	0.06			
77064	n	0.06	0.045	0.06			
76910	n	0.06	0.045	0.06			
76830 STATE HIGHWAY 36	Bridge						
76731	n	0.055	0.05	0.06			
76516	n	0.05	0.05	0.06			
76055	n	0.08	0.05	0.08			
75452 J	n	0.08	0.055	0.08			
75379	n	0.08	0.055	0.08			
75311 EULESS GRAPEVINE	Bridge						
75231 DALLAS/FORT WORT	n	0.08	0.05	0.08			
74824	n	0.1	0.055	0.08			
74356	n	0.1	0.055	0.08			
73937	n	0.1	0.055	0.08			
73465	n	0.1	0.055	0.08	0.05	0.08	
73030	n	0.1	0.055	0.1	0.06	0.05	0.06
72859	n	0.1	0.055	0.06	0.05	0.06	0.02
72680 CONFLUENCE OF TR	n	0.1	0.055	0.06	0.05	0.02	

72430	n	0.1	0.055	0.06	0.05	0.02	
71969	n	0.1	0.055	0.1	0.05		
71432	n	0.1	0.055	0.1	0.05	0.02	
71408	n	0.1	0.055	0.1	0.05	0.02	
71372	n	0.1	0.055	0.1	0.05	0.02	
71224	n	0.1	0.055	0.06	0.05	0.02	
71089	n	0.1	0.055	0.06	0.05	0.06	0.02
70862	n	0.1	0.055	0.06	0.05	0.02	
70752	n	0.1	0.055	0.06	0.05	0.045	0.02
70730	n	0.1	0.055	0.06	0.045	0.05	0.045
70689	n	0.1	0.055	0.06	0.05	0.02	
70604	n	0.1	0.055	0.06	0.05	0.02	
70309	n	0.1	0.055	0.045	0.05	0.02	
70301	n	0.1	0.055	0.045	0.05	0.1	0.02
69965	n	0.1	0.055	0.06	0.02		
69819	n	0.1	0.055	0.06	0.04		
69061	n	0.1	0.055	0.1			
68305	n	0.1	0.055	0.1			
68097	n	0.1	0.055	0.1			
67674	n	0.1	0.055	0.1			
67032	n	0.1	0.06	0.1			
66817	n	0.09	0.06	0.09			
66654	n	0.09	0.055	0.09			

66632 GLADE ROAD	Bridge						
66611	n	0.09	0.055	0.09			
66245	n	0.09	0.055	0.09			
65854	n	0.09	0.055	0.09			
65146 CONFLUENCE OF TR	n	0.09	0.055	0.09			
64107	n	0.09	0.06	0.09			
63851	n	0.09	0.06	0.09			
63279 G	n	0.09	0.06	0.09			
62867	n	0.09	0.06	0.09			
62089	n	0.09	0.055	0.09			
61612	n	0.09	0.055	0.09			
60988	n	0.08	0.055	0.08			
60177	n	0.08	0.05	0.08			
59903	n	0.08	0.05	0.08			
59386 CONFLUENCE OF TR	n	0.08	0.05	0.08			
59127	n	0.08	0.055	0.08			
58910	n	0.08	0.05	0.08			
58858	n	0.08	0.05	0.08			
58788 MID CITIES BOULE	Culvert						
58757	n	0.08	0.05	0.08			
58728	n	0.06	0.045	0.06			

58656	n	0.06	0.045	0.06			
58420 F	n	0.05	0.045	0.05			
57741	n	0.05	0.045	0.05			
57116	n	0.06	0.045	0.05			
56629	n	0.055	0.045	0.05			
56404	n	0.055	0.05	0.06			
56139	n	0.055	0.045	0.06			
55781	n	0.05	0.045	0.05			
55416 E	n	0.055	0.045	0.055			
55359	n	0.055	0.045	0.055			
55275	n	0.055	0.045	0.055			
55256 GOLF COURSE MAIN	Bridge						
55243	n	0.055	0.045	0.055			
55136	n	0.05	0.045	0.05			
54976	n	0.055	0.045	0.055			
54872	n	0.055	0.045	0.055			
54775	n	0.055	0.045	0.06			
54675	n	0.055	0.045	0.06			
54615	n	0.05	0.045	0.06			
54508	n	0.05	0.045	0.05			
54461	n	0.05	0.045	0.05			
54415	n	0.05	0.045	0.05			

54362	n	0.05	0.045	0.05			
54298	n	0.05	0.045	0.05			
54219	n	0.05	0.045	0.05			
54175	n	0.05	0.045	0.05			
54149 GOLF COURSE	Bridge						
54148	n	0.05	0.045	0.05			
54088	n	0.05	0.045	0.05			
53989	n	0.05	0.045	0.05			
53890	n	0.05	0.045	0.05			
53696	n	0.05	0.045	0.05			
53607	n	0.05	0.045	0.05			
53567	n	0.05	0.045	0.05			
53550 GOLF COURSE	Bridge						
53534	n	0.05	0.045	0.05			
53493	n	0.05	0.045	0.05			
53341	n	0.055	0.045	0.055			
52920	n	0.055	0.05	0.055			
52726	n	0.05	0.045	0.05			
52655	n	0.05	0.045	0.05			
52590	n	0.05	0.045	0.06			
52499	n	0.055	0.045	0.055			
52402 D	n	0.06	0.05	0.06			
52067	n	0.06	0.05	0.06			

51974	n	0.065	0.05	0.06			
51957 GOLF COURSE	Bridge						
51939	n	0.065	0.05	0.06			
51885	n	0.07	0.05	0.07			
51734	n	0.07	0.055	0.07			
51497	n	0.07	0.055	0.09			
51161	n	0.06	0.06	0.09			
50847	n	0.06	0.055	0.09			
50213	n	0.065	0.06	0.09			
49577	n	0.07	0.055	0.09			
49011	n	0.065	0.05	0.08			
48586	n	0.065	0.05	0.065			
48247	n	0.065	0.06	0.065			
47731	n	0.07	0.05	0.07			
47286	n	0.075	0.055	0.075			
46674	n	0.06	0.05	0.07			
46214 C	n	0.06	0.05	0.06			
46084	n	0.065	0.05	0.075			
46026 STATE HIGHWAY 97	Bridge						
45940	n	0.055	0.05	0.055			
45784	n	0.055	0.055	0.07			
45633	n	0.055	0.055	0.07			

45174	n	0.055	0.05	0.07			
45024	n	0.06	0.05	0.065			
44688	n	0.065	0.055	0.06			
44626 STATE HIGHWAY 97	Bridge						
44550	n	0.065	0.055	0.06			
44414	n	0.075	0.05	0.06			
44130	n	0.08	0.05	0.06			
43839	n	0.08	0.05	0.06			
43675 B	n	0.08	0.05	0.06			
43568	n	0.06	0.05	0.06			
43438 STATE HIGHWAY 18	Bridge						
43311	n	0.07	0.05	0.06			
43198	n	0.07	0.05	0.06			
43110	n	0.07	0.05	0.06			
43024 STATE HIGHWAY 18	Bridge						
42989	n	0.06	0.05	0.06			
42970	n	0.06	0.05	0.06			
42906 AIRPORT FREEWAY	Bridge						
42836	n	0.06	0.05	0.06			
42749	n	0.06	0.05	0.06			

42569	n	0.075	0.05	0.06			
42152 A	n	0.075	0.05	0.06			
41649	n	0.075	0.05	0.06			
41051	n	0.075	0.05	0.06			
40752	n	0.025	0.025	0.025			
40742	Bridge						
40732	n	0.025	0.025	0.025			
40682	n	0.075	0.055	0.07			
38642	n	0.075	0.055	0.07			

HEC-RAS Channel length original file

River Station	LOB	Channel	ROB
81536	433	442	437
81094	547	569	539
80525	259	294	263
80231	295	297	281
79934 CONFLUENCE OF TR	330	350	327
79584	190	174	153
79410 L	350	352	316
79058	90	135	189
78923	33	30	30
78908 WALKBRIDGE	Bridge		
78893	675	643	606
78250	349	374	428
77876 K	465	537	587
77339	177	176	167
77252 STATE HIGHWAY 36	Bridge		
77163	100	99	109
77064	152	154	153
76910	172	179	165

76830 STATE HIGHWAY 36	Bridge		
76731	210	215	208
76516	480	461	420
76055	627	603	533
75452 J	59	73	108
75379	152	148	147
75311 EULESS GRAPEVINE	Bridge		
75231 DALLAS/FORT WORT	439	407	324
74824	460	468	456
74356	422	419	424
73937	466	472	485
73465	391	435	247
73030	166	171	73
72859	128	178	231
72680 CONFLUENCE OF TR	362.4	250.8	210.2
72430	176	459.9	279.8
71969	396.2	537.4	321.7
71432	18.3	24.4	90.1
71408	15.2	35.4	91.8
71372	106.8	147.7	117.9

71224	104.1	135.7	122.4
71089	181.9	226.9	258
70862	78.7	109.9	118.7
70752	22	22	22
70730	41.2	41.2	41.2
70689	78.7	85	88.4
70604	208	295.1	363.6
70309	6.4	8.1	7.9
70301	236.3	335.9	214.8
69965	85.1	145.84	229.6
69819	796.7	758.8	629.3
69061	745	756	738
68305	214	208	181
68097	443	423	374
67674	600	642	632
67032	238	215	184
66817	162	163	161
66654	43	43	46
66632 GLADE ROAD	Bridge		
66611	330	366	349
66245	401	391	402
65854	669	708	716

65146 CONFLUENCE OF TR	983	1039	1034
64107	263	256	239
63851	566	572	530
63279 G	399	412	379
62867	747	778	764
62089	481	477	437
61612	556	624	552
60988	744	811	686
60177	210	274	291
59903	530	517	463
59386 CONFLUENCE OF TR	260	259	247
59127	210	217	214
58910	47	52	58
58858	110	101	104
58788 MID CITIES BOULE	Culvert		
58757	31	29	29
58728	79	72	56
58656	271	236	202
58420 F	674	679	681
57741	594	625	648
57116	481	487	477

56629	251	225	201
56404	218	265	277
56139	309	358	393
55781	334	365	385
55416 E	53	57	59
55359	82	84	86
55275	31	32	33
55256 GOLF COURSE MAIN	Bridge		
55243	107	107	104
55136	189	160	141
54976	129	104	83
54872	101	97	87
54775	94	100	102
54675	39	60	94
54615	84	107	108
54508	71	47	37
54461	94	46	33
54415	65	53	32
54362	67	64	54
54298	58	79	91
54219	20	44	60
54175	23	27	27

54149 GOLF COURSE	Bridge		
54148	56	60	64
54088	88	99	108
53989	93	99	103
53890	154	194	228
53696	89	89	88
53607	22	40	54
53567	32	33	41
53550 GOLF COURSE	Bridge		
53534	60	41	24
53493	201	152	107
53341	438	421	410
52920	211	194	182
52726	80	71	66
52655	77	65	59
52590	87	91	93
52499	93	97	97
52402 D	341	335	322
52067	95	93	92
51974	35	35	37
51957 GOLF COURSE	Bridge		
51939	52	54	55
51885	152	151	152

51734	217	237	226
51497	363	336	329
51161	307	314	320
50847	588	634	659
50213	561	636	668
49577	559	566	566
49011	416	425	430
48586	341	339	331
48247	508	516	521
47731	437	445	444
47286	620	612	604
46674	446	460	466
46214 C	87	130	149
46084	145	144	140
46026 STATE HIGHWAY 97	Bridge		
45940	214	156	117
45784	179	151	125
45633	469	459	445
45174	123	150	170
45024	76	336	376
44688	250	138	143

44626 STATE HIGHWAY 97	Bridge		
44550	224	136	112
44414	288	284	256
44130	365	291	233
43839	190	164	143
43675 B	127	107	97
43568	269	257	254
43438 STATE HIGHWAY 18	Bridge		
43311	72	113	122
43198	73	88	100
43110	121	120	122
43024 STATE HIGHWAY 18	Bridge		
42989	28	20	12
42970	134	134	133
42906 AIRPORT FREEWAY	Bridge		
42836	86	87	90
42749	172	180	194
42569	309	417	508
42152 A	500	503	499
41649	465	598	696

41051	299	299	299
40752	20	20	20
40742	Bridge		
40732	50	50	50
40682	2150	2040	1700
38642	2250	2970	2410

APPENDIX B

Calibrated HEC-RAS 1D/2D Manning's n 2022

River Station	n #1	n #2	n #3	n #4	n #5	n #6	n #7
74356	0.1	0.055	0.08				
74100							
74000							
73937	0.1	0.055	0.08				
73465	0.1	0.055	0.08	0.05	0.05	0.06	0.06
73030	0.1	0.055	0.1	0.05	0.05	0.05	0.05
72859	0.1	0.055	0.06	0.06	0.06	0.06	0.06
72680 CONFLUENCE OF TR	0.1	0.055	0.06	0.07	0.07		
72430	0.1	0.055	0.06	0.07	0.07		
71969	0.1	0.055	0.1	0.07			
71432	0.1	0.055	0.1	0.07	0.07		
71420							
71408	0.1	0.055	0.1	0.07	0.07		
71372	0.1	0.055	0.1	0.07	0.07		
71224	0.1	0.055	0.06	0.07	0.07		
71089	0.1	0.055	0.06	0.07	0.07	0.07	
70862	0.1	0.055	0.06	0.07	0.07		
70752	0.1	0.055	0.06	0.07	0.07	0.07	
70730	0.1	0.055	0.06	0.07	0.07	0.07	0.07

70689	0.1	0.055	0.06	0.07	0.07		
70604	0.1	0.055	0.06	0.07	0.07		
70309	0.1	0.055	0.045	0.07	0.07		
70305							
70301	0.1	0.055	0.045	0.06	0.07	0.07	0.07
69965	0.1	0.055	0.06	0.06	0.07	0.07	
69819	0.1	0.055	0.06	0.06	0.06	0.06	0.06
69061	0.1	0.055	0.1				
69000							
68305	0.1	0.055	0.1				
68097	0.1	0.055	0.1				
67674	0.1	0.055	0.1				
67500							
67032	0.1	0.06	0.1				
66817	0.1	0.06	0.09				
66654	0.1	0.055	0.09				
66632 GLADE ROAD							
66611	0.09	0.055	0.09				
66245	0.09	0.055	0.09				
65854	0.09	0.055	0.09				
65146 CONFLUENCE OF TR	0.09	0.055	0.09				
64107	0.09	0.06	0.09				

64000							
63851	0.09	0.06	0.09				
63279 G	0.09	0.06	0.09				
62867	0.09	0.06	0.09				
62089	0.09	0.055	0.09				
61612	0.09	0.055	0.09				
61000							
60988	0.08	0.055	0.08				
60177	0.08	0.05	0.08				
59903	0.08	0.05	0.08				
59386 CONFLUENCE OF TR	0.08	0.05	0.08				
59127	0.08	0.055	0.08				
58910	0.08	0.05	0.08				
58858	0.08	0.05	0.08				
58788 MID CITIES BOULE							
58757	0.08	0.05	0.08				
58728	0.06	0.045	0.06				
58710							
58656	0.1	0.07	0.08				
58420 F	0.1	0.07	0.08				
57741	0.1	0.07	0.08				
57116	0.1	0.07	0.08				

56629	0.1	0.07	0.08				
56404	0.1	0.07	0.08				
56139	0.1	0.07	0.08				
55781	0.1	0.07	0.08				
55416 E	0.1	0.07	0.08				
55359	0.1	0.07	0.08				
55275	0.1	0.07	0.08				
55256 GOLF COURSE MAIN							
55243	0.1	0.08	0.07				
55136	0.1	0.08	0.07				
54976	0.1	0.08	0.07				
54872	0.1	0.08	0.07				
54800		0.08					
54775	0.1	0.08	0.06				
54675	0.1	0.08	0.06				
54615	0.1	0.08	0.06				
54508	0.1	0.08	0.05				
54461	0.1	0.08	0.05				
54415	0.1	0.08	0.05				
54362	0.1	0.08	0.05				
54298	0.1	0.08	0.05				
54219	0.1	0.08	0.05				

54175	0.1	0.08	0.05				
54149 GOLF COURSE							
54148	0.1	0.08	0.05				
54088	0.1	0.08	0.05				
53989	0.1	0.08	0.05				
53890	0.1	0.08	0.05				
53696	0.1	0.08	0.05				
53607	0.1	0.08	0.05				
53567	0.1	0.08	0.05				
53550 GOLF COURSE							
53534	0.05	0.045	0.05				
53493	0.05	0.045	0.05				
53341	0.055	0.045	0.055				
52920	0.055	0.05	0.055				
52726	0.05	0.045	0.05				
52655	0.05	0.045	0.05				
52590	0.05	0.045	0.06				
52499	0.055	0.045	0.055				
52402 D	0.06	0.05	0.06				
52067	0.06	0.05	0.06				
51974	0.065	0.05	0.06				
51957 GOLF COURSE							
51939	0.065	0.05	0.06				

51885	0.07	0.05	0.07				
51734	0.07	0.055	0.07				
51497	0.07	0.055	0.09				
51161	0.06	0.06	0.09				
50900							
50847	0.06	0.055	0.09				
50213	0.065	0.06	0.09				
49577	0.07	0.055	0.09				
49011	0.065	0.05	0.08				
48586	0.065	0.05	0.065				
48300							
48247	0.065	0.06	0.065				
48200							
47731	0.07	0.05	0.07				
47286	0.075	0.055	0.075				
46674	0.06	0.05	0.07				
46214 C	0.06	0.05	0.06				
46084	0.065	0.05	0.075				
46026 STATE HIGHWAY 97							
45940	0.055	0.05	0.055				
45784	0.055	0.055	0.07				
45633	0.055	0.055	0.07				

45174	0.055	0.05	0.07				
45024	0.06	0.05	0.065				
44688	0.065	0.055	0.06				
44626 STATE HIGHWAY 97							
44550	0.065	0.055	0.06				
44414	0.075	0.05	0.06				
44130	0.08	0.05	0.06				
43839	0.08	0.05	0.06				
43675 B	0.08	0.05	0.06				
43568	0.06	0.05	0.06				
43438 STATE HIGHWAY 18							
43311	0.07	0.05	0.06				
43198	0.07	0.05	0.06				
43110	0.07	0.05	0.06				
43024 STATE HIGHWAY 18							
42989	0.06	0.05	0.06				
42970	0.06	0.05	0.06				
42906 AIRPORT FREEWAY							
42836	0.06	0.05	0.06				
42749	0.06	0.05	0.06				

42569	0.075	0.05	0.06				
42400							
42152 A	0.075	0.05	0.06				
41649	0.075	0.05	0.06				
41051	0.075	0.05	0.06				
40752	0.025	0.025	0.025				
40742							
40732	0.025	0.025	0.025				
40682	0.075	0.055	0.07				
38642	0.075	0.055	0.07				
33313	0.1	0.03	0.07	0.03	0.07	0.03	0.1
27811	0.1	0.07	0.045	0.07	0.1		

Calibrated HEC-RAS 1D/2D Manning's n 2017

River Station	n #1	n #2	n #3	n #4	n #5	n #6	n #7
74356	0.05	0.055	0.03				
74100							
74000							
73937	0.05	0.04	0.04				
73465	0.05	0.04	0.04	0.05	0.05	0.06	0.06
73030	0.05	0.04	0.04	0.05	0.05	0.05	0.05
72859	0.05	0.04	0.04	0.06	0.06	0.06	0.06
72680 CONFLUENCE OF TR	0.05	0.04	0.04	0.07	0.07		
72430	0.05	0.04	0.04	0.07	0.07		
71969	0.05	0.04	0.04	0.07			
71432	0.05	0.04	0.04	0.07	0.07		
71420							
71408	0.06	0.04	0.07	0.07	0.07		
71372	0.06	0.04	0.07	0.07	0.07		
71224	0.06	0.04	0.07	0.07	0.07		
71089	0.06	0.04	0.07	0.07	0.07	0.07	

70862	0.06	0.04	0.07	0.07	0.07		
70752	0.06	0.04	0.07	0.07	0.07	0.07	
70730	0.06	0.04	0.07	0.07	0.07	0.07	0.07
70689	0.06	0.04	0.07	0.07	0.07		
70604	0.06	0.04	0.07	0.07	0.07		
70309	0.06	0.055	0.07	0.07	0.07		
70305							
70301	0.07	0.03	0.07	0.06	0.07	0.07	0.07
69965	0.07	0.03	0.07	0.06	0.07	0.07	
69819	0.07	0.03	0.07	0.06	0.06	0.06	0.06
69061	0.07	0.03	0.07				
69000							
68305	0.06	0.055	0.06				
68097	0.06	0.055	0.06				
67674	0.06	0.055	0.06				
67500							
67032	0.06	0.06	0.05				
66817	0.06	0.06	0.05				
66654	0.06	0.055	0.05				
66632 GLADE ROAD							
66611	0.06	0.055	0.07				
66245	0.06	0.055	0.07				
65854	0.06	0.055	0.07				

65146 CONFLUENCE OF TR	0.06	0.055	0.07				
64107	0.06	0.06	0.07				
64000							
63851	0.09	0.06	0.09				
63279 G	0.09	0.06	0.09				
62867	0.09	0.06	0.09				
62089	0.09	0.055	0.09				
61612	0.09	0.055	0.09				
61000							
60988	0.08	0.055	0.08				
60177	0.08	0.05	0.08				
59903	0.08	0.05	0.08				
59386 CONFLUENCE OF TR	0.08	0.05	0.08				
59127	0.08	0.055	0.08				
58910	0.08	0.05	0.08				
58858	0.08	0.05	0.08				
58788 MID CITIES BOULE							
58757	0.08	0.05	0.08				
58728	0.06	0.045	0.06				
58710							
58656	0.06	0.07	0.06				

58420 F	0.06	0.07	0.06				
57741	0.06	0.07	0.06				
57116	0.06	0.07	0.06				
56629	0.06	0.07	0.06				
56404	0.06	0.07	0.06				
56139	0.06	0.07	0.06				
55781	0.06	0.07	0.06				
55416 E	0.06	0.07	0.06				
55359	0.06	0.07	0.06				
55275	0.06	0.07	0.06				
55256 GOLF COURSE MAIN							
55243	0.06	0.08	0.07				
55136	0.06	0.08	0.07				
54976	0.06	0.08	0.07				
54872	0.06	0.08	0.07				
54800		0.08					
54775	0.1	0.08	0.06				
54675	0.1	0.08	0.06				
54615	0.1	0.08	0.06				
54508	0.1	0.08	0.05				
54461	0.1	0.08	0.05				
54415	0.1	0.08	0.05				

54362	0.1	0.08	0.05				
54298	0.1	0.08	0.05				
54219	0.1	0.08	0.05				
54175	0.1	0.08	0.05				
54149 GOLF COURSE							
54148	0.1	0.08	0.05				
54088	0.1	0.08	0.05				
53989	0.1	0.08	0.05				
53890	0.1	0.08	0.05				
53696	0.1	0.08	0.05				
53607	0.1	0.08	0.05				
53567	0.1	0.08	0.05				
53550 GOLF COURSE							
53534	0.05	0.045	0.05				
53493	0.05	0.045	0.05				
53341	0.055	0.045	0.055				
52920	0.055	0.05	0.055				
52726	0.05	0.045	0.05				
52655	0.05	0.045	0.05				
52590	0.05	0.045	0.06				
52499	0.055	0.045	0.055				
52402 D	0.06	0.05	0.06				
52067	0.06	0.05	0.06				

51974	0.065	0.05	0.06				
51957 GOLF COURSE							
51939	0.065	0.05	0.06				
51885	0.07	0.05	0.07				
51734	0.07	0.055	0.07				
51497	0.07	0.055	0.09				
51161	0.06	0.06	0.09				
50900							
50847	0.06	0.055	0.09				
50213	0.065	0.06	0.09				
49577	0.07	0.055	0.09				
49011	0.065	0.05	0.08				
48586	0.065	0.05	0.065				
48300							
48247	0.065	0.06	0.065				
48200							
47731	0.07	0.05	0.07				
47286	0.075	0.055	0.075				
46674	0.06	0.05	0.07				
46214 C	0.06	0.05	0.06				
46084	0.065	0.05	0.075				
46026 STATE HIGHWAY 97							

45940	0.055	0.05	0.055				
45784	0.055	0.055	0.07				
45633	0.055	0.055	0.07				
45174	0.055	0.05	0.07				
45024	0.06	0.05	0.065				
44688	0.065	0.055	0.06				
44626 STATE HIGHWAY 97							
44550	0.065	0.055	0.06				
44414	0.075	0.05	0.06				
44130	0.08	0.05	0.06				
43839	0.08	0.05	0.06				
43675 B	0.08	0.05	0.06				
43568	0.06	0.05	0.06				
43438 STATE HIGHWAY 18							
43311	0.07	0.05	0.06				
43198	0.07	0.05	0.06				
43110	0.07	0.05	0.06				
43024 STATE HIGHWAY 18							
42989	0.06	0.05	0.06				
42970	0.06	0.05	0.06				

42906 AIRPORT FREEWAY							
42836	0.06	0.05	0.06				
42749	0.06	0.05	0.06				
42569	0.075	0.05	0.06				
42400							
42152 A	0.075	0.05	0.06				
41649	0.075	0.05	0.06				
41051	0.075	0.05	0.06				
40752	0.025	0.025	0.025				
40742							
40732	0.025	0.025	0.025				
40682	0.075	0.055	0.07				
38642	0.075	0.055	0.07				
33313	0.1	0.03	0.07	0.03	0.07	0.03	0.1
27811	0.1	0.07	0.045	0.07	0.1		

REFERENCES

[1] A. A. AL-Hussein, S. Khan, K. Ncibi, N. Hamdi, and Y. Hamed, "Flood analysis using HEC-ras and HEC-hms: A case study of khazir river (middle east—northern iraq)," Water, vol. 14, no. 22, p. 3779, 2022.

[2] H. Rashid, M. M. Manzoor, S. Mukhtar, et al., "Urbanization and its effects on water resources: An exploratory analysis," Asian Journal of Water, Environment and Pollution, vol. 15, no. 1, pp. 67–74, 2018.

[3] S. Prasood, M. Mukesh, V. Rani, K. Sajinkumar, and K. Thrivikramji, "Urbanization and its effects on water resources: Scenario of a tropical river basin in south india," Remote Sensing Applications: Society and Environment, vol. 23, p. 100556, 2021.

[4] M. Y. Onanuga, A. O. Eludoyin, and I. E. Ofoezie, "Urbanization and its effects on land and water resources in ijebuland, southwestern nigeria," Environment, Development and Sustainability, vol. 24, no. 1, pp. 592–616, 2022.

[5] A. Sengupta, S. K. Adams, B. P. Bledsoe, E. D. Stein, K. S. McCune, and R. D. Mazor, "Tools for managing hydrologic alteration on a regional scale: Estimating changes in flow characteristics at ungauged sites," Freshwater Biology, vol. 63, no. 8, pp. 769–785, 2018.

[6] H. Meresa, "Modelling of river flow in ungauged catchment using remote sensing data: application of the empirical (scs-cn), artificial neural network (ann) and hydrological model (HEC-hms)," Modeling Earth Systems and Environment,

vol. 5, pp. 257–273, 2019.

[7] D. Halwatura and M. Najim, “Application of the HEC-hms model for runoff simulation in a tropical catchment,” Environmental modelling & software, vol. 46, pp. 155–162, 2013.

[8] C. G. Quinonez, Development of HEC-HMS and HEC-RAS models for urban floodplain mapping and flood damage reduction in Brownsville, Texas. Rice University, 2005.

[9] A. Shabani, S. A. Woznicki, M. Mehaffey, J. Butcher, T. A. Wool, and P.-Y. Whung, “A coupled hydrodynamic (HEC-ras 2d) and water quality model (wasp) for simulating flood-induced soil, sediment, and contaminant transport,” Journal of flood risk management, vol. 14, no. 4, p. e12747, 2021.

[10] E. Hut ̧anu, A. Mihu-Pintilie, A. Urzica, L. E. Paveluc, C. C. Stoleriu, and A. Grozavu, “Using 1d HEC-ras modeling and lidar data to improve flood hazard maps accuracy: A case study from jijia floodplain (ne romania),” Water, vol. 12, no. 6, p. 1624, 2020.

[11] E. Ghimire, S. Sharma, and N. Lamichhane, “Evaluation of one-dimensional and two-dimensional HEC-ras models to predict flood travel time and inundation area for flood warning system,” ISH Journal of Hydraulic Engineering, vol. 28, no. 1, pp. 110–126, 2022.

[12] T. K. Eckermann, D. S. Hunt, and A. M. Kinoshita, “Impacts of vegetation removal on urban mediterranean stream hydrology and hydraulics,” Hydrology, vol. 9, no. 10, p. 170, 2022.

[13] S. Zafar and A. Zaidi, “Impact of urbanization on basin hydrology: a case study

of the malir basin, karachi, pakistan," Regional Environmental Change, vol. 19, pp. 1815–1827, 2019.

[14] A. Aniskin, T. Mkilima, Z. Shakhmov, G. Kozina, et al., "Potential impact of land-use changes on river basin hydraulic parameters subjected to rapid urbanization," Tehniˇcki vjesnik, vol. 28, no. 5, pp. 1519–1525, 2021.

[15] V. A. Rangari, V. Sridhar, N. Umamahesh, and A. K. Patel, "Floodplain mapping and management of urban catchment using HEC-ras: a case study of hyderabad city," Journal of The Institution of Engineers (India): Series A, vol. 100, pp. 49–63, 2019.

[16] A. Alsubeai and S. R. Burckhard, "Rainfall-runoff simulation and modelling using HEC-hms and HEC-ras models: Case study tabuk, saudi arabia," Natural Resources, vol. 12, no. 10, pp. 321–338, 2021.

[17] K. Nagarajan, A. P. Raju Narwade, S. Panhalkar, V. S. Kulkarni, and A. P. Hingmire, "Employing digital elevation model (dem) for floodplain mapping with applications of HEC-hms, HEC-ras, and arcgis: A review," 2022.

[18] A. G. Cowles, Effects of Historical Land-use Change on Surface Runoff and Flooding in the Amite River Basin, Louisiana, USA Using Coupled 1D/2D HEC-RAS–HEC-HMS Hydrological Modeling. Louisiana State University and Agricultural & Mechanical College, 2021.

[19] E. F. Lambin, H. J. Geist, and E. Lepers, "Dynamics of land-use and land-cover change in tropical regions," Annual review of environment and resources, vol. 28, no. 1, pp. 205–241, 2003.

[20] F. Pervaiz, "Evaluation of ice loads on beitstadsundet bridge by deterministic

and probabilistic approaches." Master's thesis, NTNU, 2019.

[21] F. Pervaiz and M. Hummel, "Numerical simulation of hydrodynamic forces on bridges subjected to high-velocity flows," 2021.

[22] S. Lim, D. Popov, N. Raza, F. Pervaiz, and M. Al-Qadi, "Feasibility study of submerged floating crossing," 2018.

[23] H. Ahmari, M. Hummel, S.-H. S. Chao, S. M. I. Kabir, F. Pervaiz, B. R. Acharya, M. Dean, Q. A. Mowla, et al., "Identify and analyze inundated bridge superstructures in high velocity flood events," University of Texas at Arlington, Tech. Rep., 2021.

[24] J. Ahmad and J. A. Eisma, "Capturing small-scale surface temperature variation across diverse urban land uses with a small unmanned aerial vehicle," Remote Sensing, vol. 15, no. 8, p. 2042, 2023.

[25] J. Ahmad, "Merging satellite rainfall estimates in scarcely gauged basin: A case study of indus basin," 2018.

[26] B. Bhattacharya and J. Ahmad, "K nearest neighbour in merging satellite rainfall estimates from diverse sources in sparsely gauged basins," in EGU General Assembly Conference Abstracts, 2021, pp. EGU21–14 650.

[27] Q. Hu, Q. Wang, T. Zhang, C. Zhao, K. H. Iltaf, S. Liu, and Y. Fukatsu, "Petrophysical properties of representative geological rocks encountered in carbon storage and utilization," Energy Reports, vol. 9, pp. 3661–3682, 2023.

[28] B. Thakur, R. Parajuli, A. Kalra, S. Ahmad, and R. Gupta, "Coupling HEC-ras and HEC-hms in precipitation runoff modelling and evaluating flood plain inundation map," in World Environmental and Water Resources Congress 2017,

2017, pp. 240–251.

[29] D. P. Patel, J. A. Ramirez, P. K. Srivastava, M. Bray, and D. Han, “Assessment of flood inundation mapping of surat city by coupled 1d/2d hydrodynamic modeling: a case application of the new HEC-ras 5,” Natural Hazards, vol. 89, pp. 93–130, 2017.

[30] L. Dasallas, Y. Kim, and H. An, “Case study of HEC-ras 1d–2d coupling simulation: 2002 baeksan flood event in korea,” Water, vol. 11, no. 10, p. 2048, 2019.

[31] F. Pervaiz and M. Hummel, “Evaluation of climate change and urbanization impacts on bridges in harris county, texas,” in World Environmental and Water Resources Congress 2022, pp. 499–507.

BIOGRAPHICAL STATEMENT

Machiraju P Kashyap was born in New Delhi, India, in 1995. He received his Btech in civil Engineering in SRM University, Tamil Nadu, in 2016. He is an avid sport enthusiast. He worked in the construction management industry for 4 years and project management knowledge while he got to travel all around the country for different industrial and residential construction projects. He came to USA in the fall of 2021 seeking a master's degree in water resources engineering and since been pursuing his degree in the Civil Engineering Department at the University of Texas at Arlington. His favorite courses are water resources planning and hydraulics.